9-26-2012

Effect of Accessory Power Take-off Variation on a Turbofan Engine Performance

Anis Faidi

EFFECT OF ACCESSORY POWER TAKE-OFF VARIATION ON A TURBOFAN ENGINE PERFORMANCE

THESIS

Anis Faidi, Lieutenant, TUNIAF

AFIT/GAE/ENY/12-S26

DEPARTMENT OF THE AIR FORCE
AIR UNIVERSITY

AIR FORCE INSTITUTE OF TECHNOLOGY

Wright-Patterson Air Force Base, Ohio

AFIT/GAE/ENY/12-S26

EFFECT OF ACCESSORY POWER TAKE-OFF VARIATIONS ON A TURBOFAN ENGINE PERFORMANCE

DISSERTATION

Presented to the Faculty

Department of Aeronautics and Astronautics

Graduate School of Engineering and Management

Air Force Institute of Technology

Air University

Air Education and Training Command

In Partial Fulfillment of the Requirements for the

Degree of Master of science in Aeronautical Engineering

Anis Faidi, BS

Lieutenant, TUNAF

September 2012

AFIT/GAE/ENY/12-S26

EFFECT OF ACCESSORY POWER TAKE-OFF VARIATION ON A TURBOFAN ENGINE PERFORMANCE

Anis Faidi, BS

1st Lieutenant, TUNAF

Approved:

_____	_____
Paul King, PhD (Chairman)	Date
_____	_____
Lt. Col Ronald Simmons (Member)	Date
_____	_____
Lt. Col Jeremy Agte (Member)	Date

AFIT/GAE/ENY/12-S26

Abstract

Engine fuel efficiency of aerospace vehicles can be reached by different techniques. One way to do that is to reduce aircraft subsystems power supply effects on the engine performance. Previous research work has showed that extracting bleed air from the high pressure compressor exit is more efficient than extracting the equivalent amount of energy from the low pressure spool shaft. A high bypass turbofan engine was modeled using the Numerical Propulsion System Simulation (NPSS). The baseline engine performance was evaluated at different flight conditions of Mach number and altitude. To better understand the effect of air bleed take-off and shaft power extraction, four simulation cases are investigated at constant fuel flow and constant high pressure turbine inlet temperature setting. The first two cases extract bleed air from compressors while the last two cases extract equivalent power from engine shafts. Appropriate model modifications and port connections are made to consider the power extraction method. The effect of a bleed air fraction off-take from 1% to 10% and equivalent shaft power extraction on engine performance of thrust and thrust specific fuel consumption was investigated. Engine compressors operating lines and HPT inlet temperature were also checked. Results proved that shaft power extraction is more efficient for engine performance than bleeding an equivalent air fraction from compressors. Those results were shown to be consistent with a simulation run on the AEDsys simulation tool.

Acknowledgments

I would like to warmly thank my family for the moral support they have never stopped giving me during my master's degree training in AFIT. My greatest thanks are addressed to my father, may God blessings be upon him. I would like to thank my US social sponsors, Ms. and Mr. Graiziers, for the great time we spent together and their unlimited help. I would specifically like to thank the international student military office manager, Ms. Annette Robb for her unconditional support and her dedication for the international students even beyond her duty scope. I also want to thank my thesis advisor, Dr. Paul King for not only being patient with me but also for the knowledge I have got from him during classes as well as during my research.

Anis Faidi

Table of Contents

Page

Abstract iv
Acknowledgments v
Table of Contents vi
List of Figures viii
List of Tables xiv
List of Symbols xv
List of Abbreviations xix
I. Introduction 1
I.1 Numerical Propulsion System Simulation program. 2
I.2 Problem Statment 3
I.3 Research Focus. 3
II. Background and Previous Work 4
II.1 Turbofan Engine Cycle Analysis and Performance 4
II.2 Power Extraction Techniques 8
II.3 NPSS Modeling And Simulation 9
II.4 Previous Work On Power Extraction Effects On Air Breathing Engine Performance 18
III. Methodology and Simulation Setup 25
III.1 Engine NPSS Model 25
III.2 Engine Performance And Limitations 28
III.3 Running Cases 31
III.4 Turbomachinery Map Scaling 33
IV. Simulation Results and Analysis 37

IV.1 Engine Thrust And TSFC Performance at Design Point 37
IV.2 Engine Performance Sensitivity to Maximum HPT Inlet Temperature.....52
IV.3 Study of The Sensitivity of The engine Performance Trends to the Altitude Change 57
IV.4 Engine Turbomachinery Components Performance 60
IV.5 AEDsys simulation results.....65
V. Conclusion and Recommendations 68
V.1 Findings and Results.....68
V.2 Recommendations and Future Work 69
Appendix-A.....71
1. Engine Model File.....71
2. Engine Run File.....79
3. Engine Control File 79
4. HPC Exit Bleed Air Off-take Case File 82
5. Viewer File.....85
6. User Function File.....88
Appendix-B.....91
Appendix-C.....93
Bibliography 107

List of Figures

Page

Figure II.1. High bypass turbofan engine sketch 6

Figure II.2. An example of NPSS engine block model..... 10

Figure II.3. NPSS solver sketch..... 11

Figure II.4. NPSS Solver solution searching method 13

Figure II.5. NPSS elements ports connection 16

Figure II.6. Typical engine compressor map 17

Figure II.7. Effect of 0 to 7500 kW Exergy off-take in the form of bleed air or electrical energy, on the thrust and specific fuel consumption, assuming constant fuel flow... 21

Figure II.8. Typical commercial aircraft mission profile legs 22

Figure II.9. Effect of bleeding air (4.73 kg/s) and electrical power off-take on the performance of the CF6-80E1 over the complete flight cycle..... 23

Figure III.1. High bypass turbofan baseline engine model with NPSS 25

Figure III.2. Baseline engine thrust at military power..... 30

Figure III.3. Baseline engine TSFC at military power..... 30

Figure III.4. Baseline engine air mass flow at military power..... 31

Figure III.5. Engine fan scaled map..... 35

Figure III.6. Engine low pressure compressor scaled map 35

Figure III.7. Engine high pressure compressor scaled map..... 36

Figure IV.1. Compared bleed air off-take equivalent horsepower for bleed air off take simulation cases at standard day 39

Figure IV.2. Specific thrust versus CTO: mf = 0.35 lbm/s, Mach = 0.8, Alt = 35 kft on a standard day 41
Figure IV.3 Inlet mass flow rate increment percentage versus CTO: mf = 0.35 lbm/s, Mach = 0.8, Alt = 35 kft on a standard day..... 43
Figure IV.4. TSFC versus CTO: mf = 0.35 lbm/s, Mach = 0.8, Alt = 35 kft on a standard day 43
Figure IV.5. % Tt4 increment versus CTO: mf = 0.35 lbm/s, Mach = 0.8, Alt = 35 kft on a standard day..... 44
Figure IV.6. Specific thrust versus CTO: Tt4 = 2770 R, Mach = 0.8, Alt = 35 kft on a standard day 45
Figure IV.7. Inlet mass flow rate increment percentage versus CTO: Tt4 = 2770 R, Mach = 0.8, Alt = 35 kft on a standard day..... 45
Figure IV.8. TSFC versus CTO: Tt4 = 2770 R, Mach = 0.8, Alt = 35 kft on a standard day 46
Figure IV.9. Specific thrust versus CTO: mf = 0.35 lbm/s, Mach = 0.8, Alt = 35 kft on a cold day 47
Figure IV.10. TSFC versus CTO: mf = 0.35 lbm/s, Mach = 0.8, Alt = 35 kft on a cold day 47
Figure IV.11. Specific thrust versus CTO: Tt4 = 2770 R, Mach = 0.8, Alt = 35 kft on a cold day 48
Figure IV.12. TSFC versus CTO: Tt4 = 2770 R, Mach = 0.8, Alt = 35 kft on a cold day48
Figure IV.13. Tt4 versus CTO: mf = 0.35 lbm/s, Mach = 0.8, Alt = 35 kft on a cold day49

Figure IV.14. Specific thrust versus CTO: mf = 0.35 lbm/s, Mach = 0.8, Alt = 35 kft on a hot day 50
Figure IV.15. TSFC versus CTO: mf = 0.35 lbm/s, Mach = 0.8, Alt = 35 kft on a hot day 50
Figure IV.16. Specific thrust versus CTO: Tt4 = 2770 R, Mach = 0.8, Alt = 35 kft on a hot day 51
Figure IV.17. TSFC versus CTO: Tt4 = 2770 R, Mach = 0.8, Alt = 35 kft on a hot day. 51
Figure IV.18. Tt4 versus CTO: mf = 0.35 lbm/s, Mach = 0.8, Alt = 35 kft on a hot day. 52
Figure IV.19. Thrust sensitivity to Tt4: Mach = 0.8, Alt = 35 kft on a standard day 53
Figure IV.20. TSFC sensitivity to Tt4: Mach = 0.8, Alt = 35 kft on a standard day 54
Figure IV.21. TSFC versus CTO: Mach = 0.8, Alt = 35 kft, Fn = 1849 lbf on a standard day 56
Figure IV.22. Tt4 versus CTO: Mach = 0.8, Alt = 35 kft, Fn = 1849 lbf on a standard day 56
Figure IV.23. TSFC versus CTO: Mach = 0.8, Alt = 20 kft on a standard day 58
Figure IV.24. TSFC versus CTO: Mach = 0.8, Alt = 10 kft on a standard day 58
Figure IV.25. % Tt4 increment versus CTO: Mach = 0.8, Alt = 20 kft on a standard day 59
Figure IV.26. % Tt4 increment versus CTO: Mach = 0.8, Alt = 10 kft ft on a standard day 59
Figure IV.27. Fan operating lines: mf = 0.35 lbm/s, Mach = 0.8, Alt = 35 kft on a standard day 61

Figure IV.28. LPC operating lines: mf = 0.35 lbm/s, Mach = 0.8, Alt = 35 kft on a standard day 61
Figure IV.29. Fan operating lines: Tt4 = 2770 R, Mach = 0.8, Alt = 35 kft t on a standard day 62
Figure IV.30. LPC operating lines : Tt4 = 2770 R, Mach = 0.8, Alt = 35 kft on a standard day 62
Figure IV.31. HPC operating lines : mf = 0.35 lbm/s, Mach = 0.8, Alt = 35 kft on a standard day 64
Figure IV.32. HPC operating lines : Tt4 = 2770 R, Mach = 0.8, Alt = 35 kft on a standard day 64
Figure IV.33. AEDsys engine model in ONX 66
Figure IV.34. Thrust versus CTO using AEDsys: mf = 0.35 lbm/s, Mach = 0.8, Alt = 35 kft on a standard day 66
Figure IV.35. Thrust versus CTO using AEDsys : Tt4 = 2770 R, Mach = 0.8, Alt = 35 kft on a standard day 67
Figure B.1. MIL-STD-210A day type definition: US unit system 91
Figure C.1. Thrust versus exergy: mf = 0.35 lbm/s, Mach = 0.8, Alt = 35 kft on standard day 93
Figure C.2. TSFC versus exergy: mf = 0.35 lbm/s, Mach = 0.8, Alt = 35 kft on standard day 93
Figure C.3. Thrust versus exergy: Tt4 = 2270 R, Mach = 0.8, Alt = 35 kft on standard day 94

Figure C.4. TSFC versus exergy: Tt4 = 2270 R, Mach = 0.8, Alt = 35 kft on standard day 94
Figure C.5. Tt4 versus exergy: mf = 0.35 lbm/s, Mach = 0.8, Alt = 35 kft on standard day 95
Figure C.6. Thrust versus exergy: mf = 0.35 lbm/s, Mach = 0.8, Alt = 35 kft on cold day 95
Figure C.7. TSFC versus exergy: mf = 0.35 lbm/s, Mach = 0.8, Alt = 35 kft on cold day 96
Figure C.8. Thrust versus exergy: Tt4 = 2270 R, Mach = 0.8, Alt = 35 kft on cold day . 97
Figure C.9. TSFC versus exergy: Tt4 = 2270 R, Mach = 0.8, Alt = 35 kft on cold day .. 97
Figure C.10. Tt4 versus exergy: mf = 0.35 lbm/s, Mach = 0.8, Alt = 35 kft on cold day 97
Figure C.11. Thrust versus exergy: mf = 0.35 lbm/s, Mach = 0.8, Alt = 35 kft on hot day 98
Figure C.12. TSFC versus exergy: mf = 0.35 lbm/s, Mach = 0.8, Alt = 35 kft on hot day 98
Figure C.13. Thrust versus exergy: Tt4 = 2770 R, Mach = 0.8, Alt = 35 kft on hot day . 99
Figure C.14. TSFC versus exergy: Tt4 = 2770 R, Mach = 0.8, Alt = 35 kft on hot day .. 99
Figure C.15. Tt4 versus exergy: wf = 0.35 lbm/s, Mach = 0.8, Alt = 35 kft on hot day 100
Figure C.16. Fan operating lines : wf = 0.35 lbm/s, Mach = 0.8, Alt = 35 kft on cold day 100
Figure C.17. LPC operating lines : wf = 0.35 lbm/s, Mach = 0.8, Alt = 35 kft on cold day 101

Figure C.18. HPC operating lines : wf = 0.35 lbm/s, Mach = 0.8, Alt = 35 kft on cold day 101
Figure C.19. Fan operating : Tt4 = 2270 R, Mach = 0.8, Alt = 35 kft on cold day..... 102
Figure C.20. LPC operating lines Tt4 = 2270 R, Mach = 0.8, Alt = 35 kft on cold day 102
Figure C.21. HPC operating lines:Tt4 = 2270 R, Mach = 0.8, Alt = 35 kft on cold day 103
Figure C.22. Fan operating : wf = 0.35 lbm/s, Mach = 0.8, Alt = 35 kft on hot day..... 103
Figure C.23. LPC operating lines : wf = 0.35 lbm/s, Mach = 0.8, Alt = 35 kft on hot day 104
Figure C.24. HPC operating lines : wf = 0.35 lbm/s, Mach = 0.8, Alt = 35 kft on hot day 104
Figure C.25. Fan operating lines :Tt4 = 2270 R, Mach = 0.8, Alt = 35 kft on hot day.. 105
Figure C.26. LPC operating lines :Tt4 = 2270 R, Mach = 0.8, Alt = 35 kft on hot day. 105
Figure C.27. HPC operating lines :Tt4 = 2270 R, Mach = 0.8, Alt = 35 kft on hot day 106

List of Tables

Page

Table II-1. Engine components total pressure and enthalpy ratios 8

Table II-2. NPSS on-design and off-design default independent parameters 14

Table II-3. NPSS on-design and off-design default dependent conditions 15

Table III-1. Ambient flight condition parameters 26

Table III-2. InletStart and Inlet design input parameters 26

Table III-3. Engine compressors and turbines design point main parameters 27

Table III-4. Engine cooling bleed air parameters 28

Table III-5. Simulation cases description 32

Table III-6. Engine map scaling factors 34

Table IV-1. Bleed air off-take cases equivalent extracted horsepower 37

List of Symbols

A_9	total nozzle exit area, in^2
A_{19}	total secondary exit area, in^2
a_0	free stream speed of sound, ft/s
CTO	coefficient of power extraction
$diaPump$	effective pumping diameter used to calculate the power used to accelerate the bleed flow to the rotational speed of the turbine blades, in^2
dT_s	delta temperature from selected atmosphere used value, R
eff	adiabatic efficiency
$effDes$	adiabatic efficiency at design point
$eRamBase$	uninstalled ram pressure recovery
$errorNONdim$	non dimensional error
eq_{lhs}	equation left hand side
eq_{rhs}	equation right hand side
E_x	total exergy extraction, Btu
f	fuel-air ratio
F	uninstalled total thrust, lbf
F_c	core uninstalled thrust, lbf
F_F	bypass stream uninstalled thrust, lbf
$fracBldW$	ratio of bleed flow to compressor inlet flow
$fracBldP$	fraction of total pressure rise in the bleed flow

$fracBldWork$	fraction of the total enthalpy rise in bleed flow
g_c	Newton constant,
h_t	station total enthalpy, Btu/lbm
M	Mach number
$\dot{m}_{25}$	LPC exit air mass flow, lbm/s
$\dot{m}_{251}$	HPC entry air mass flow rate, lbm/s
$\dot{m}_3$	HPC exit air mass flow rate, lbm/s
$\dot{m}_{31}$	burner entry air mass flow rate, lbm/s
$\dot{m}_4$	burner exit air mass flow rate, lbm/s
$\dot{m}_{41}$	HPT air mass flow rate, lbm/s
$\dot{m}_{44}$	HPC exit air mass flow rate, lbm/s
$\dot{m}_{45}$	LPT entry mass flow rate, lbm/s
$\dot{m}_5$	LPT exit air mass flow rate, lbm/s
$\dot{m}_9$	nozzle exit mass flow rate, lbm/s
$\dot{m}_c$	corrected mass flow, lbm/s
$\dot{m}_{core}$	core air mass flow, lbm/s
$\dot{m}_F$	bypass stream air mass flow, lbm/s
$\dot{m}_f$	fuel mass flow rate, lbm/s
N_c	corrected rotational speed, rpm
N_cDes	design point corrected rotational speed, rpm
N_{HP}	rotational speed of the high pressure spool. rpm
N_{LP}	rotational speed of the low pressure spool, rpm

$Nmech$	rotational speed of engine shafts, rpm
NR	ratio of the load to the shaft speed, rpm
P_{19}	secondary nozzle exit stream static pressure, psia
P_9	nozzle exit static pressure, psia
P_t	station total pressure, psia
$\dot{Q}_{in}$	rate of thermal energy released,
s	station entropy
S_F	thrust sensitivity to HPT inlet temperature
S_{F_n}	specific thrust
S_{TSFC}	TSFC sensitivity to HPT inlet temperature
Trq_{LP}	net torque of the low pressure spool
Trq_{HP}	net torque of the high pressure spool
Trq_{LPC}	torque load of the low pressure compressor
Trq_{Fan}	torque load of the fan compressor
Trq_{LPT}	torque load of the low pressure turbine
Trq_{HPC}	torque load of the high pressure compressor
Trq_{HPT}	torque load of the high pressure turbine
TSFC	Thrust Specific Fuel Consumption, lbm/(lbf. hr)
T_t	station total temperature, R
V_9	nozzle exit airflow velocity, ft/s
V_0	inlet airflow velocity, ft/s
V_{19}	bypass stream exit velocity, ft/s

W	station mass flow rate, lbm/s
W_in	inlet airflow at design, lbm/s
$\dot{w}_{out}$	net power out of engine
α	bypass ratio
β	surge bleed air fraction
θ	dimensionless static temperature
δ	dimensionless static pressure
π_i	total pressure ratio of component i
τ_i	total temperature ratio for component i
$\varepsilon_1, \varepsilon_2, \varepsilon_3$	cooling bleed air fractions
ε_x	specific total exergy
η_O	overall engine efficiency
η_P	propulsive engine efficiency
η_{TH}	engine thermal efficiency
$\sum_{LP} PX$	LP spool shaft total power extraction
$\sum_{HP} P$	HP spool shaft total power extraction
$\sum_{LP} I$	total inertia of the LP spool
$\sum_{HP} I$	total inertia of the HP spool

List of Abbreviations

AEDsys	Aircraft Engine Design system
BPR	Bypass Pressure Ratio
ECS	Environmental control system
FPR	Fan Pressure Ratio
GE	General Electric
GSP	Gas turbine Simulation Program
HPT	High Pressure Turbine
HPC	High Pressure Compressor
HP	High Pressure
NPSS	Numerical Propulsion System Simulation
NASA	National Aeronautics and Space Administration
LP	Low Pressure
LPC	Low Pressure Compressor
LPT	Low Pressure Turbine
OPR	Overall Pressure Ratio
SPS	Secondary Power System

EFFECT OF ACCESSORY POWER TAKE-OFF VARIATION ON A TURBOFAN ENGINE PERFORMANCE

I. Introduction

Optimization of engine fuel consumption for both commercial and military aircraft engines is becoming increasingly a matter of concern more than at any previous time due to high engine acquisition, operation and maintenance costs. In a commercial aircraft, engine fuel efficiency is crucial for an airline company as well as for its customers in determining flight ticket cost. For a military aircraft, engine fuel efficiency could directly affect the aircraft range and how much payload it could carry for a specific mission.

In the early 1970s, the energy crisis pushed jet engine and aerospace industries to focus on jet engine fuel consumption optimization. Consequently, studies have been conducted in a variety of areas such as material strength improvement and weight reduction, combustion optimization and fuel quality, and airframe drag reduction through aerodynamic improvements. A large amount of work has also been dedicated to engine system integration.

Engine system integration includes all studies seeking optimal engine component integration efficiency, engine control techniques, thermal management techniques and power off-take techniques. Different power extraction scenarios have shown different impact on engine performance, and the analysis of their influence on fuel consumption as

well as on engine component behavior has been made easier with the availability of high fidelity simulation codes such as NPSS.

I.1 Numerical Propulsion System Simulation program.

The traditional serial design process method for complex aerospace systems involves mainly three phases. Starting from a request for proposal, the conceptual design phase seeks to determine the requirements that drive the design, to define the geometry of the system, and the technologies that should be used. Then, the system configuration is frozen in the preliminary phase to develop a test and analytical data base, to design major components, and to estimate actual product cost. Finally, is the detail design phase where actual design pieces are built and design tooling and fabrication processes are initiated.

Although the design wheel offers an opportunity to improve design through an iterative process, redesign or modification of one system components for a specific disciplinary consideration can cause not only redesign of other components but also cycle time to be longer than what is scheduled and fabrication cost to increase. With ever-increasing market demands of reduced acquisition cost and highly efficient systems, engineers can no longer rely on the traditional serial design process. Therefore, new design tools are needed to take into consideration simultaneous modification or redesign of system components, multidisciplinary team communication, and communication between teams of different phase levels of the design process.

To overcome these challenges, U.S. government agencies such as NASA Glenn Research center has joined with industrial partners such as General Electric (GE) and

Rolls Royce corporation to develop the Numerical Propulsion System Simulation. (NPSS).

Comment [a1]: use AIAA 2004-371 as refer

I.2 Problem Statment

The intent of this research dissertation is mainly to study the influence of different power extraction techniques on jet engine performance in terms of thrust, thrust specific fuel consumption (TSFC), HPT inlet temperature, and turbomachinery components operating lines. Furthermore, engine performance sensitivities to HPT inlet temperature maximum value will be studied. The simulation cases will be run at on-design point cruise conditions; however results sensitivity to the flight condition altitudes will also be made.

I.3 Research Focus.

The research will proceed as follows: a thorough survey of the literature will summarize the current state-of-the-art of engine performance improvement in fuel consumption. This concept will be implemented with other power extraction techniques to see their feasibility and influence on engine performance. The remainder of this document is arranged as follows: Chapter II provides a summary of previous work described in the literature in the field gas turbine propulsion performance analysis when power is extracted to feed aircraft accessories, while Chapter III describes the simulation setup and methodology and Chapter V summarizes the results and analysis of this research simulations.

II. Background and Previous Work

II.1 Turbofan Engine Cycle Analysis and Performance

For all types of gas turbine engine (turbojet, turbofan, turboprop, and ramjet), the gas generator has basically the same component configuration with a turbine, compressor and a burner at its heart. The main function of the gas generator is to convert an air-fuel mixture into a hot gas having a high pressure and temperature. For a turbojet engine as an example, thrust is produced by a nozzle that mainly converts hot gas at the turbine exit into high momentum flow while the work extracted by the turbine is used to drive engine compressor stages and the fan.

The primary measures of the engine's overall performance are the engine uninstalled thrust (F) and the thrust specific fuel consumption (TSFC). The uninstalled thrust for a non-mixed turbofan engine is basically the combination of the thrust produced by the bypass flow stream and the thrust produced by the main stream (core). Thrust produced by the fan, thrust produced by the engine core and the overall uninstalled thrust is given by Eqs. 1, 2 and 3 respectively.

$$F_c = \frac{1}{g_c}(\dot{m}_9 V_9 - \dot{m}_c V_0) + A_9(P_9 - P_0) \tag{1}$$

$$F_F = \frac{1}{g_c}\dot{m}_F(V_{19} - V_0) + A_{19}(P_{19} - P_0) \tag{2}$$

$$F = F_c + F_F \tag{3}$$

These expressions of thrust are widely used for gas turbine engine cycle analysis. However, non dimensional expressions are used for parametric engine design or when

engine performance is required to be compared with available equivalent results. For that reason, specific thrust, S_F, is introduced and will be used in our engine simulation results.

$$S_F = \frac{g_c F}{\dot{m}_o a_o} \tag{4}$$

where,

$$\dot{m}_o = \dot{m}_F + \dot{m}_c \tag{5}$$

Thrust specific fuel consumption (TSFC) is a crucial engine performance parameter that reflects engine fuel consumption and allows an easy comparison of one engine fuel consumption efficiency among various engines. The TSFC is given by Eq. 6.

$$TSFC = \frac{\dot{m}_f}{F} \tag{6}$$

Some other parameters that are also useful in judging engine performance are the thermal efficiency, the propulsive efficiency and the overall engine efficiency. The thermal efficiency characterizes the net energy output extracted (shaft work) from the engine divided by the available thermal energy (fuel). The propulsive efficiency defines the ratio between the engine power output and the power being used to run the aircraft. The overall performance of a propulsion system is given by the combination between thermal and propulsive efficiencies. Those performance parameters are given by Eqs. 7-9

$$\eta_{TH} = \frac{\dot{w}_{out}}{\dot{Q}_{in}} \tag{7}$$

$$\eta_P = \frac{T.V_0}{\dot{w}_{out}} \tag{8}$$

$$\eta_O = \eta_P \eta_{TH} \tag{9}$$

For a valid engine cycle point, engine parameters must allow at least conservation of mass, conservation of momentum, and conservation of energy across any engine

component. Based on the turbofan engine cycle model of Figure II-1, the conservation of mass throughout the engine different stations is depicted by Eqs. 10-21.

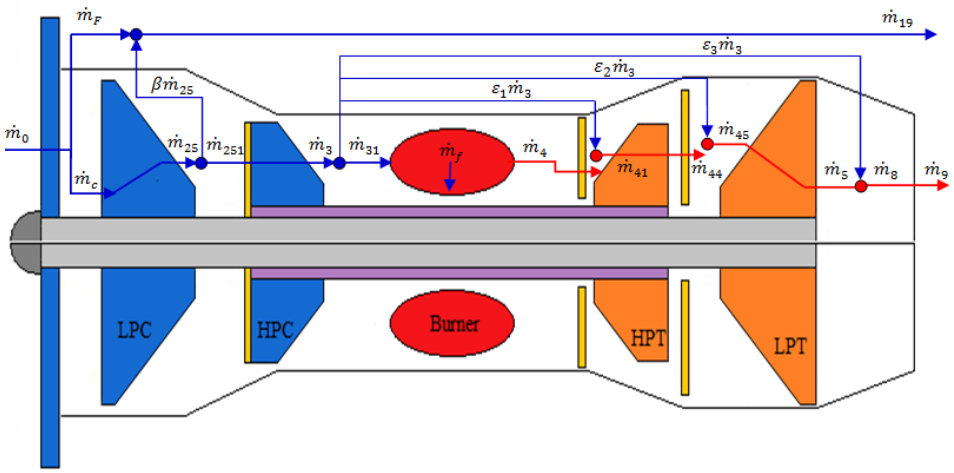

Figure II.1. High bypass turbofan engine sketch

$$\dot{m}_0 = \dot{m}_c + \dot{m}_F = (1+\alpha)\dot{m}_c \tag{10}$$

$$\dot{m}_{25} = \dot{m}_c \tag{11}$$

$$\dot{m}_{251} = (1-\beta)\dot{m}_c \tag{12}$$

$$\dot{m}_3 = \dot{m}_{251} \tag{13}$$

$$\dot{m}_{31} = (1-\beta)(1-\varepsilon_1-\varepsilon_2-\varepsilon_3)\dot{m}_c \tag{14}$$

$$\dot{m}_4 = (1+f)(1-\beta)(1-\varepsilon_1-\varepsilon_2-\varepsilon_3)\dot{m}_c \tag{15}$$

$$\dot{m}_{41} = (1-\beta)\{1-\varepsilon_2-\varepsilon_3+f(1-\varepsilon_1-\varepsilon_2-\varepsilon_3)\}\dot{m}_c \tag{16}$$

$$\dot{m}_{44} = \dot{m}_{41} \tag{17}$$

$$\dot{m}_{45} = (1-\beta)\{1-\varepsilon_3+f(1-\varepsilon_1-\varepsilon_2-\varepsilon_3)\}\dot{m}_c \tag{18}$$

$$\dot{m}_5 = \dot{m}_{45} \tag{19}$$

$$\dot{m}_8 = (1-\beta)\{1+f(1-\varepsilon_1-\varepsilon_2-\varepsilon_3)\}\dot{m}_c \tag{20}$$

$$\dot{m}_9 = \dot{m}_8 \tag{21}$$

The conservation of energy across engine components basically concerns power or torque balance between elements mounted on each shaft element. In fact, at steady state regime the low pressure turbine produced work should balance the work needed to turn the low pressure compressor, fan and loads consuming work. Also, the high pressure turbine produced work should equate to the amount of work used to drive the high pressure compressor and other possible loads such as electric power generators.

For the engine model of Figure II.1, the torque conservation across engine shafts is governed by Eqs. 22 and 23.

$$Trq_{LP} = Trq_{LPT} - \left(Trq_{LPC} + Trq_{Fan} + \frac{\sum_{LP} PX}{N}\right) = 0 \tag{22}$$

$$Trq_{HP} = Trq_{HPT} - \left(Trq_{HPC} + \frac{\sum_{HP} PX}{N}\right) = 0 \tag{23}$$

In transient mode, the HP spool shaft and LP spool shaft mechanical speeds are governed by Eqs. 24 and 25.

$$\frac{dN_{HP}}{dt} = {}^{60}/_{2\pi} \cdot \frac{Trq_{HP}}{\sum I_{HP}} \tag{24}$$

$$\frac{dN_{LP}}{dt} = {}^{60}/_{2\pi} \cdot \frac{Trq_{LP}}{\sum I_{LP}} \tag{25}$$

Engine components total property ratios are presented in Table II-1.

Table II-1. Engine components total pressure and enthalpy ratios

	Total pressure Ratio	Total enthalpy ratio
Fan	$\pi_F = \frac{P_{t13}}{P_{t2}}$	$\tau_F = \frac{h_{t13}}{h_{t2}}$
Low Pressure compressor (LPC)	$\pi_{LPC} = \frac{P_{t25}}{P_{t2}}$	$\tau_{LPC} = \frac{h_{t25}}{h_{t2}}$
High Pressure compressor (HPC)	$\pi_{HPC} = \frac{P_{t3}}{P_{t251}}$	$\tau_{HPC} = \frac{h_{t3}}{h_{t251}}$
Burner	$\pi_B = \frac{P_{t4}}{P_{t31}}$	$\tau_B = \frac{h_4}{h_{t31}}$
High pressure turbine (HPT)	$\pi_{HPT} = \frac{P_{t44}}{P_{t41}}$	$\tau_{HPT} = \frac{h_{t44}}{h_{t41}}$
Low pressure turbine (LPT)	$\pi_{LPT} = \frac{P_{t5}}{P_{t45}}$	$\tau_{LPT} = \frac{h_{t5}}{h_{t45}}$
Exhaust nozzle	$\pi_n = \frac{P_{t9}}{P_{t8}}$	$\tau_n = \frac{h_{t9}}{h_{t8}}$

II.2 Power Extraction Techniques

Secondary power systems (SPS) are the power distributed around the engine and airframe systems and not used for propulsion. On most aircraft SPS are distributed in three forms:

Comment [a2]: use Israel.pdf as reference

- Electric (avionics, lights, instruments, entertainment).
- Hydraulics (primary and secondary flight controls, landing gears, brakes, steering, doors, and other actuation functions).
- Bleed air or pneumatics (environmental control system (ECS), cabin pressurization, engine cowl and wing ice protection, engine starting).

Past and current turbofan and turbojet engines are capable of supplying SPS in two forms:

- Shaft power is extracted from the engine's high pressure shaft to drive a gearbox on which SPS components are mounted in addition to the engine's fuel and oil pumps.
- Hot, pressurized air is extracted from the engine's compressors.

II.3 NPSS Modeling And Simulation

The performance of an air breathing engine basically depends on engine components performance as well as operational conditions. In NPSS, the engine model consists of a set of connected elements in cascade. For a double spool turbofan, elements typically include a fan, a low pressure compressor, a high pressure compressor, a burner, a high pressure turbine, low pressure turbine and a nozzle. Engine NPSS model operational conditions includes flight conditions such as Mach number, altitude and day type, and effects basically are the engine mechanical loads and bleeding air. Figure II.2 presents a typical NPSS model of a double spool turbofan engine. Detailed information about the model is given in section III.1.

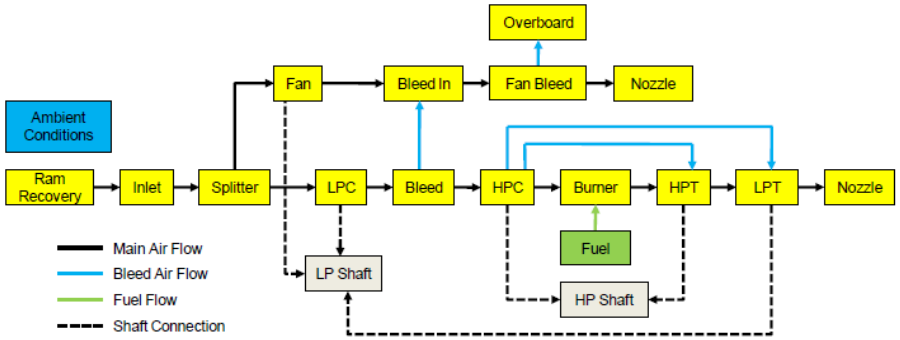

Figure II.2. An example of NPSS engine block model

The NPSS solver converges the engine model cycle set of equations into a balanced state in terms of mass, momentum and energy conservation. The engine cycle basically consists of an interconnected set of equations that need to be solved simultaneously to obtain a consistent solution. To do that, the solver starts with a guess of the model input parameters. Depending on the solver running mode (on-design or off-design) and on the user requirements, one or more of the input parameters is varied progressively in an iterative approach until the final solution tolerance is met. In NPSS language the varied parameter is called the independent variable while the equation to be solved is called the dependent condition or variable. The number of independent variables must equate to the number of dependent conditions to be satisfied. Figure II.3 represents the NPSS solver basic solution method.

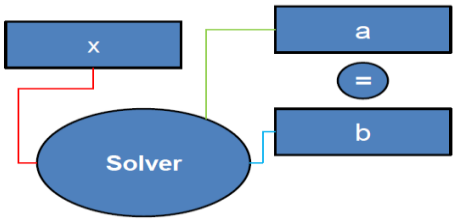

Figure II.3. NPSS solver sketch

Consider Eq. 26. In this equation example, the variable x represents the independent variable while the equation itself represents the dependent condition. Commonly, in NPSS programming the equation is called the dependent variable. As given this equation cannot be solved explicitly. However, we can get a numeric solution very close to the real one just by varying the independent variable until the error between the equation left hand side and right side within the tolerance order of magnitude.

$$\underbrace{4\boldsymbol{x}^2 - 7.25}_{\textbf{eq\_lhs}} = \underbrace{\boldsymbol{x}^3 + sin(\tfrac{\boldsymbol{x}}{4})}_{\textbf{eq\_rhs}} \tag{26}$$

Basically, the absolute error of Eq. 27 is used to monitor the accuracy of the solution regarding how far it is from the tolerance criteria. However, for a system of equations each equation could have a different order of magnitude. Therefore, using the absolute error tolerance could lead to inaccurate solution for all the equations.

$$error = eq\_lhs - eq\_rhs \tag{27}$$

For example, say that the user is targeting a value of thrust specific fuel consumption and burner exit temperature given by Eqs. 28 and 29. If the absolute error tolerance is set to be of the order of 0.5, we would have 65.4% error on *TSFC* and 0.01% error on T_{t41} when the solver is converged. In a case where the tolerance is chosen to be

very small, on the order of 0.01, to minimize the error on the TSFC calculated value, the convergence of the solver for the solution of Eq. 26 will be difficult to obtain and may take many iterations. In fact, the independent variable that affects the value of T_{t41} is the fuel-air ratio. When this variable is varied the change in T_{t41} value could be more than the error tolerance (0.001). Therefore, no matter how little the independent variable is changed, the absolute error of Eq. 27 will more than the tolerance, and the convergence will not be obtained.

$$TSFC = 0.765\ lbm/(hr.lbf) \tag{28}$$

$$T_{t41} = 3200\ R \tag{29}$$

For that reason, the fractional or non dimensional error tolerance is used and a reasonable error value for all orders of magnitude is obtained regardless of how many equations the system has. The non-dimensional error is given by Eq. 30. In NPSS, the user has the option to set the type of tolerance desired.

$$errorNonDim = (eq_{lhs} - eq_{rhs})/eq_{ref} \tag{30}$$

Independently from the type of error tolerance used, the NPSS solver algorithm varies x so that error converges to the tolerance (theoretically zero). In fact, for each independent variable x value, the solver algorithm calculates the slope of the error and looks for the value of x at which the error is more closer to zero. This is done iteratively until convergence is achieved. Figure II.4 shows the solver algorithm process.

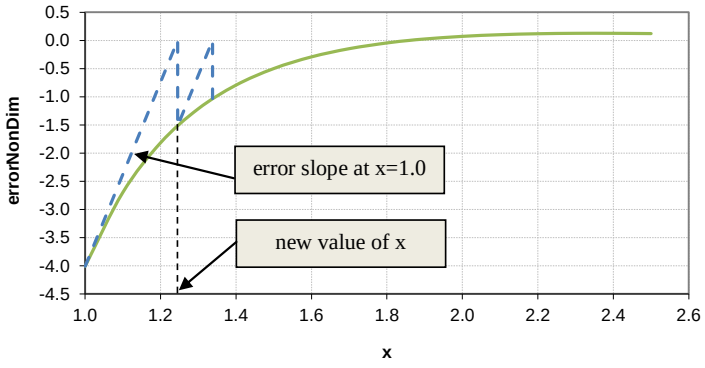

Figure II.4. NPSS Solver solution searching method

Different solver algorithms within NPSS could be used to track how errors are refined. The basic method is Newton's method, but other methods such as Modified and Quasi Newton's methods are also used. The difference among those algorithms is the way the slope is calculated and the new value of x is obtained. This can affect the time an iteration could take and, therefore, how fast the convergence is. When dealing with a system of equations, such as in our simulation case, a matrix of slopes is obtained instead and updated at each iteration. This matrix is called the Jacobian.

The NPSS solver setup basically comprises three major steps for the simulation to run correctly. First, engine model elements have to be executed in the correct order. By default, the solver executes elements in the order of their alignment. However, if they are not aligned in the correct order, the user must set the correct execution order using the *executionSequence* function. The next step is to set the solver running mode. In fact, two running mode options are possible within NPSS. At on-design running mode, the solver uses the on-design parameter values and flight conditions to perform engine performance

necessary calculations. At off-design running mode, flight conditions in terms and Mach number and altitude are different from what are at on-design mode. Therefore, to find a consistent cycle solution at off-design mode, the solver varies more independent variables than in the case of on-design mode. Initial values of these independent variables are obtained when on-design mode is run, and only then can the off-design mode can be run. Finally, to complete the solver setup, the global function *autoSolverSetup* is called to set the default solver to the appropriate independent and dependent variables. These variables can also be set manually. Tables II-2 and II-3 show default independent and dependent variables for on-design and off-design modes for a high bypass, double spool, turbofan engine respectively.

Table II-2. NPSS on-design and off-design default independent parameters

Solver Mode	Solver Independents	
	Solver Variable	Description
On-Design	TrbH.S_map.ind_parmMap	HPT map Parameter (used by efficiency subelement to read the map)
	TrbL.S_map.ind_parmMap	LPT map Parameter (used by efficiency subelement to read the map)
Off-design	InletStart.ind_W	Inlet air flow at design
	SpltFan.ind_BPR	Bypass ratio
	CmpFsec.S_map.ind_RlineMap	Fan map R line
	CmpL.S_map.ind_RlineMap	LPC map R line
	CmpL.S_map.ind_RlineMap	HPC map R line
	TrbH.S_map.ind_parmMap	Same as On-design
	TrbL.S_map.ind_parmMap	Same as On-design
	ShH.ind_Nmech	High pressure shaft rpm
	ShL.ind_Nmech	Low pressure shaft rpm

When the model is run in NPSS, thermodynamic calculations are performed for each element in cascade. Besides the on-design parameters values, the NPSS solver

requires additional parameter values, such as entry thermodynamic conditions and mass flow rate, to perform necessary calculations within an element. These parameter values are made available for use within an element through element connection ports (fluid input port of the element and output port of the previous joint element) as illustrated by Figure II.5. The high pressure compressor (HPC) element of Figure II.5 has its design point parameters of pressure ratio, efficiency and corrected shaft speed defined as $\pi_{HPC} = 10.0$, $\eta_{HPC} = 0.8522$, and $N_c = 1.0$ consecutively. However, to perform thermodynamic calculations of pressure ratio for example, the input mass flow rate, W, is required. For the example illustrated in Figure II.5, compressor input mass flow rate is obtained from the bleed element fluid output port.

Table II-3. NPSS on-design and off-design default dependent conditions

Solver Mode	Solver dependents	
	Solver Variable	Description
Off-design	NozSec.dep_Area	Error between flow into the nozzle and nozzle flow based on area and PR
	CmpL.S_map.dep_errWc	Error between flow into the compressor and compressor map flow based on Rline and Nc
	Trb.S_map.dep_errWp	Error between flow into the turbine And turbine map flow based on PR and Nc
	Sh.integrate_Nmech	torque/work required for all compressors and loads torque/work delivered by all turbines

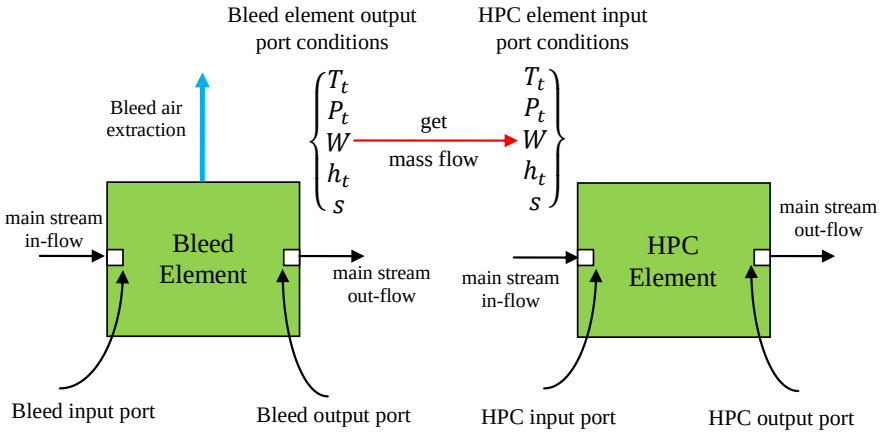

Figure II.5. NPSS elements ports connection

The engine is sized by the choice of the design point parameter values. Design point is commonly specified in terms of operating Mach number and altitude while design point parameters typically include the overall pressure ratio, OPR, fan pressure ratio, low pressure compressor pressure ratio, high pressure compressor pressure ratio, bypass ratio, BPR, and high pressure turbine inlet temperature, T_{t4}. The design point parameter values make together an engine consistent cycle solution that preserves conservation of mass, momentum, and energy. However, due to the large number of parameters used when the engine is modeled in NPSS, some mismatches could be generated. These inconsistencies can be solved internally within the element level or within the model level by varying one independent parameter until a valid cycle solution is obtained.

In on-design mode, the NPSS solver uses on-design parameters to compute the on-design cycle solution. In off-design mode, the solver requires the engine maps in order that a valid engine cycle solution can be obtained. The performance of engine

turbomachinery components are typically given in a map format, commonly known as engine maps. Figure II.6 is a typical example of an engine compressor map. Compressor maps present pressure ratio and efficiency as functions of the compressor inlet corrected mass flow and the shaft corrected speed. These two parameters are given by Eqs. 31 and 32.

$$\dot{m}_c = \dot{m}\sqrt{\theta}/_{\delta} \tag{31}$$

$$N_c = N/_{\sqrt{\theta}} \tag{32}$$

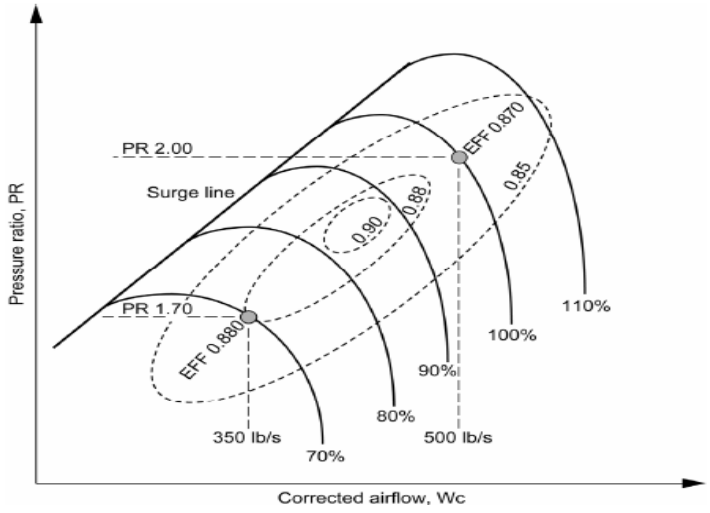

Figure II.6. Typical engine compressor map

II.4 Previous Work On Power Extraction Effects On Air Breathing Engine Performance.

A. Yuhas and R. Ray [1] investigated an experimental test of the effects of bleed air extraction on the thrust level of the F404-GE-400 turbofan engine. The experiment was part of a program initiated by NASA to study the maneuverability of high performance aircraft at high angle of attack. The problem was that the aircraft maneuverability at high angle of attack degrades as control surface effectiveness is degraded. Extensive experimental tests in a wind tunnel were conducted and had shown that bleed air from engine is an adequate control method that meets mass flow requirements over an extended time for the pneumatic forebody flow control (FFC). However, bleeding air form the high pressure compressor decreases engine performance in term of thrust. A ground experiment was conducted to investigate engine performance when bleed air was extracted from the high pressure compressor exit. The F/A-18 aircraft was tied to a ground platform to measure installed thrust while bleed air was extracted at three engine power settings: 92% high pressure spool shaft speed, military power and maximum power. Measured thrust was shown to be reduced linearly with bleed air extracted for the three different power settings. Higher thrust losses were shown for military and maximum power.

Ronald and Sijmen [2] studied the performance of a commercial aircraft gas turbine engine when bleed air was tapped-off from the HPC exit or equivalent power was extracted from the LP spool shaft. The extracted bleed air was measured in kg/s while the electric power extracted from shaft was measured in kW. Therefore, a relationship

between the two measurements was developed to compute the bleed air equivalent energy. To do that, the authors used an exergy based calculation. As mentioned in [2], a flow stream specific exergy is given by:

$$\varepsilon_x = \underbrace{(h - h_{ref})}_{1st\ thermodynamic\ law\ term} + \underbrace{T_{ref}(s - s_{ref})}_{2nd\ thermodynamic\ law\ term} \quad (33)$$

By definition, exergy is the combination of the 1st and 2nd law of thermodynamics. With that combination, the conservation of energy (basically 1st law of thermodynamics) is constrained by the conservation of entropy (basically the 2nd law of thermodynamics). In other words, when a process produces an amount of energy, not of all the energy released will be useful. In fact, some of it will be dissipated in chaotic motion of particles within the flow stream. This energy is known as the "dead" energy. Consequently, if energy calculations do not take into consideration the lost energy while computing bleed air equivalent power, comparison with the engine performance when equivalent electrical power is extracted from the low pressure spool shaft will not be valid.

John H. Doty, José A.Camberos and Davis J.Moorhouse [3,4], further investigated the utility of exergy based focus over energy based focus for aerospace applications. The performance of a modeled turbojet engine was investigated for one or more of its components performance (duct heat exchange; for example) modified using energy or exergy based calculations. It turned out that when using an energy alone focus, physically non-possible operating conditions were allowed. However, exergy based analysis provided the only possible physical combinations of operating conditions.

Ronald and Sijmen [2] used the CF6-80E1 engine which powers the medium size A300-200 aircraft. For the purpose of the simulation, they modeled the engine using their own simulation code known as the Gas turbine Simulation Program (GSP).

Initially, they studied the bleed air and electrical power extraction effect on engine performance at two different simulation settings: constant fuel flow rate setting and constant high pressure turbine inlet temperature. Then, they investigated the effect of exergy extraction strategies on the engine performance over a typical commercial aircraft mission.

The first simulation setup was done keeping fuel flow constant while a bleed air fraction of 1% to 10% of the main stream was removed at the high pressure compressor exit. This bleed air fraction was intended to power aircraft accessories such as ECS. However, it was not mentioned how bleed air is removed away from the engine. The equivalent amount of exergy was computed and then extracted from the low pressure spool shaft. The electrical power extracted from the LP spool shaft was to power different accessories on board the aircraft such as electronic navigation devices. For each power extraction technique, the engine performance in terms of thrust and thrust specific fuel consumption was plotted against the equivalent amount of exergy extracted. For both setting methods, constant fuel flow and constant high pressure turbine inlet temperature, exergy extraction in bleed air was more efficient than exergy extraction in low pressure spool shaft power for both thrust and thrust specific fuel consumption at on-design point (see Figure II.7).

For both power off-take strategies, effects on engine compressor operating conditions were also investigated. Actually, when air bleed fraction is increased, the rotational speed of HP and LP compressors decreased. However, when equivalent shaft power was extracted from LP spool shaft, the rotational speed of the HP spool shaft increased at constant fuel flow setting. In fact, in that case, both compressor pressure ratios and rotational speeds increased. Obviously, bleed air off-take is safer until a more detailed investigation of power off-take on compressor operating conditions can be performed.

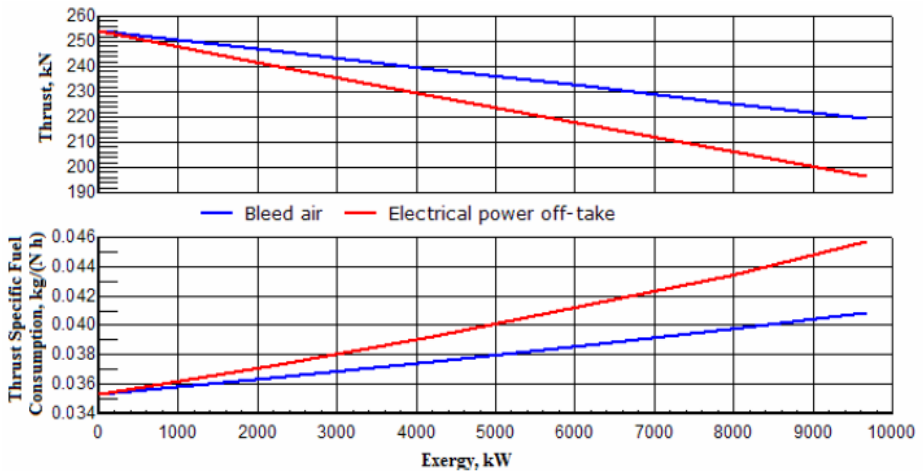

Figure II.7. Effect of 0 to 7500 kW Exergy off-take in the form of bleed air or electrical energy, on the thrust and specific fuel consumption, assuming constant fuel flow

The second part of the simulation of the effect of exergy extraction strategy on engine performance was carried out on a typical commercial aircraft mission. The profile of the mission is shown in Figure II.8.

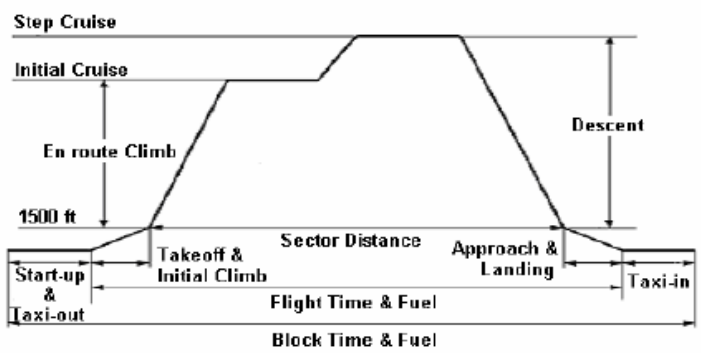

Figure II.8. Typical commercial aircraft mission profile legs

For this simulation, bleed air mass flow of 4.73 kg/s was tapped off at the end of the HPC and half way from HPC. The equivalent amount of exergy was extracted from the shaft power of the low pressure spool. For comparison between bled air off-take and electrical energy off-take, the simulation was set so that both cases have the same cruise thrust. Therefore, in order to preserve the same cruise thrust for both techniques, different power settings were used.

Again, the bleed air off-take was shown to be more efficient, in terms of TSFC, over the complete flight cycle notably during cruise and ground idling legs (see Figure II.8). It was noted that the electrically powered systems would need to be 10-25% more efficient than bleed air powered systems in order for the equivalent power extraction technique to be more efficient than the bleed air extraction technique.

The investigation of an electrically powered environmental control system ECS and bleed air powered ECS over the entire flight profile showed that the electrically powered ECS is more efficient than pneumatically powered ones in terms of thrust

specific fuel consumption. However, this efficiency is only due to the efficiency of the ECS system itself and not to electric power extraction from the LPC shaft.

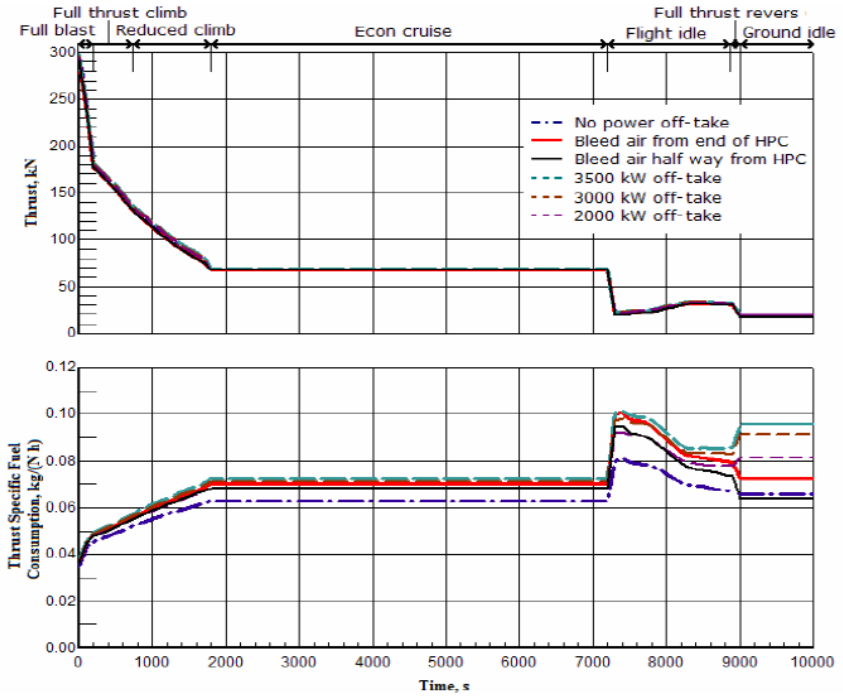

Figure II.9. Effect of bleeding air (4.73 kg/s) and electrical power off-take on the performance of the CF6-80E1 over the complete flight cycle

In conclusion, the simulations of Ronald and Sijmen [2] showed that the bleed air extraction is more efficient than electric power extraction, in terms of thrust and thrust specific fuel consumption. In fact, engine performance degrades more when equivalent power is extracted from LPC shaft than bleeding air from HPC exit. However, fuel saving depends on the efficiency of the subsystems when powered by one or another technique. This favorably gave advantage to electrically powered ECSs over bleed air powered ECS. This simulation [2] gave an insight into the effect of some power extraction techniques on

the performance of the engine, but for several reasons the results given should be considered more qualitatively than quantitatively. First, the engine modeling on the turbine simulation program (GSP), the accuracy of the solver, the fidelity of the simulation were not explained. Second, the over-estimated results of exergy extraction (up to 8,000 kW) are more than typical power requirement for commercial aircraft systems. For example, the B787 commercial aircraft subsystems require about 1000 kW of power generation.

III. Methodology and Simulation Setup

III.1 Engine NPSS Model

Fig III-1 depicts the high bypass turbofan engine NPSS block diagram model. Each block represents an NPSS engine element. The blue colored blocks together represent the engine low temperature section, which includes both compressors, the fan, and the secondary nozzle. The red colored elements represent the engine hot gas section, which comprises the combustor, both turbines and the primary nozzle.

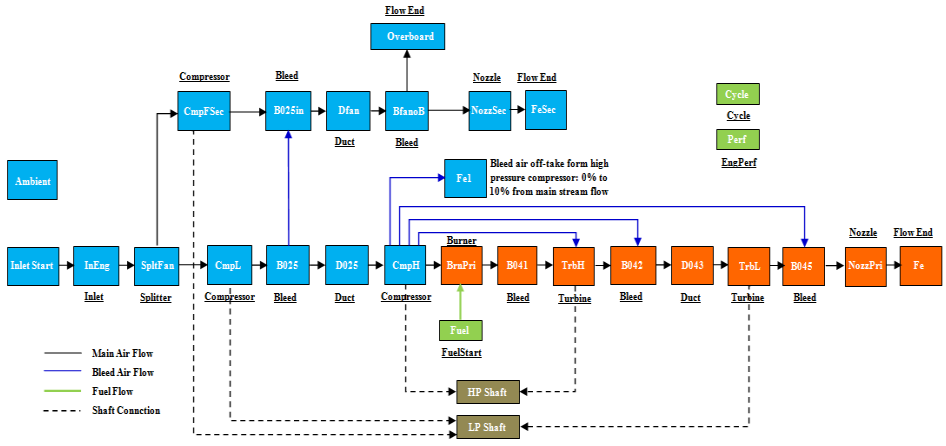

Figure III.1. High bypass turbofan baseline engine model with NPSS

The ambient element, despite not being an effective engine element, represents the engine operational condition for computing the flight condition properties based on a set of input parameters, of which most critical are the flight Mach number and altitude.

Table III-1. Ambient flight condition parameters

Mach number	Altitude (ft)	Day Type	dTs
0.80	35,000.0	Ambient	0.0

Based on those flight conditions, the inlet start element (InletStart) defines the starting conditions for flow into the engine inlet (InEng). The starting conditions include the inlet airflow and corrected airflow. The inlet cannot start the flow, and for that reason there must be an upstream element, which is the inlet start element (InletStart), to start the flow. Provided with the flow, the inlet element calculates the performance of a standard inlet such as capture area and ram drag. Table III-2 summarizes on-design parameter of the InletStart and Inlet elements.

Table III-2. InletStart and Inlet design input parameters

	W_In (lbm/s)	eRamBase
InletStart	100.0	
Inlet (InEng)		0.995

The Split element is used for a bypass turbofan engine to split the free stream flow into the main stream and the bypass stream based on the bypass ratio (BPR), which is set at the design point. The core stream passes through the low pressure compressor, the high pressure compressor and the engine hot section.

Both the CmpL and the CmpH type elements perform compressor performance calculations in terms of pressure ratio, temperature ratio and efficiency. In on-design mode, those performance parameters are set as input parameters. In off-design mode, compressor performance is obtained from the compressor maps, which are implemented

as a subelement of the compressor element. Table III-3 presents main compressors and turbines parameter values at on-design mode. These parameters mainly include adiabatic efficiency, pressure ratio and corrected speed.

The area separating the two compressors (LPC and HPC) is modeled as a duct element. Duct elements are used throughout the engine to model pressure losses between engine elements. D025, D043, and Dfan are duct elements which model pressure loss between the two compressors, the two engine turbines, and fan and bypass stream nozzle, respectively. The user can set the pressure loss parameter so the element duct performs an adiabatic pressure loss calculation.

Table III-3. Engine compressors and turbines design point main parameters

	PR	effDes	RlineMap	NcDes	parmMapDes
CmpFSec	1.5	0.8589	2.0	1.0	
CmpL	3.0	0.8720	2.0	1.0	
CmpH	10.0	0.8522	2.0	1.0	
TrbH		0.8900		100.0	4.975
TrbL		0.8770		100.0	4.271

The model of Figure III.1 includes three bleed types: surge bleed air is extracted from the low pressure compressor exit (B025), cooling bleed air mainly for the high pressure turbine (TrbH, B042, B045), is extracted from the high pressure compressor exit, and aircraft bleed powered accessory systems (Fel, for example) can be extracted from both compressors. For the bleed off-take from the main stream, three main parameters have to be specified: the fraction of the compressor inlet flow that is extracted as bleed (fracBldW), the fraction of the total pressure rise in the bleed flow (fracBldP), and the fraction of the total enthalpy rise in the bleed flow (fracBldWork). The user

should notice that only compressor and bleed elements are bleed sources, while the turbine and bleed can be bleed sinks. All of the bleeds parameter settings are summarized in Table III-4.

Table III-4. Engine cooling bleed air parameters

	fracBldW	fracBldP	fracBldWork	Pfract	diaPump
CmpH → TrbH	10.0%	100.0%	100.0%	100.0%	0
CmpH → B042	4.0%	100.0%	100.0%		
CmpH → B045	1.0%	50.0%	50.0%		

For a bypass turbofan, two engine nozzle elements are modeled: the main stream nozzle (NozzPri) and the secondary stream nozzle (NozzSec). The amount of flow that can pass through the nozzle is determined by the fixed throat area, which is calculated at the design point. FlowEnd elements (Fe, Fel, FeSec) are designed to terminate the flow.

III.2 Engine Performance And Limitations

The NPSS engine model execution file can be put in one sole file. However, from an organizational point of view and for simulation robustness, the use of different file types, each having a specific task, is recommended. Commonly, we use the model file, the user function file, the control file, the viewer file, the case file and the run file. In the model file, elements are defined, ports are connected, on-design point engine element parameters are set, and turbomachinery maps for the off-design mode are included. The function file defines a user customized function to do a specific task. In the function file example of Section 6 of Appendix-A, three user functions were created. One function was created to make an engine envelope search. The second function is used to obtain engine maximum performance in terms of thrust, TSFC and mass flow at military power.

The last function purpose is to run the engine throttle hooks. The control file (see Appendix-A, Section 3) gathers specific engine parameter values for fan mechanical shaft speed and high pressure turbine inlet temperature to limit their maximum values. In the viewer file (see Appendix-A, Section 3), targeted engine performance parameters and simulation case monitoring parameters are set to be viewed. The main engine parameters include the engine net thrust, TSFC, and HPT inlet temperature. The simulation monitoring parameters are day running type, the thermodynamic package used and the engine throttle setting. The case file contains all cases to be simulated. The case file example of section 4 of Appendix-A includes an on-design point case simulation and eleven HPC exit bleed air off-take cases. The run file is the model execution file where all file types mentioned previously are included using a special NPSS command (see Appendix-A, section 2) . The day type option, the thermodynamic package and the throttle setting values can also be set up in the run file.

Figures III.2-III.4 show baseline engine maximum thrust, thrust specific fuel consumption and mass flow over several flight conditions of Mach number and altitude. To obtain those curves, the engine throttle was set to its maximum value. This is done by setting the power lever angle to 50 (CONTROL.PLACS = 50) which corresponds to maximum fan mechanical speed. The altitude and range of Mach number were set on the maxPerf function (see Appendix-A, section 6) and the simulation was run.

At cruise design point, (altitude = 35 kft, M = 0.8) all engine performance parameters clearly indicate a small size turbofan engine. Actually, at that flight condition the engine can only produce 1,849 pounds of thrust. Although the engine can be scaled to

be adapted to common commercial aircraft mission performance requirements, by scaling the inlet mass flow at the design point, we will use this engine model for the simulation since the engine size does not affect the simulation trends (see Chapter IV).

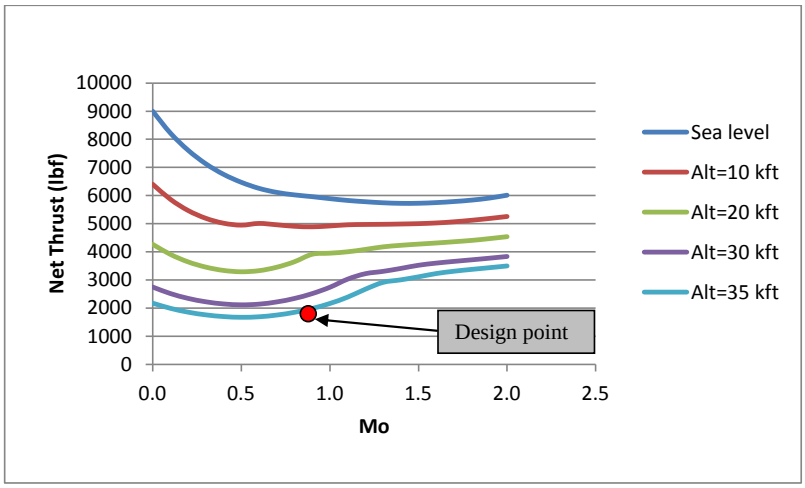

Figure III.2. Baseline engine thrust at military power

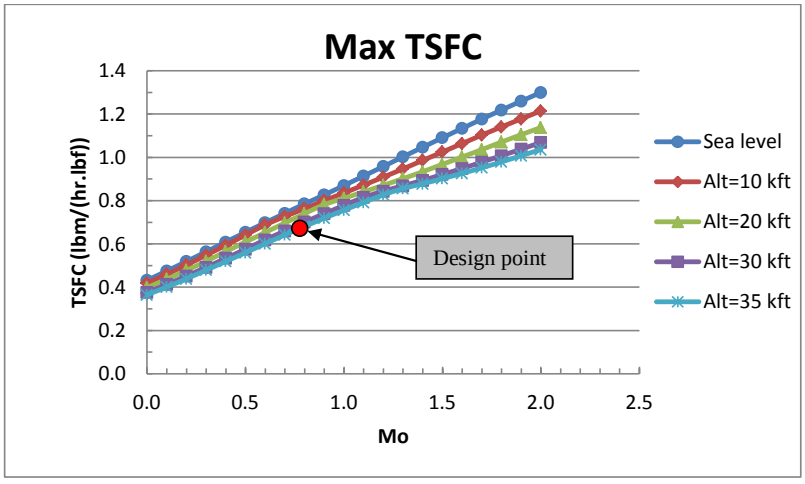

Figure III.3. Baseline engine TSFC at military power

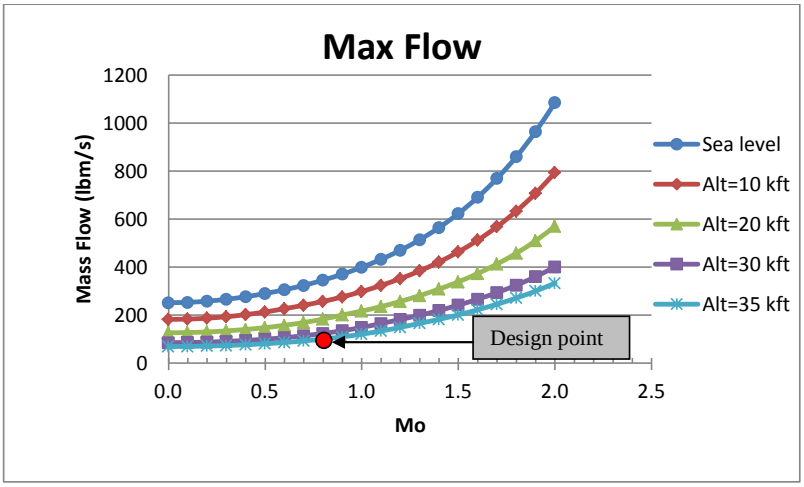

Figure III.4. Baseline engine air mass flow at military power

III.3 Running Cases

As mentioned previously, four main simulation cases were performed during this study. The first two cases included extraction of bleed air from both engine compressor exits. The other two cases extract an equivalent power from both spool shafts. Each of these two cases was run at two different settings. One setting kept fuel flow constant. The other setting maintained a constant high pressure turbine inlet temperature. The fuel flow parameter is not by default considered as a solver independent variable (see Table II-2 for the list of the NPSS by default independent variables). Therefore, for off-design mode, at each case running, no extra setting is needed to run the simulation at constant fuel flow. In fact, the solver will maintain the fuel flow rate the same as at the design point. However, to run the cases at constant HPT entry temperature, the fuel flow parameter is added to the solver as an independent variable and the HPT inlet temperature is added as

a dependent variable while fixing its targeted value. In this case, the solver will vary the fuel flow until the air fuel mixture combustion (which is a simple energy balance with a specified combustion efficiency) produces the targeted maximum high pressure turbine inlet temperature. For reference, all the cases considered in this simulation are summarized in Table III-5.

Table III-5. Simulation cases description

Case Name	Description	T_{t4}(R^o)	Fuel Flow (lbm/s)
Case 1	Bleed air extraction from HPC exit	Non constant	0.35
Case 2	Power extraction from HP spool shaft	Non constant	0.35
Case 3	Bleed air extraction from LPC exit	Non constant	0.35
Case 4	Power extraction from LP spool shaft	Non constant	0.35
Case 5	Bleed air extraction from HPC exit	2770.0	Non constant
Case 6	Power extraction from HP spool shaft	2770.0	Non constant
Case 7	Bleed air extraction from LPC exit	2770.0	Non constant
Case 8	Power extraction from LP spool shaft	2770.0	Non constant

Based on the NPSS default element and tools, there are two options for power extraction from engine LP and HP spool shafts. The first option includes adding a load element on the targeted spool shaft. When linked to the shaft, the load element consumes shaft power by applying a torque load on it. The amount of power extracted is proportional to the product of shaft speed and the load torque as illustrated by Eq. 34:

$$P = trq_{load} * N_{mech} * NR \tag{34}$$

The advantage of the shaft load applying power extraction option is that it takes into account the electrical power generator characteristics. In fact, practically, not all of the power extracted mechanically from the shaft will be transformed into useful electrical

energy. Actually, useful power depends on the connection gear efficiency and other parameters. A disadvantage, however, is the difficulty to find in the open data bases typical technical characteristics of an air breathing engine electrical power generator that matches the engine size of the current study.

The second option for spool shaft power extraction is to directly use the governing shaft power calculation as defined by Eqs. 22-23. The shaft element HPX variable is the targeted parameter and represents the amount of horsepower extracted from the shaft. Although this method does not really take into account the efficiency of the load element, it is simple to use and makes the study independent of the technology used, giving the results a broad interpretation. For that reason, the second power off-take option was used.

III.4 Turbomachinery Map Scaling

Gas turbine engine turbomachinery maps basically depend on blade geometry characteristics. Therefore, maps used to test small engine prototypes can be scaled and used for a real sized model. The maps included within the NPSS engine model do not necessarily match the engine modeled size, but the user can choose a customized engine size for a particular purpose by setting the inlet air mass flow at the design point. Consequently, in off-design mode, compressors and turbine maps must be scaled to perform the necessary engine performance calculations. The NPSS solver automatically scales the engine maps by varying some independent variables. For compressor maps, the solver varies RlineMap parameter until the mismatch between flow going into the

compressor and the flow map based on Rline and N_c converges to zero. For turbine maps, the solver varies the parmMap independent parameter until the mismatch between flow going into the turbine and the map flow based on *PR* and N_c is minimized.

Comment [a3]: don't forget to add those variables on the list of varaible names a the begining of the thesis

Although map scaling is automated within the NPSS solver, scaled maps have to be obtained manually, at least for the fan and compressor maps, in order that different simulation cases operating lines can be plotted and the compressor behavior for each case can be revealed. The compressor maps parameters to be scaled are the compressor corrected entry mass flow, pressure ratio and efficiency. The scaling is performed using the design point and according to Eqs. 35-37

$$W_c\ scale\ factor = \frac{W_c\ desired}{W_c\ unscaled} \tag{35}$$

$$PR\ scale\ factor = \frac{PR\ desired-1}{PR\ unscaled-1} \tag{36}$$

$$\eta\ scale\ factor = \frac{\eta\ desired}{\eta\ unscaled} \tag{37}$$

Table III-6. Engine map scaling factors

	Desired (on-design)					Unscaled (map)			Scale factors		
	PR	eff	W_c(lbm/s)	Rline	N_c	PR	Eff	W_c(lbm/s)	PR	eff	W_c
Fan	1.5	0.86	216	2.0	1.0	1.67	0.87	1441.7	0.73	0.98	0.15
LPC	3.0	0.87	43.2	2.0	1.0	1.71	0.90	187.7	2.81	0.97	0.23
HPC	10.0	0.85	17.2	2.0	1.0	24.1	0.82	123.58	0.39	1.03	0.14

Comment [a4]: don't forget to tweak maps the same as in results and analysis chapter, do the same thing for maps on Appendix-C

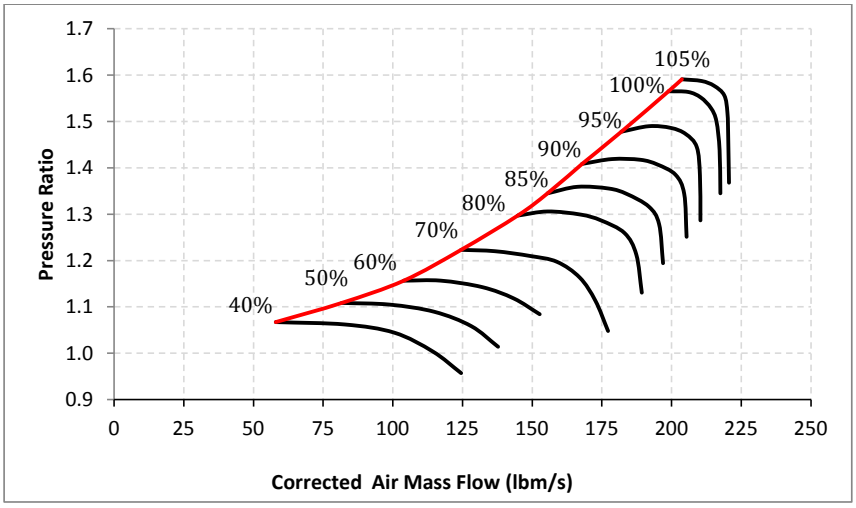

Figure III.5. Engine fan scaled map

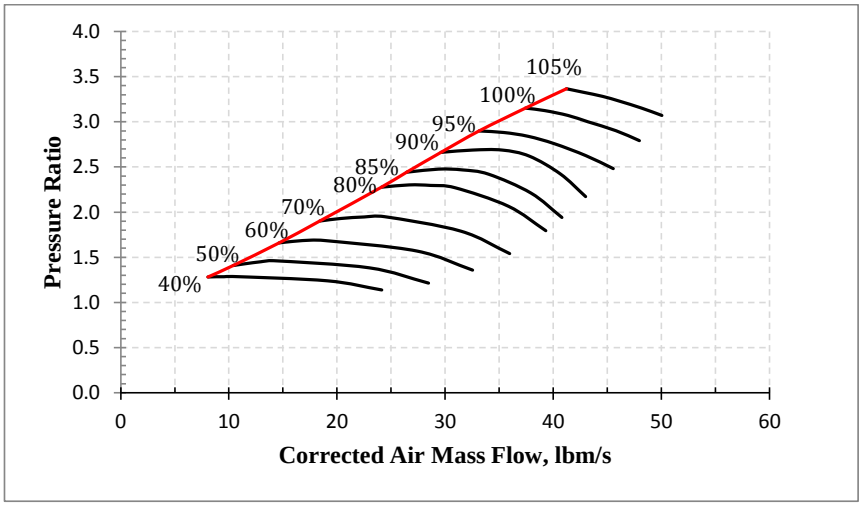

Figure III.6. Engine low pressure compressor scaled map

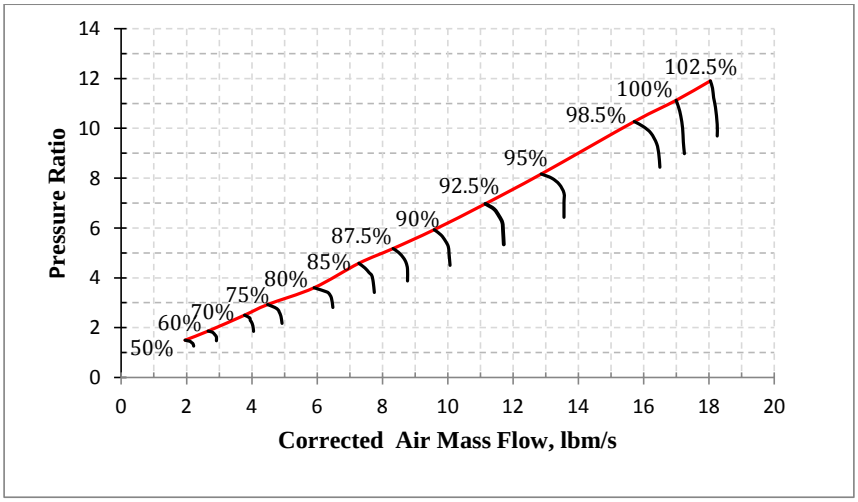

Figure III.7. Engine high pressure compressor scaled map

IV. Simulation Results and Analysis

IV.1 Engine Thrust And TSFC Performance at Design Point

The first step in the simulation was to determine the bleed air off-take equivalent power for the bleed extraction cases (cases 1, 3, 5 and 7). After setting each for up to 10 % bleed air fraction from the corresponding compressor exit, the solution yields bleed air mass flow rate and specific exergy as well as engine performance. The exergy is obtained by applying Eq. 33; however, some unit manipulations from British unit system to International unit system were necessary since power extraction from engine shafts is by default in horsepower. Table IV-1 summarizes equivalent horsepower of bleed air off-take for cases 1, 3, 5 and 7. The obtained equivalent power is then extracted from engine shafts to simulate cases 2, 4, 6, and 8.

Table IV-1. Bleed air off-take cases equivalent extracted horsepower

	Equivalent power (hp)			
Bleed Fraction	Case 1	Case 3	Case 5	Case 7
0.0%	0.00	0.00	0.00	0.00
1.0%	41.65	32.06	41.39	31.85
2.0%	83.16	64.42	81.61	63.96
3.0%	124.27	97.08	121.16	96.14
4.0%	165.26	130.04	159.54	128.58
5.0%	206.10	163.49	197.28	161.07
6.0%	246.58	197.02	233.66	193.79
7.0%	286.71	231.04	269.41	226.54
8.0%	327.01	265.50	304.14	259.31
9.0%	366.72	300.06	337.54	292.31
10.0%	406.14	335.03	369.66	325.49

Equivalent horsepower of Table IV-1 is plotted against bleed air fraction up to 10% in Figure IV.1. It can be seen that equivalent power from the HPC exit (case 1 and 5), at both settings of constant fuel flow rate and constant HPT inlet temperature, is higher than when bleed air is extracted from the LPC exit (case 3 and 7). As can be inferred from Eq. 38, this is basically due to bleed air mass flow rate since the specific exergy is the same for both HPC and LPC exit bleed air cases. In fact, when bleed air is tapped off, the engine inlet swallows a larger air mass flow when done from the HPC exit rather than from the LPC exit, especially at high bleed air fraction rates. This gives HPC exit air bleed off-take an advantage over LPC bleed air off take since less bleed air fraction will be needed to produce the same desired equivalent power. However, this result is tentative until the impact of air bleed effects on engine performance is shown later.

$$E_x = \dot{m}_b * \varepsilon_x \tag{38}$$

Equivalent power values for constant HPT inlet temperature setting cases (case 5 and 7) are less than those for corresponding constant fuel flow setting cases (case 1 and 3). In fact, fixing the HPT inlet temperature to maximum value limits engine performance.

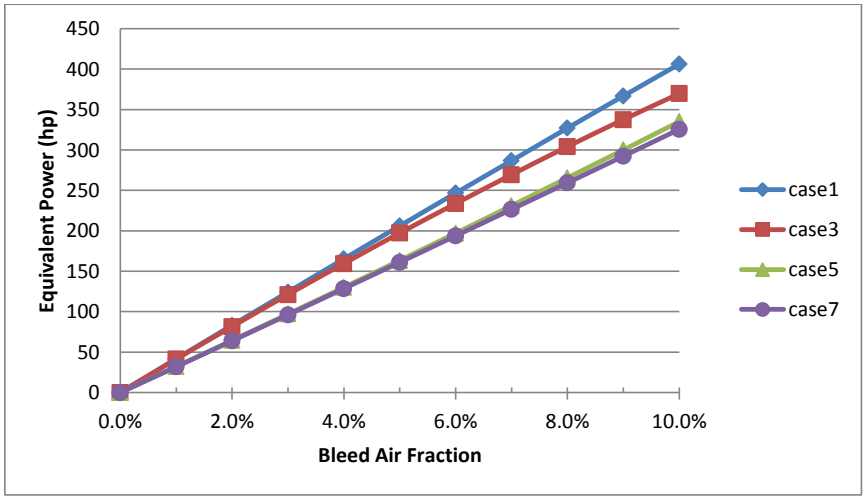

Figure IV.1. Compared bleed air off-take equivalent horsepower for bleed air off take simulation cases at standard day

For each case, at each bleed air fraction or equivalent power extraction value, engine performance including thrust, TSFC, T_{t4} and other parameters are gathered. Engine thrust and TSFC values are obtained from the engine performance element (Perf, see Figure III.1). Other performance parameters such as T_{t4} are obtained from engine station state parameters. All parameters of concern are gathered together on the same viewer and presented as in the viewer output file example of Appendix-A.

Comment [a5]: don't forget to put caseout and viewout results file in one Appendix

For the results to be more broad and used for comparison with other equivalent simulations, non dimensional engine performance parameters are given. A coefficient of equivalent power extraction, *CTO*, is used to reflect how much power is extracted from engine in bleed air or in shaft power. Similarly, specific thrust coefficient, S_{F_n}, is used to indicate engine non-dimensional thrust performance. Therefore, using *CTO* and S_{F_n}, a

fair comparison of other simulation results using different engine sizes, could be very likely to take place. Results using dimensional parameters for the specific engine of the current study are presented in Appendix-C as reference. The non-dimensional CTO and S_{F_n} parameters are defined according to Eqs. 39 and 40 respectively.

$$CTO = \frac{\dot{m}_b * \varepsilon_x}{\dot{m}_o * h_o} \tag{39}$$

$$S_{F_n} = \frac{F_n * g_c}{\dot{m}_o * a_o} \tag{40}$$

The on-design value of the HPT inlet temperature, T_{t4} = 2270 R, is used for simulation cases run at constant T_{t4} setting. Although maximum allowable turbine inlet temperature is greater (T_{t4} = 3206 R), the choice of the constant temperature does not affect the result trends since cases with the same settings were compared to each other. Moreover, constant T_{t4} setting simulation cases were only intended to show the impact of the maximum allowable HPT inlet temperature on engine performance when bleed air from compressor exits or power is directly extracted from shafts.

For a standard day, the effect of compressor exits bleed air off-take and equivalent power extraction from engine shafts on engine performance are plotted against the coefficient of equivalent power extraction, CTO. At constant fuel flow rate setting, as illustrated by Figure IV.2, engine specific thrust performance of HPC exit air bleeding (case1) is less efficient among all cases. Based on obtained equivalent power of Table IV-1, HPC exit bleed air was expected to be more efficient than LPC exit air bleed. The reason is likely to be the cooling bleed air from HPC exit. In fact, at the HPC exit not

only is power generation bleed air extracted but in addition 15 % of bleed air used for turbine cooling. While it is true that cooling bleed air is reintroduced into the main stream, that air could produce much more energy if burned in the combustor, which would affect the engine cycle and improve engine thrust.

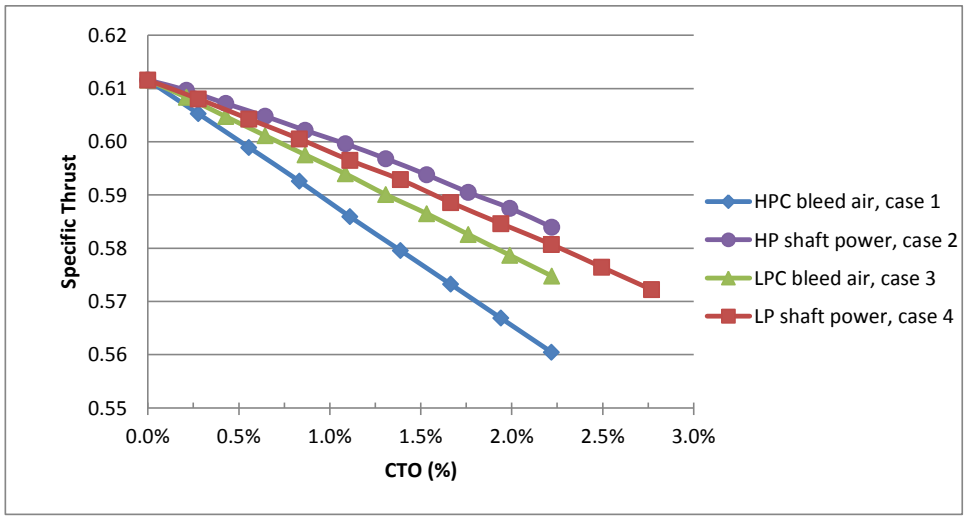

Figure IV.2. Specific thrust versus CTO: mf = 0.35 lbm/s, Mach = 0.8, Alt = 35 kft on a standard day

Based on the results of Figure IV.2, HP shaft power extraction has better specific thrust than air bleeding from LPC exit or equivalent power extraction from LP shaft cases. However, the specific thrust results should not be considered alone without taking into account the inlet mass flow. In fact, according to Eq. 39, thrust is a function of the inlet mass flow. A look at Figure IV.3 shows that engine inlet mass flow percentage increment, relative to on-design inlet mass flow rate, increases up to 0.5% when bleeding air from LPC exit, while it decreases down to -2.3%, -2.5% and -4.7% when bleeding air

from HPC exit, extracting power from HP and LP shafts respectively. Based on that, for the engine of the current study, at constant fuel flow setting, HP spool shaft power extraction (case 2) and LPC exit bleed air off-take (case 3) nearly have the same thrust efficiency at low power extraction levels, when CTO is less than 1% (see Figure C.1; Appendix-C). However, when coefficient of power extraction is increased above 1%, bleeding air from LPC exit is more efficient, in terms of thrust, than extracting an equivalent power from HP spool shaft. In fact, at maximum CTO (2.25%), case 3 is 1.38% more efficient than case 2 in terms of thrust.

The thrust specific fuel consumption, according to Figure IV.4, follows the same trends as those of thrust. This is predictable since fuel flow is constant. The effect of the coefficient of power extraction on the HPT inlet temperature is investigated too. Figure IV.5 represents the percentage of increment in HPT inlet temperature, relative to T_{t4} value at design point, due to power extraction coefficient up to 2.5%. Obviously, cases 2, 3 and 4 have nearly the same T_{t4} value for up to 1.0% of CTO power extraction. However, when CTO is high enough, case 2 HPT inlet temperature increases by 4% compared to 2% for cases 3 and 4. Air bleeding from HPC exit case has the highest HPT turbine inlet temperature reaching about 6.8% at 2.5% CTO power extraction. The increment in HPT inlet temperature when power is extracted, in bleed air or in shaft power, could be detrimental to the engine performance in terms of thrust and thrust specific fuel consumption especially when maximum allowable T_{t4} is low. This is the subject of the study of the different cases effect on engine performance at constant HPT inlet temperature.

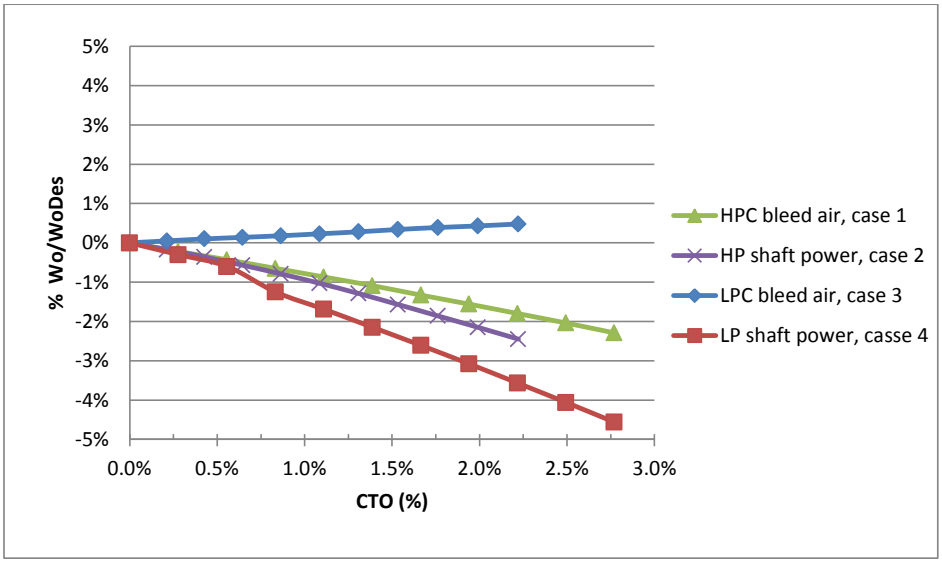

Figure IV.3 Inlet mass flow rate increment percentage versus CTO: mf = 0.35 lbm/s, Mach = 0.8, Alt = 35 kft on a standard day

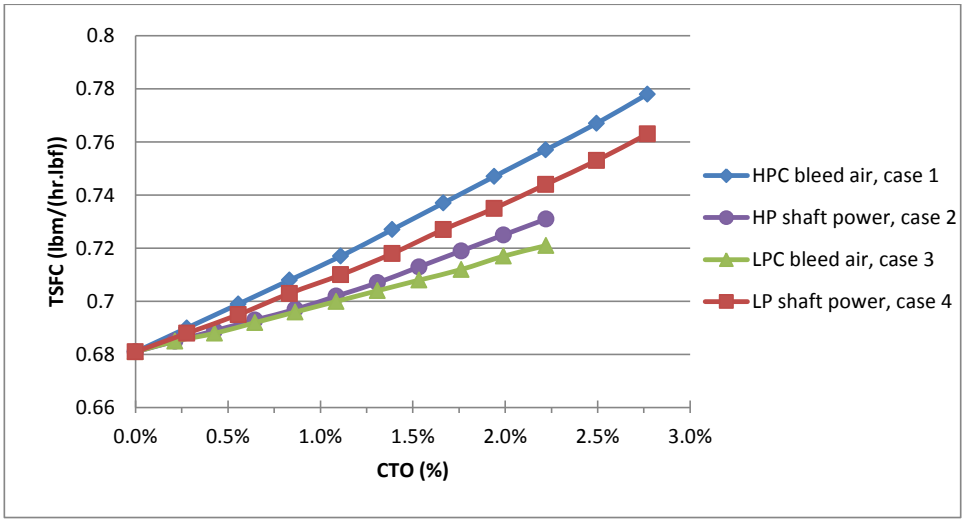

Figure IV.4. TSFC versus CTO: mf = 0.35 lbm/s, Mach = 0.8, Alt = 35 kft on a standard day

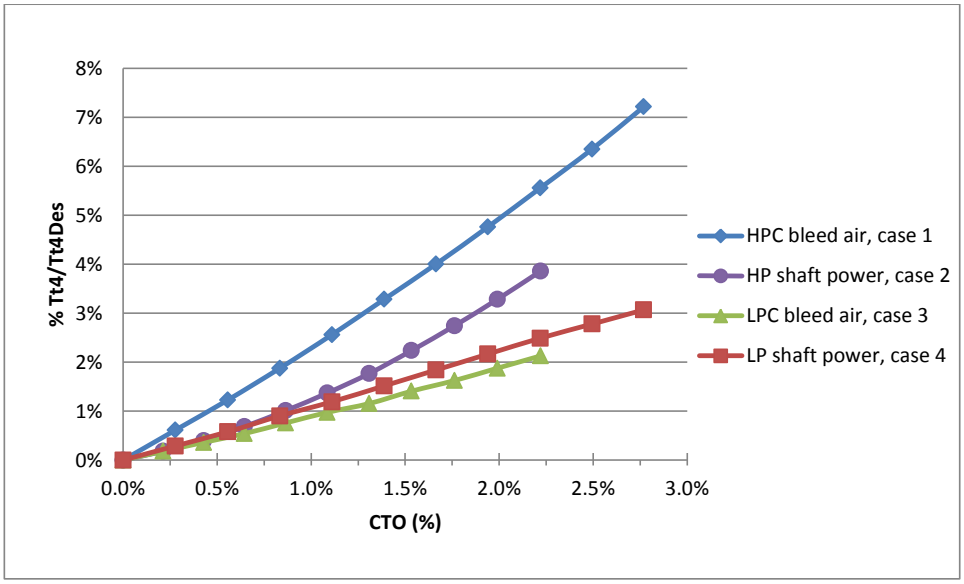

Figure IV.5. % Tt4 increment versus CTO: mf = 0.35 lbm/s, Mach = 0.8, Alt = 35 kft on a standard day

At constant temperature setting, the HPT inlet temperature kept constant at on-design value (T_{t4} = 2770 R) while bleeding air from the LPC or HPC exits, or extracting equivalent power from the LP or HP spool shafts. According to Figure IV.6 specific thrust of cases 6,7 and 8 is nearly the same for up to 1% CTO power extraction. When maximum allowable T_{t4} value is fixed, specific thrust performance degraded (Figure IV.6), especially for cases where high burner exit temperature were released. In fact, specific thrust of case 1 decreased from 0.56 to 0.52 at 2.25% CTO power extraction. This means a loss of about 300 lbf of thrust for the engine of the current study (see Figure C.4; Appendix-C). It can be noticed from Figure IV.7, at constant HPT inlet temperature, that when bleeding air from the LPC, the inlet mass flow approximately maintain the same value as on-design point. However, cases 5, 6, and 8 have more decrease in inlet

mass flow than at constant fuel flow setting, reaching -6.75% at 2.5% CTO power extraction.

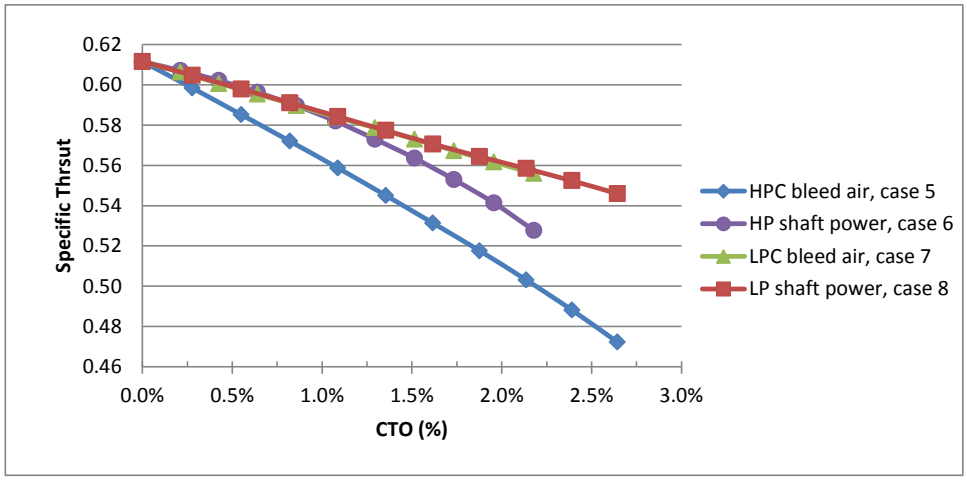

Figure IV.6. Specific thrust versus CTO: Tt4 = 2770 R, Mach = 0.8, Alt = 35 kft on a standard day

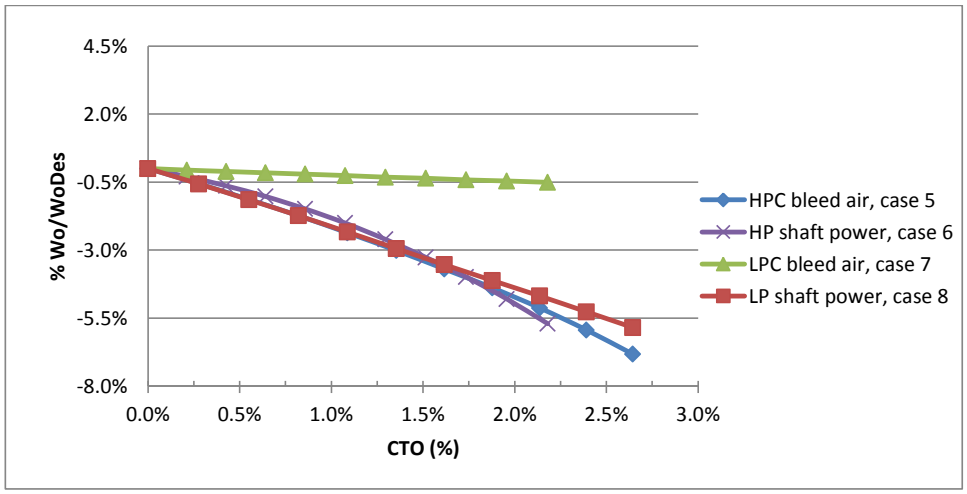

Figure IV.7. Inlet mass flow rate increment percentage versus CTO: Tt4 = 2770 R, Mach = 0.8, Alt = 35 kft on a standard day

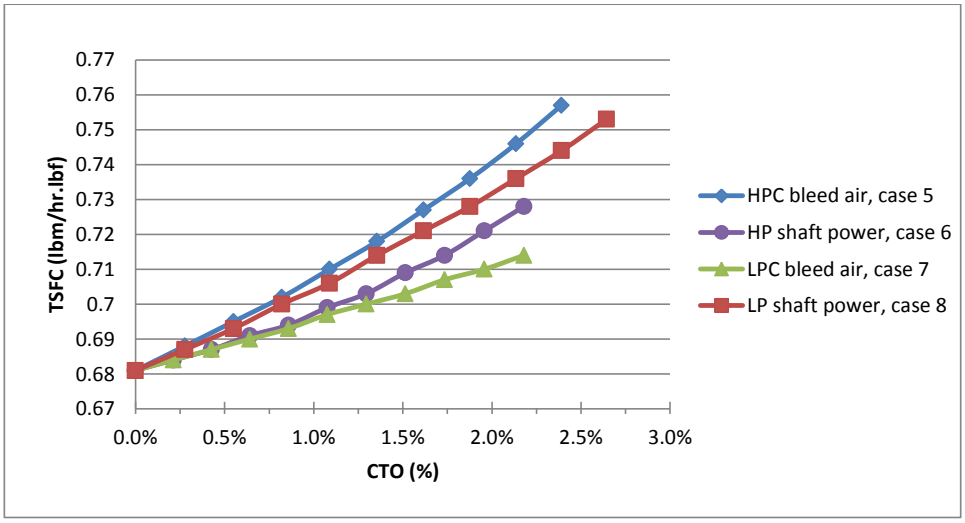

Figure IV.8. TSFC versus CTO: Tt4 = 2770 R, Mach = 0.8, Alt = 35 kft on a standard day

The different simulation cases were also run on a cold day (see Figure B.1 and B.2; Appendix-B) setting. Qualitatively, engine performance of specific thrust and thrust specific fuel consumption, of Figures IV.9 and IV.10 respectively, have the same trends as for a standard day discussed previously. However, some quantitative results need to be mentioned. Specific thrust and thrust specific fuel consumption are about 1% more efficient than for the standard day case. For example, at constant temperature setting, HP shaft power extraction is more efficient than in standard day for both thrust and thrust specific fuel consumption.

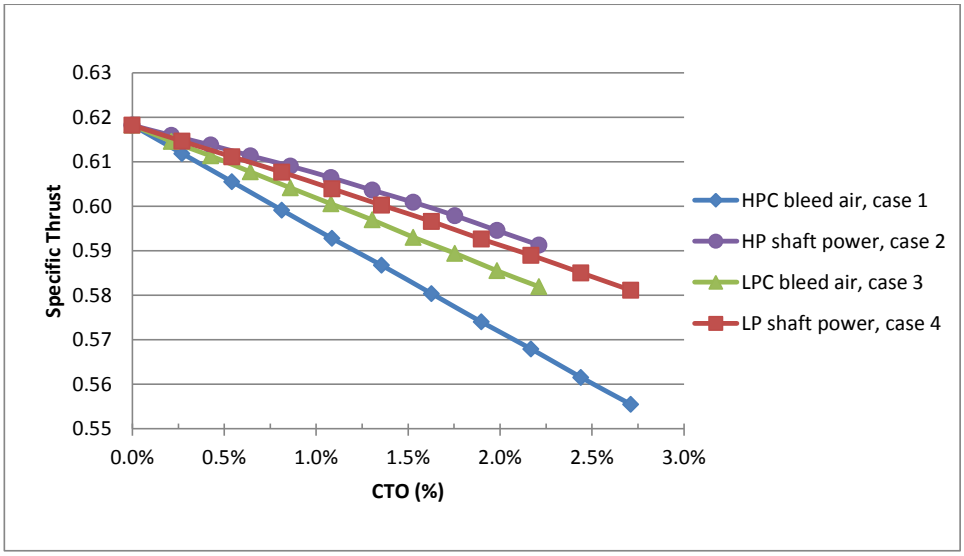

Figure IV.9. Specific thrust versus CTO: mf = 0.35 lbm/s, Mach = 0.8, Alt = 35 kft on a cold day

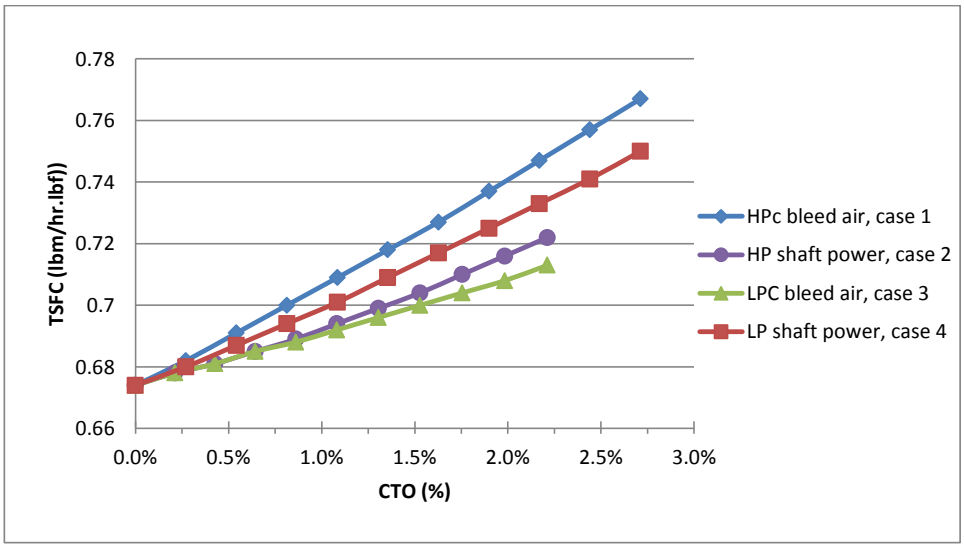

Figure IV.10. TSFC versus CTO: mf = 0.35 lbm/s, Mach = 0.8, Alt = 35 kft on a cold day

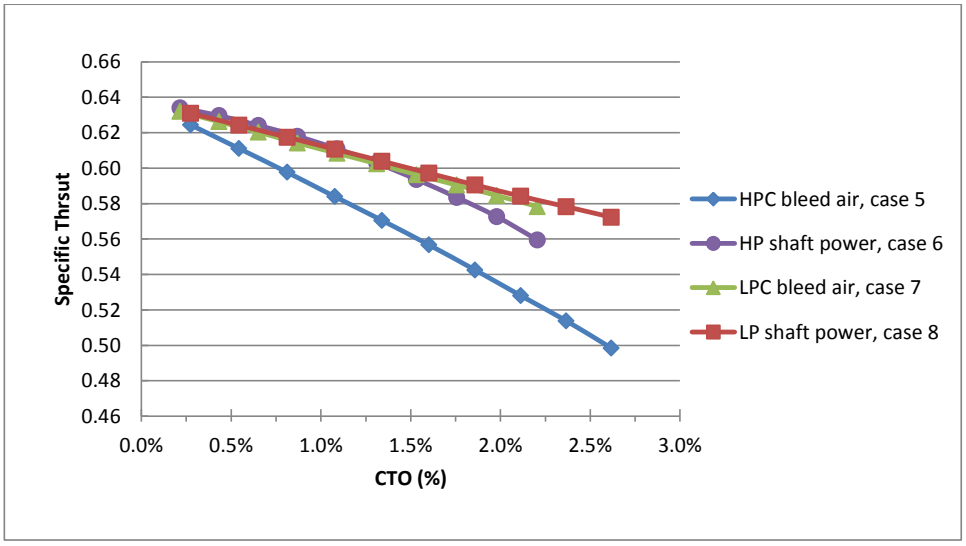

Figure IV.11. Specific thrust versus CTO: Tt4 = 2770 R, Mach = 0.8, Alt = 35 kft on a cold day

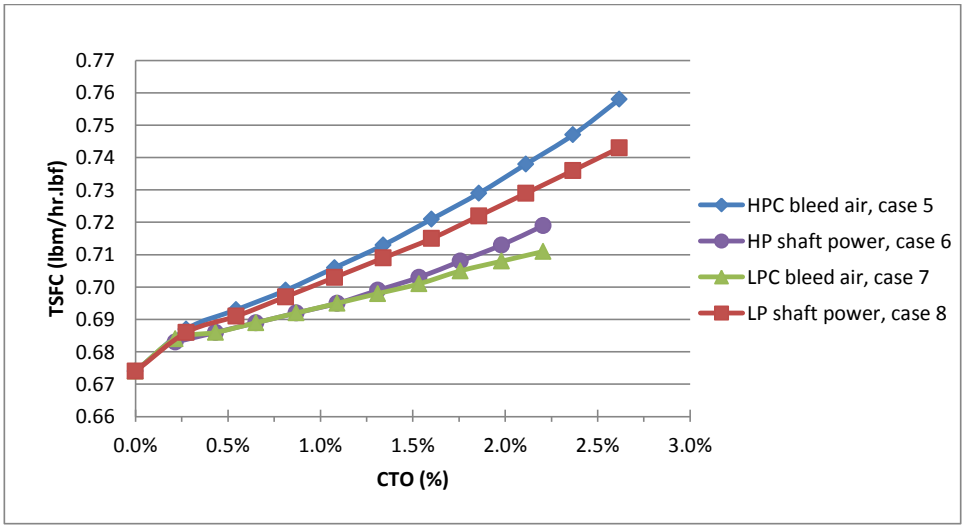

Figure IV.12. TSFC versus CTO: Tt4 = 2770 R, Mach = 0.8, Alt = 35 kft on a cold day

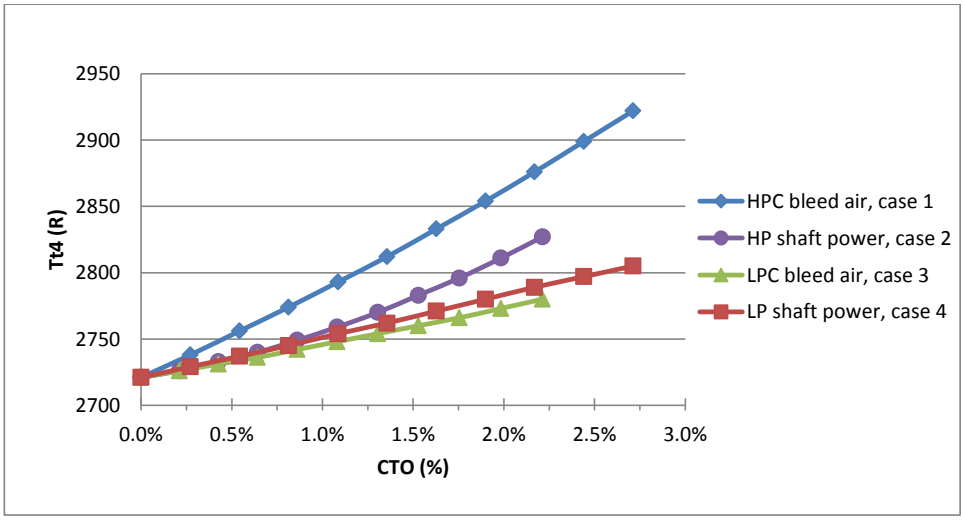

Figure IV.13. Tt4 versus CTO: mf = 0.35 lbm/s, Mach = 0.8, Alt = 35 kft on a cold day

All power extraction techniques effects on engine performance were simulated for a hot day (see Figure B.1 and B.2; Appendix-B) also. The overall trends match with those obtained for the standard and cold day cases, as depicted by Figures IV.14-IV.18. However, in comparison with standard day cases, there is about 2.2% performance degradation shift in terms of thrust and thrust specific fuel consumption. At constant temperature setting, HP shaft power extraction is less efficient than in a standard day for both thrust and thrust specific fuel consumption.

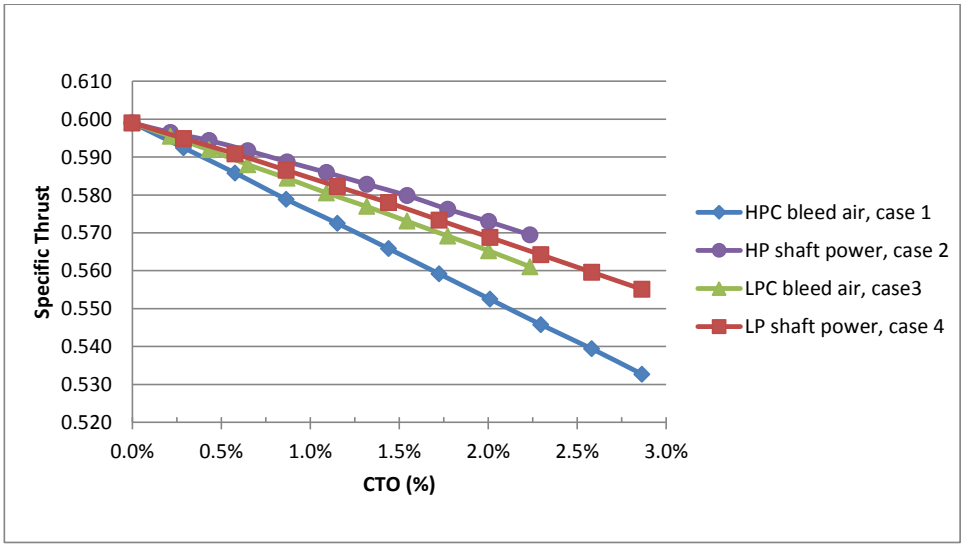

Figure IV.14. Specific thrust versus CTO: mf = 0.35 lbm/s, Mach = 0.8, Alt = 35 kft on a hot day

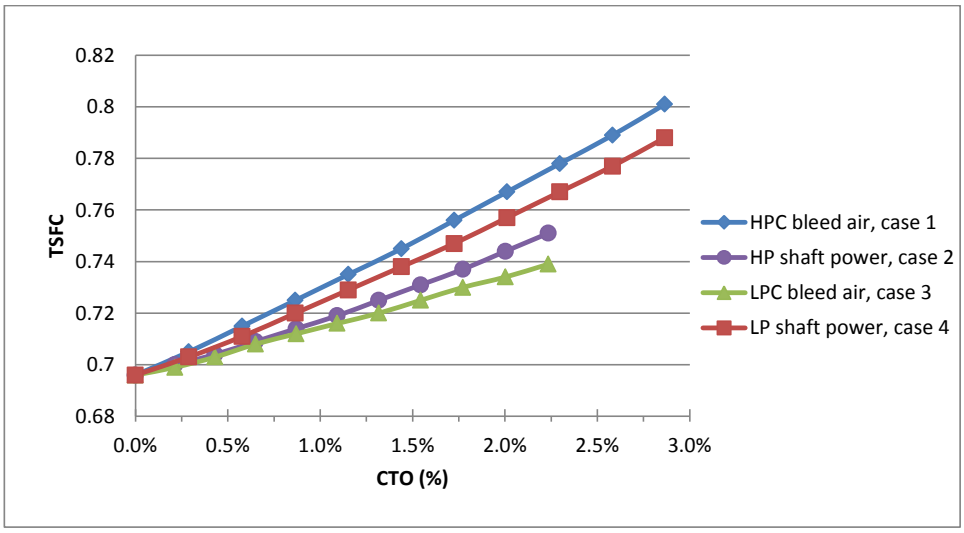

Figure IV.15. TSFC versus CTO: mf = 0.35 lbm/s, Mach = 0.8, Alt = 35 kft on a hot day

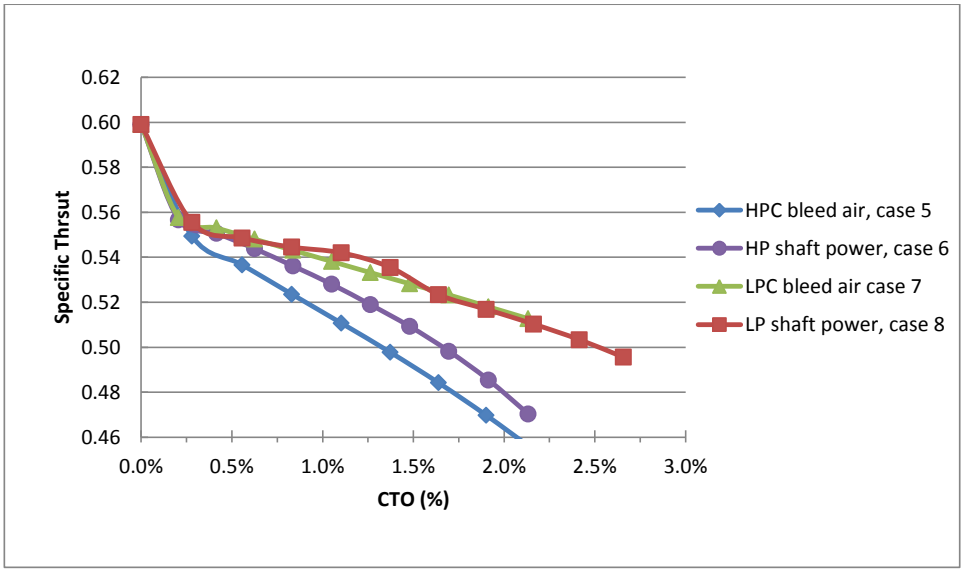

Figure IV.16. Specific thrust versus CTO: Tt4 = 2770 R, Mach = 0.8, Alt = 35 kft on a hot day

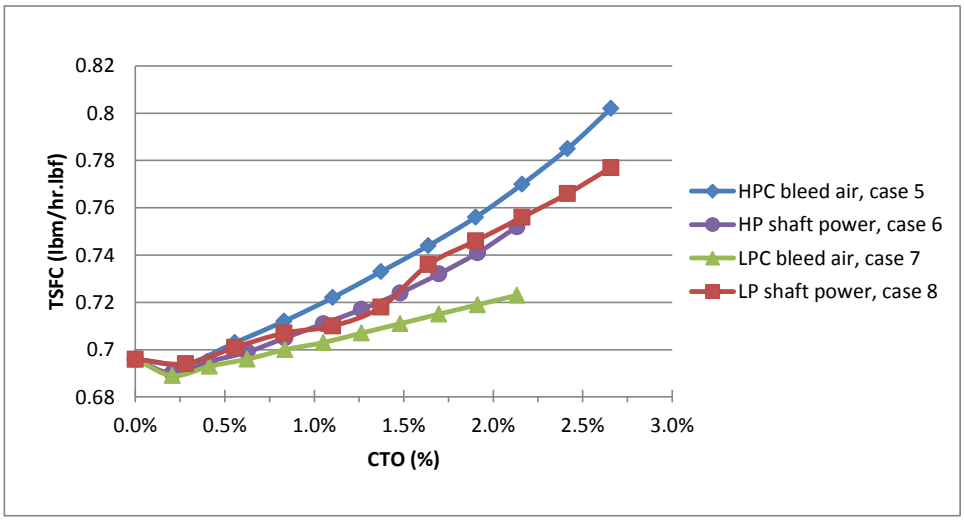

Figure IV.17. TSFC versus CTO: Tt4 = 2770 R, Mach = 0.8, Alt = 35 kft on a hot day

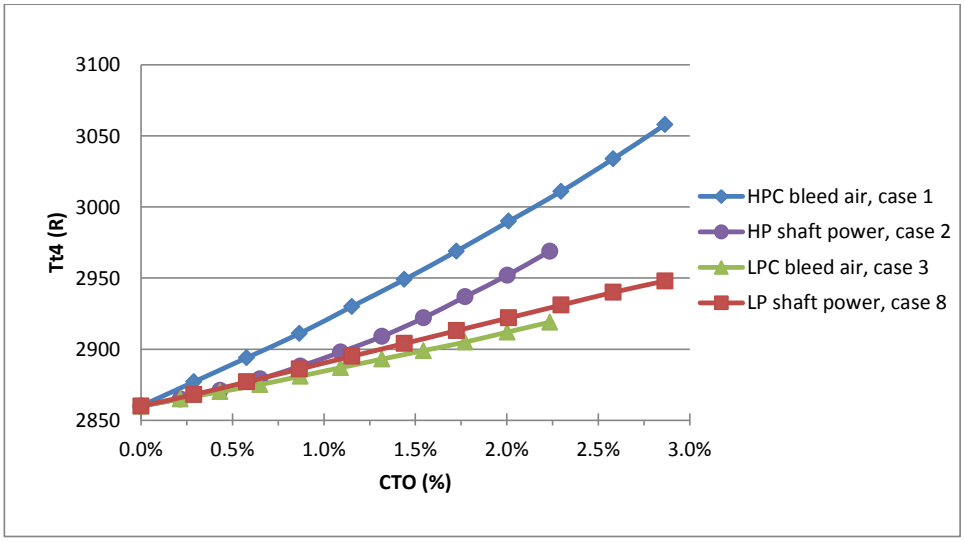

Figure IV.18. Tt4 versus CTO: mf = 0.35 lbm/s, Mach = 0.8, Alt = 35 kft on a hot day

IV.2 Engine Performance Sensitivity to Maximum HPT Inlet Temperature

The effect of the maximum allowable HPT inlet temperature on the engine performance makes necessary the study of the sensitivity of both thrust and thrust specific fuel consumption to the change of maximum T_{t4} value. The sensitivity of thrust and TSFC were obtained by running the different simulation cases at different T_{t4} setting values up to 3206 R. For each T_{t4} value setting, Eqs. 41 and 42 were used to compute sensitivities of thrust and thrust specific fuel consumption respectively.

$$S_F = \frac{F_n - F_n|_{Design}}{T_{t4} - T_{t4}|_{Design}} \tag{41}$$

$$S_{TSFC} = \frac{TSFC - TSFC|_{Design}}{T_{t4} - T_{t4}|_{Design}} \tag{42}$$

The overall sensitivity of thrust and thrust specific fuel consumption is the average of sensitivities obtained at each value of constant HPT inlet temperature setting. Thrust and TSFC overall sensitivities are plotted against coefficient of power extraction, CTO, as depicted by Figures IV.19 and IV.20 respectively. For the region of CTO values where simulation cases curves are above sensitivity zero line, available thrust is higher than at the design point. On the bottom side of the Figure IV.19 , thrust is less than that at the design point. Also, the sooner a case curve crosses the sensitivity zero line, the worst are the chances to extract power without deteriorating engine thrust performance. The higher the thrust sensitivity curve is, the better the thrust engine performance will be when HPT maximum allowable inlet temperature is raised. Based on that, bleeding air from HPC exit (case 1 or 5) would be the worst case. HP shaft power extraction looks the best although having comparable sensitivity with LP shaft power extraction or air bleeding from LPC exit.

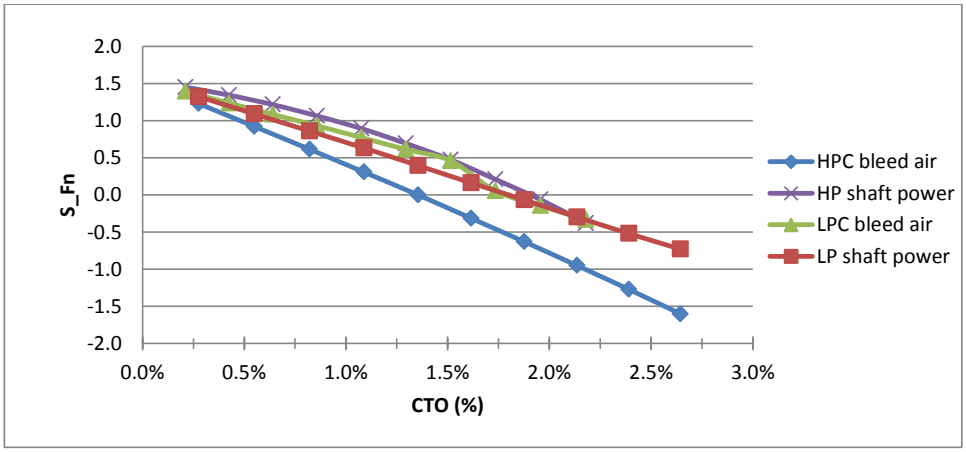

Figure IV.19. Thrust sensitivity to Tt4: Mach = 0.8, Alt = 35 kft on a standard day

For thrust specific fuel consumption sensitivity curves of Figure IV.20, the lower the sensitivity curve is placed to the bottom, the better that is for the engine performance. In fact, that means that thrust specific fuel consumption is less affected when HPT inlet temperature is changed and required power extraction is increased. Obviously, bleeding air from LPC exit or extracting equivalent power from HP spool shaft are the most promising power extraction techniques for better fuel consumption.

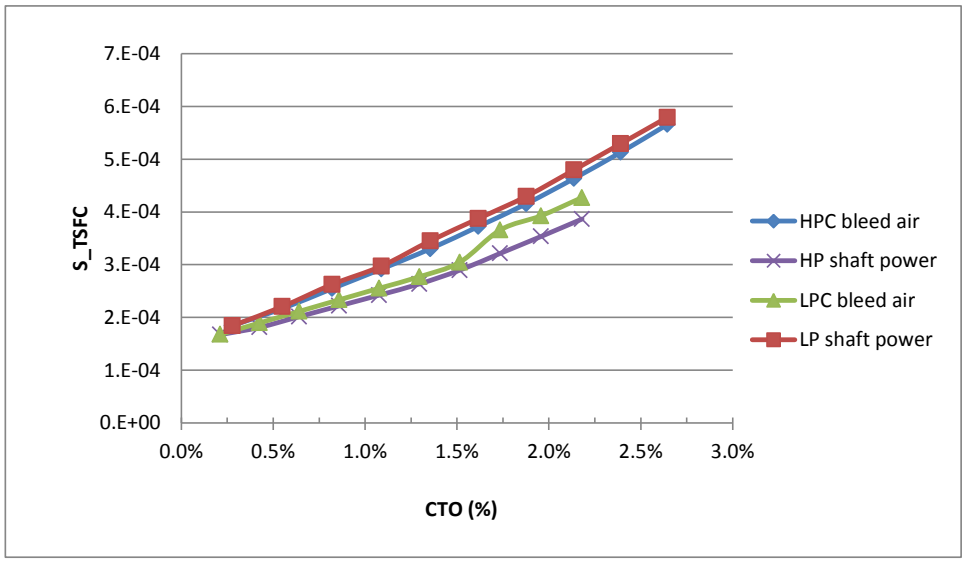

Figure IV.20. TSFC sensitivity to Tt4: Mach = 0.8, Alt = 35 kft on a standard day

It was obvious from previous analysis of engine performance in terms of thrust, thrust specific fuel consumption and HPT inlet temperature that bleeding air from HPC exit is the worst case scenario technique that could be used. However, it is hard to be decisive on which technique is the most efficient among LPC (case 3 or 7) exit air off-take, LP shaft power extraction (case 4 or 8) and HP (case 2 or 6) shaft power extraction.

In fact, from cases simulated at constant fuel flow, cases 2 and 4 are of comparable efficiency at lower power extraction levels (less than 150 kW or CTO less than 1.25 %) and case 4 is better for higher power extraction levels. Power extraction from LP spool was shown to be less efficient than cases 2 and 3. However, when power extraction techniques were simulated at constant T_{t4} setting, case 8 effect on engine performance turned to approach those of cases 6 and 7.

For that reason, engine thrust is kept the same for all power extraction techniques (air bleeding and power extraction cases) and thrust specific fuel consumption and HPT inlet temperature are compared. Thrust specific fuel consumption and HPT inlet temperature are plotted against the coefficient of power extraction as shown in Figures IV.19 and IV.20 respectively. Obviously, LPC air bleeding, LP shaft power extraction and HP shaft power extraction are comparable with same TSFC efficiency, while LPC air bleeding case is slightly better. However, for a required thrust, power extraction from HP spool shaft has higher HPT inlet temperature than when bleed air is tapped off LPC exit or an equivalent power is extracted from LP spool shaft.

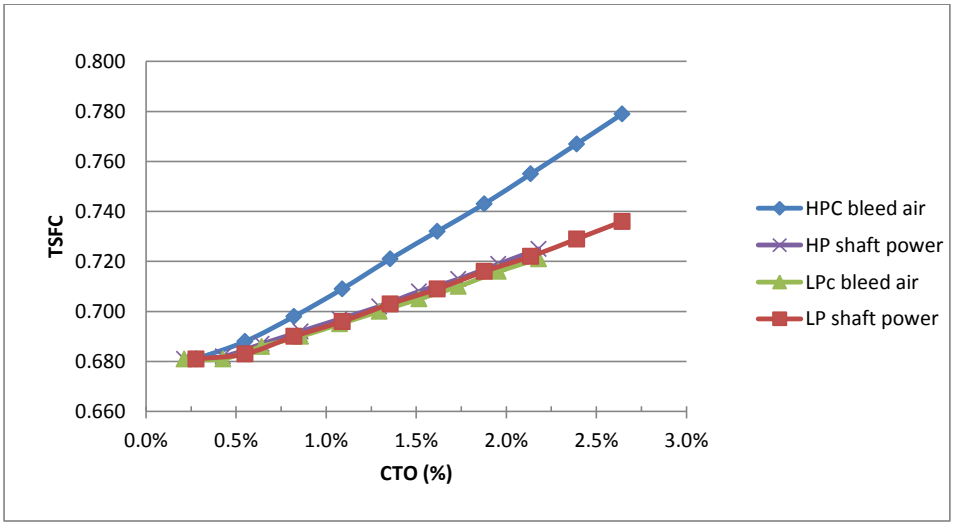

Figure IV.21. TSFC versus CTO: Mach = 0.8, Alt = 35 kft, Fn = 1849 lbf on a standard day

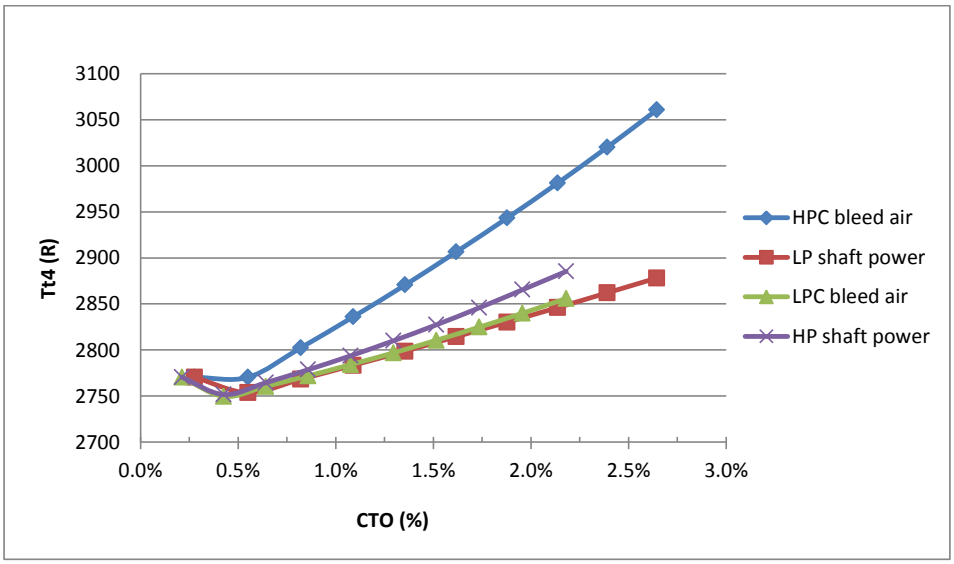

Figure IV.22. Tt4 versus CTO: Mach = 0.8, Alt = 35 kft, Fn = 1849 lbf on a standard day

IV.3 Study of The Sensitivity of The engine Performance Trends to the Altitude Change

The results obtained previously were done at cruise condition design point with a Mach number of 0.8 and an altitude of 35,000 ft. These flight conditions represent the typical commercial aircraft cruise conditions where most of the fuel consumption reduction should be done. However, effect of air bleeding from the LPC and HPC exits or power extraction from The LP and HP spool shafts on engine performance, for different flight condition altitudes is simulated. Thrust specific fuel consumption trends of Figures IV.23 (altitude = 20,000) and IV.24 (altitude = 10,000) as well as HPT inlet temperature of Figures IV.2 (altitude = 20,000) and IV.26 (altitude = 10,000) are nearly the same as those obtained for 35,000 of altitude. Therefore, this suggest that results obtained previously are independent of engine size as well as the flight altitude.

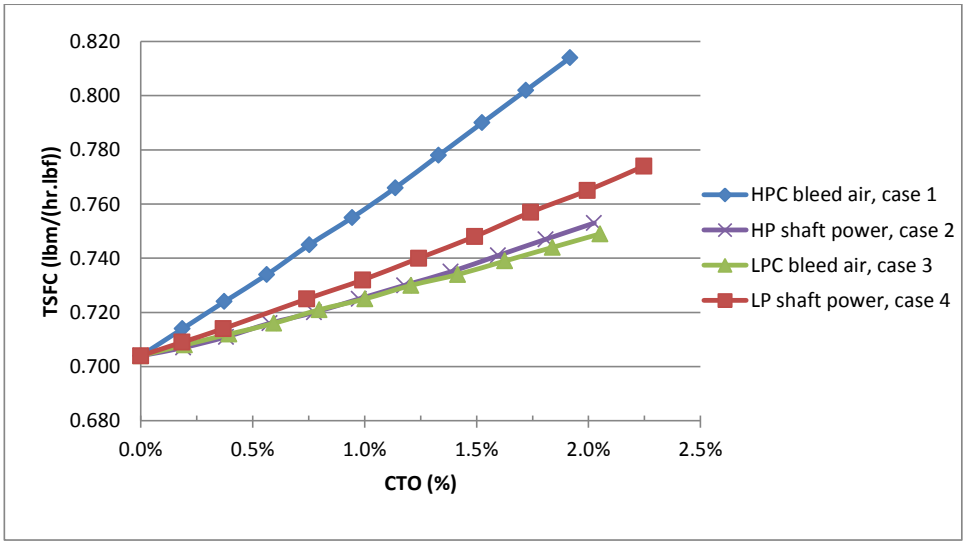

Figure IV.23. TSFC versus CTO: Mach = 0.8, Alt = 20 kft on a standard day

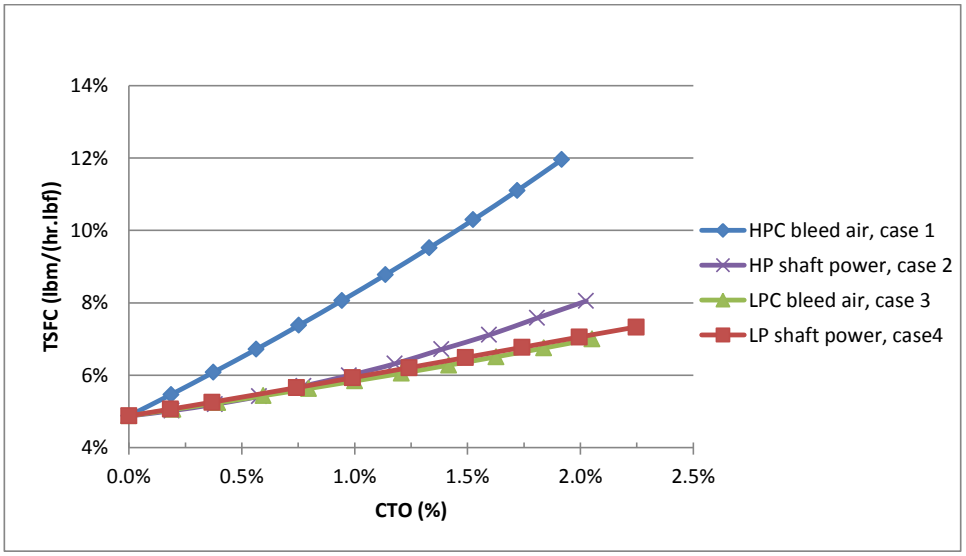

Figure IV.24. TSFC versus CTO: Mach = 0.8, Alt = 10 kft on a standard day

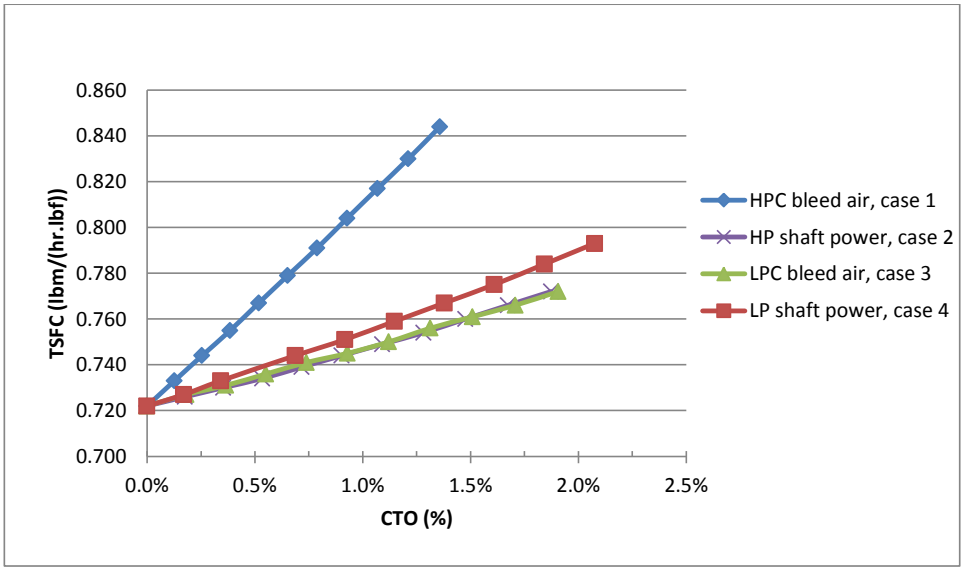

Figure IV.25. % Tt4 increment versus CTO: Mach = 0.8, Alt = 20 kft on a standard day

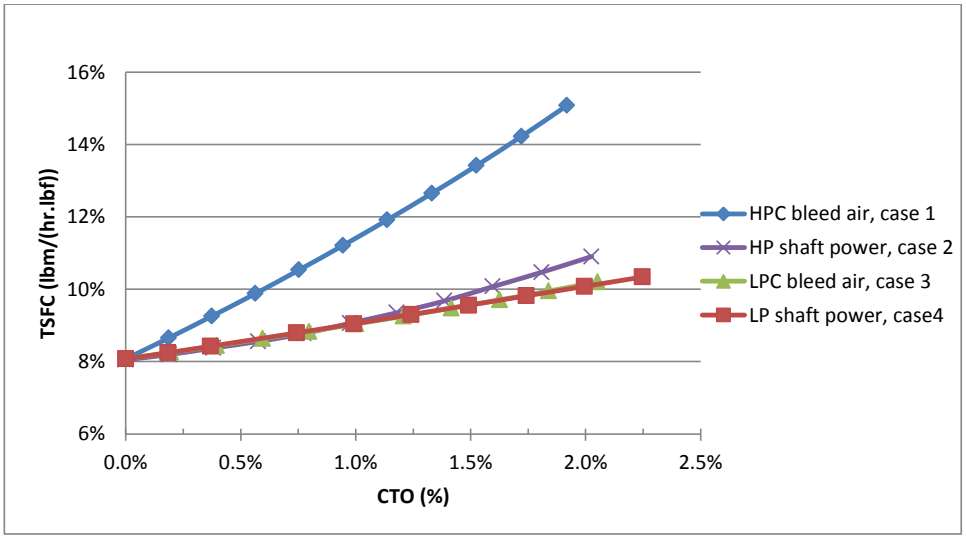

Figure IV.26. % Tt4 increment versus CTO: Mach = 0.8, Alt = 10 kft ft on a standard day

IV.4 Engine Turbomachinery Components Performance

Operational lines for fan, low and high pressure compressors were obtained by running all the cases and gathering the values of efficiency, pressure ratio, and corrected mass flow parameters. These parameters are plotted on the corresponding scaled compressor map. Efficiency contour plots were not ploted within the map as data was presented in a table form which was difficult to plot in the form of contour plots, However, compressor adiabatic efficiency variation due to power extraction are given in Appendix-C.

As depicted by Figures IV.27 to IV.30, the corrected speeds of the fan and the low pressure compressor decrease when bleeding air from HP or LP compressors, or an equivalent power is extracted from engine shafts, and at both settings of constant fuel flow rate and constant high pressure inlet temperature. In fact, fan and LPC corrected speeds more when bleeding air from the HPC exit or equivalent power is extracted from the LP spool shaft than when air bleeding from the LPC exit or equivalent power is extracted from the HP spool shaft. In fact, corrected speed of the fan and the LPC decreases by about 0.5% for cases 2 and 3, and 2% for cases 1 and 4, for each 1% CTO power extraction. However, at constant HPT inlet temperature setting as depicted by Figures IV.29 and IV.30, the LP spool shaft corrected speed decreases faster than at constant fuel flow setting. Therefore, apparently all power extraction techniques cause no problem for LP shaft functioning.

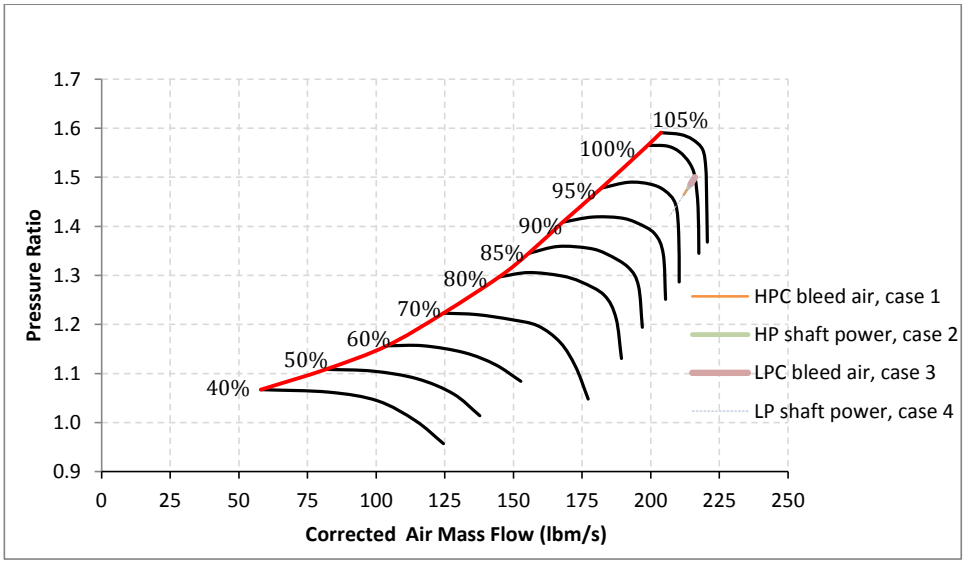

Figure IV.27. Fan operating lines: mf = 0.35 lbm/s, Mach = 0.8, Alt = 35 kft on a standard day

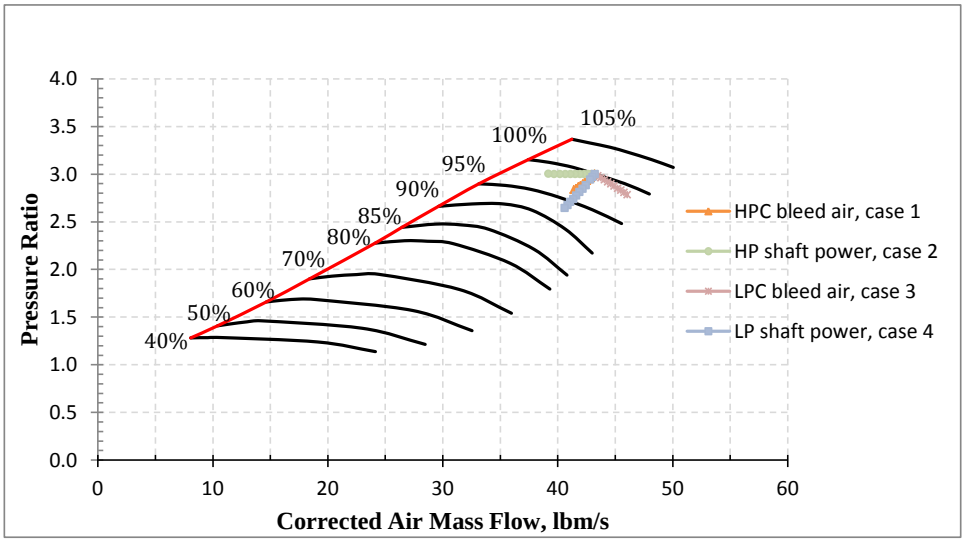

Figure IV.28. LPC operating lines: mf = 0.35 lbm/s, Mach = 0.8, Alt = 35 kft on a standard day

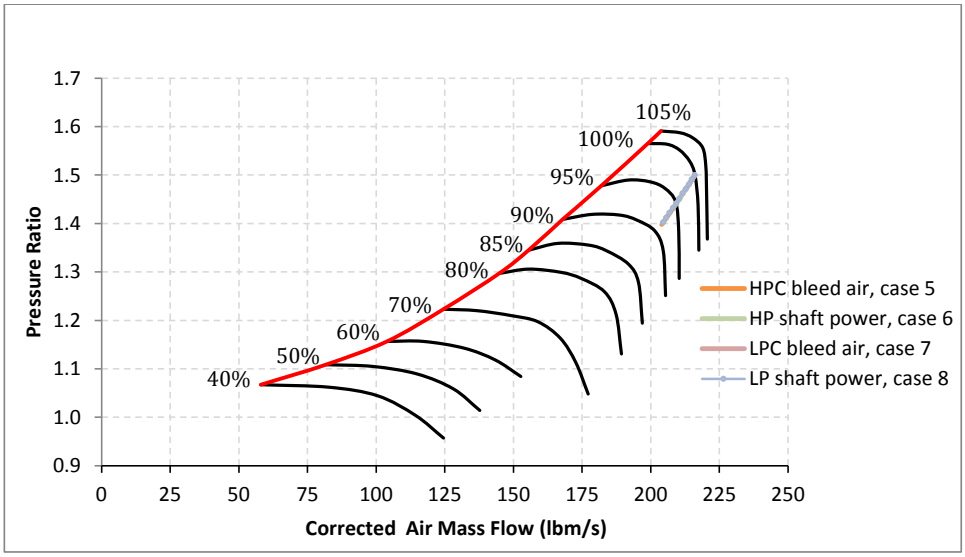

Figure IV.29. Fan operating lines: Tt4 = 2770 R, Mach = 0.8, Alt = 35 kft t on a standard day

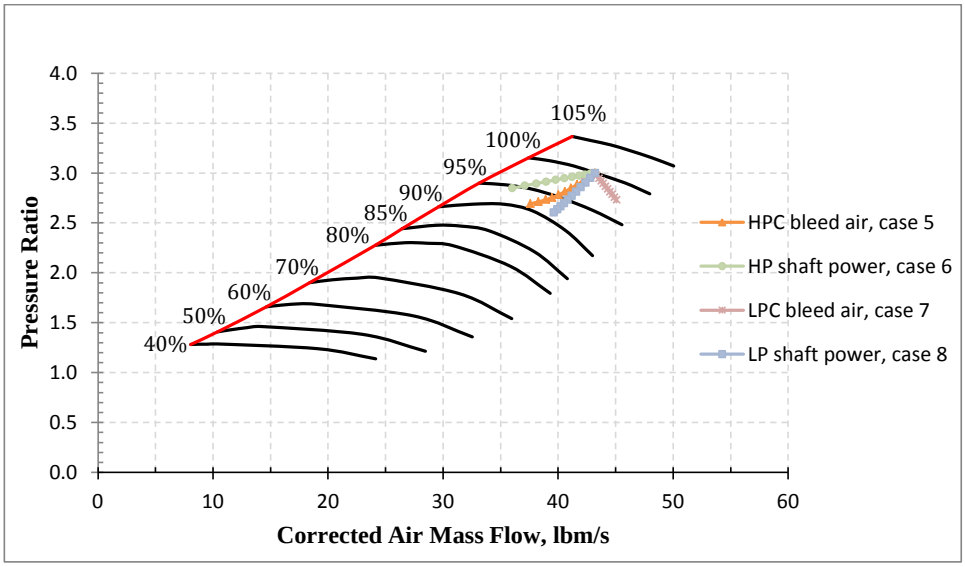

Figure IV.30. LPC operating lines : Tt4 = 2770 R, Mach = 0.8, Alt = 35 kft on a standard day

As depicted by the HPC operating lines shown in Figures IV.31 and IV.32, the corrected speed of the high pressure compressor increases when bleeding air from LPC exit or extracting power from the low pressure spool shaft at both settings of constant fuel flow and constant HPT inlet temperature. However, it is obvious that HP spool corrected speed is more sensitive for power extraction from the LP spool shaft (cases 4 and 8) rather than bleeding air from LPC exit (cases 3 and 7). In fact, HP shaft corrected speed increases by about 0.1% for cases 3 and 7, and 0.15% for cases 4 and 8, for each 1% CTO power extraction. The HPC corrected speed is nearly constant when bleeding air from the HPC, however it decreases by about 0.95% for each 1% CTO power extraction when power is extracted from the HP spool shaft. Consequently, there should be no problem, when bleeding air from the HPC exit or extracting equivalent power from HP spool shaft, on the HP shaft behavior. Contrarily, depending on the HP shaft rotational speed limit, it could be a problem when bleeding air from LPC exit or extracting equivalent power from the LP spool, especially when higher power extractions are needed and engine is run at high throttle settings.

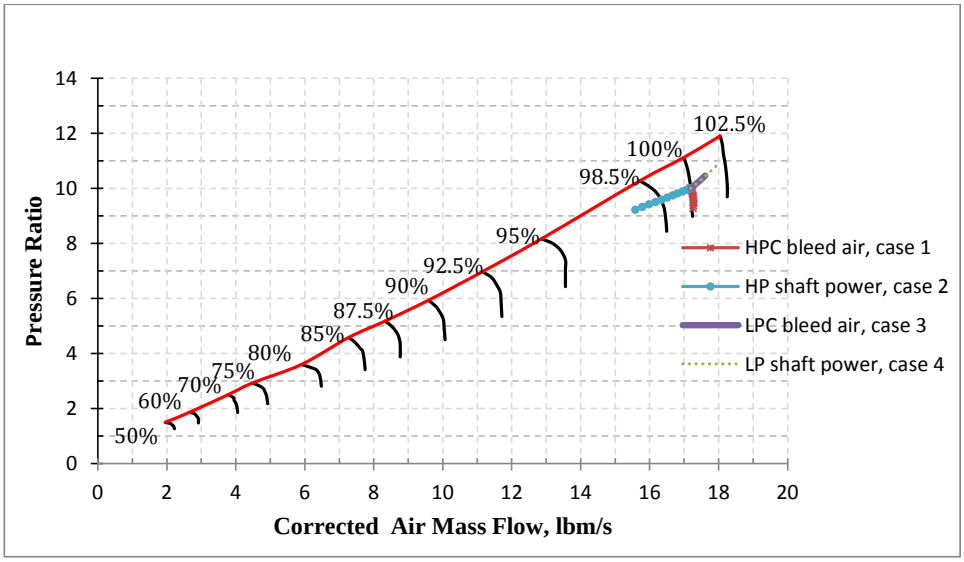

Figure IV.31. HPC operating lines : mf = 0.35 lbm/s, Mach = 0.8, Alt = 35 kft on a standard day

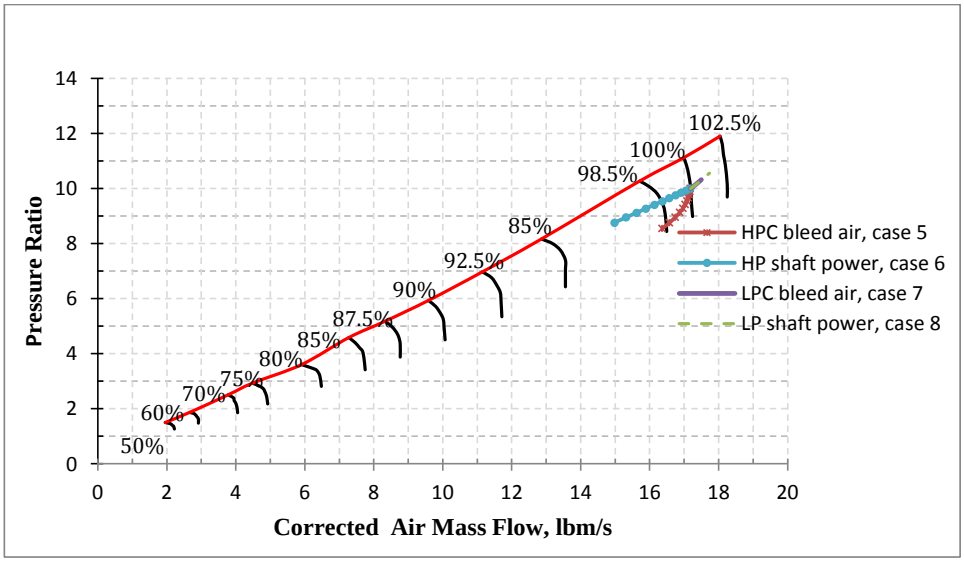

Figure IV.32. HPC operating lines : Tt4 = 2770 R, Mach = 0.8, Alt = 35 kft on a standard day

IV.5 AEDsys simulation results

It is always good to verify simulation against available experimental results. However, with unavailability of experimental result, using a second tool method simulation is an adequate way to verify results. For that reason, the Aircraft Engine Design system code (AEDsys) is used to run power extraction technique cases previously run using NPSS simulation environment. For AEDsys, bleed air extraction is only possible from high pressure compressor exit. Therefore, only three power extraction techniques will be simulated within AEDsys which are HPC air bleeding, LP spool shaft power extraction and HP spool shaft power extraction. The engine model design parameters are implemented within AEDsys as illustrated by Figure IV.33.

At both simulation settings of constant fuel flow and constant HPT inlet temperature, LP shaft power extraction and HP shaft power extraction are more efficient in terms of thrust than bleed equivalent amount of air at the HPC exit. This confirms results obtained within NPSS that air bleed off-take is the worst case scenario to extract energy from the engine .

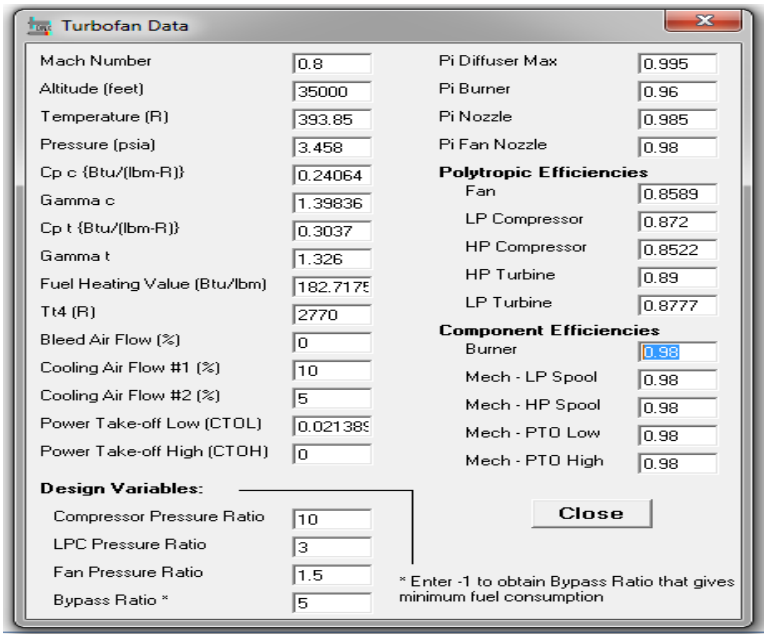

Figure IV.33. AEDsys engine model in ONX

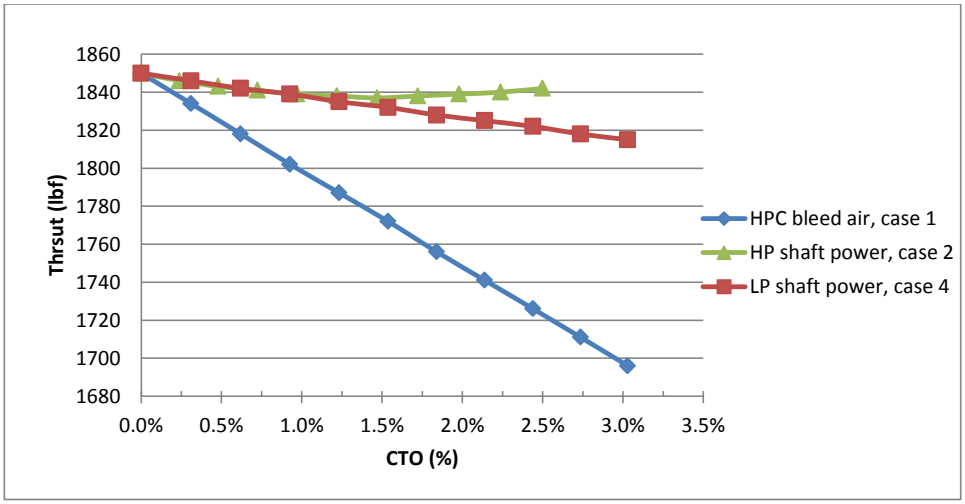

Figure IV.34. Thrust versus CTO using AEDsys: mf = 0.35 lbm/s, Mach = 0.8, Alt = 35 kft on a standard day

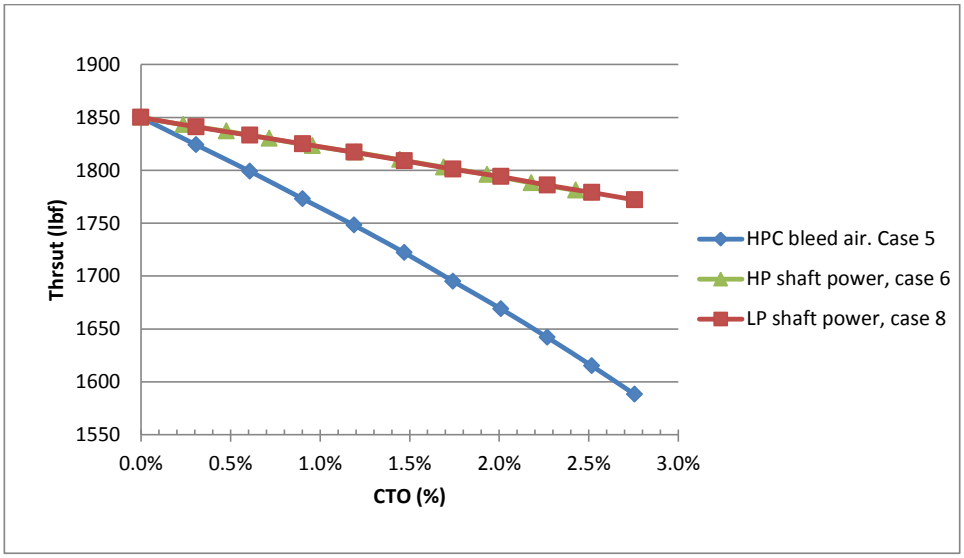

Figure IV.35. Thrust versus CTO using AEDsys : Tt4 = 2770 R, Mach = 0.8, Alt = 35 kft on a standard day

V. Conclusion and Recommendations

V.1 Findings and Results

This works objective was to understand the impact of the different techniques of power extraction from a high bypass air breathing engine and determine which technique is more efficient in terms of thrust and thrust specific fuel consumption. For the simulation, engine was modeled using the Numerical Propulsion System Simulation code (NPSS).

Basically, four cases were simulated. The first case was to bleed air at the high pressure compressor exit with a fraction of 1 to 10 % of the main stream. The second case was to extract equivalent power from the high pressure spool shaft. The third case was bleeding air at the low pressure compressor exit with a fraction of 1 to 10 % of the main stream. The last case was to extract equivalent power from the low pressure spool shaft. Two engine simulation settings are used for each case: constant fuel flow and constant high pressure turbine inlet temperature settings. The engine simulation was run at cruise flight condition with a Mach number of 0.8 and an altitude of 35,000 feet.

Simulation results showed that, while bleeding air from high pressure compressor exit is the worst case scenario that can be used for power generation, air bleeding from the low pressure compressor, extracting equivalent power from high or low spool shafts are the most efficient techniques for power extraction in terms of fuel saving. Although, when extracting power from the HP spool shaft, HPT inlet temperature was higher than for the other two cases (LPC bleeding and LP shaft power cases), it was not high enough

to cause a big problem. Actually, T_{t4} increased by only 50 R at the maximum power extraction coefficient, CTO, when power is extracted from the HP spool shaft. Moreover, HP shaft power extraction and LPC exit air bleed showed to have the best efficiency in the terms of sensitivity to HPT maximum allowable inlet temperature with HP power extraction being slightly better.

Engine turbomachinery components performance was investigated too. Fan, low pressure compressor and high pressure compressor operating lines were plotted on corresponding maps. The results suggest that there should be no problem using any of the simulated power extraction techniques on the LP spool shaft maximum speed limit. However, it was shown that bleeding air from the HPC or extracting equivalent power from the LP spool shaft could be a problem regarding rotation speed especially at high power extraction coefficient and high engine throttle settings.

V.2 Recommendations and Future Work

In this research air bleeding from both HPC and LPC exits, bleed air ducts pressure drops were not modeled. In fact, pressure losses that could happen within the bleeding duct could it required more bleed air to fulfill subsystems power requirements and this could be increasingly worse for the engine performance. Similarly, during equivalent power extraction from the LP spool shaft as well as from HP spool shaft, I did not model losses due to power generation gears and efficiency to transform mechanical work into electricity. Therefore, it is recommended for future work to take that into account. I would also recommend to simulate a full typical commercial aircraft mission

using one of the power extraction techniques at a time. Aircraft mission can be modeled on Matlab and wrapped up to NPSS. However, I would recommend to model the whole thing in NPSS. On one hand, NPSS gives necessary tools to do that, and on the other hand it is easier to control the simulation accuracy within NPSS than using another code.

Appendix-A

1. Engine Model File

```
//--------------------------------------------------------------------------
//   F A N J E T   E N G I N E                                              |
//                                                                          |
//   File Name:     fanjet.mdl                                              |
//   Version:       2.0                                                     |
//   Date(s):       11 November 1998                                        |
//                  5 Dec 2006  - ARP5571 standard nomenclature             |
//   Modified By:   1st Lieutenant Anis Faidi/Air Force Institute of        |
//                  Technology on July 2012                                 |
//                                                                          |
//   This fan jet model has been developed to use as example in User
//   Guide document.  Model uses E3 compressor and turbine maps.

AUTHOR = " ";
MODELNAME = "fanjet";
string Model_ID = "fanjet for documentation example";


// ------------------------------
//        Ambient Amb
// ------------------------------

Element Ambient Amb {
  switchMode = "ALDTMN";
  alt_in      = 35000.;
  dTs_in     = 0.;
  MN_in       = 0.8;
} // END Amb
```

```
// ------------------------------
//      Splitter SpltFan
// ------------------------------

Element Splitter SpltFan {
  BPRdes = 5.;
} // END SpltFan


// ------------------------------
//      Compressor CmpFSec
// ------------------------------

Element Compressor CmpFSec {
#include "fanE3.map";
  S_map.PRdes  = 1.5;
  S_map.effDes= 0.8589;
  S_map.RlineMap = 2.0;
  S_map.NcDes = 1.0;
  //Sh_O.inertia = 10.;     // slugs-ft**2.

} //END CmpFSec


// ------------------------------
//      Bleed B025in
// ------------------------------

Element Bleed B025in {
}
// ------------------------------
//      Duct Dfan
// ------------------------------

Element Duct Dfan {
} // END FanDuct


// ------------------------------
//      Bleed BFanOB
// ------------------------------

Element Bleed BFanOB {
  BleedOutPort BFanOB {
    hscale = 1.0;
    Pscale = 1.0;
    fracW = .00;
  }
}
```

```
// ------------------------------
//      Nozzle NozSec
// ------------------------------

Element Nozzle NozSec {
  PsExhName = "Amb.Ps";
} //END NozSec


// ------------------------------
//      Compressor CmpL
// ------------------------------

Element Compressor CmpL {
#include "lpcE3.map";

InterStageBleedOutPort Bld1out{
       fracBldW=0.0;
       fracBldP=1.0;
       fracBldWork=1.0;
       }

  S_map.PRdes  = 3.0;
  S_map.effDes= 0.872;
  S_map.RlineMap = 2.0;
  S_map.NcDes = 1.0;
  //Sh_O.inertia = 10.;     // slugs-ft**2.
} //END CmpL


// ------------------------------
//      Bleed B025
// ------------------------------

Element Bleed B025 {
}
//------------------------------
//      Duct D025
//------------------------------

Element Duct D025{
         switchDP="OFF";
         dPqP_in=0.002;
     //numRakes=1;

} // END D025


// ------------------------------
//      Compressor CmpH
// ------------------------------
```

```
Element Compressor CmpH {
#include "hpcE3.map";

InterStageBleedOutPort Bld1out{
       fracBldW=0.0;
       fracBldP=1.0;
       fracBldWork=1.0;
       }

  //Commemt out this Subelement to run the CEA thermo package
  Subelement ThermalMass S_Qhx {
    Ahx = 35743.5;
    CpMat = 1.0;
    ChxDes = .0003858;
    massMat = 500;
    wtdAvg_Fl = .5;
  }

  S_map.PRdes  = 10.0;
  S_map.effDes= 0.8522;
  S_map.RlineMap = 2.0;
  S_map.NcDes = 1.0;
  //Sh_O.inertia = 10.;     // slugs-ft**2.
} //END CmpH


// ------------------------------
//      FuelStart FusEng
// ------------------------------

Element FuelStart FusEng {
    hFuel = 182.7175;
} // END FusEng
// ------------------------------
//      Burner BrnPri
// ------------------------------

Element Burner BrnPri {
  dPqP_dmd          = 0.05;
  effBase           = 0.98;

  switchHotLoss    =  "input";
  switchBurn       = "FUEL";
  Wfuel = .35;
  tolRayleigh       = 0.0001;

} // END BrnPri
```

```
// ------------------------------
//      Bleed B041
// ------------------------------

Element Bleed B041 {
}


// ------------------------------
//      Turbine TrbH
// ------------------------------

Element Turbine TrbH {
#include "hptE3.map";
  S_map.parmMapDes   = 4.975;
  S_map.parmNcDes = 100.0;
  S_map.effDes       = 0.89;
  //Commemt out this Subelement to run the CEA thermo package
  Subelement ThermalMass S_Qhx {
    Ahx = 3574.35;
    CpMat = 1.0;
    ChxDes = .0003858;
    massMat = 100;
    wtdAvg_Fl = .5;
  }

} //END TrbH


// ------------------------------
//      Bleed B042
// ------------------------------

Element Bleed B042 {
}
// ------------------------------
//      Duct D043
// ------------------------------

Element Duct D043 {
  switchDP = "INPUT";
  void preexecute() {
    dPqP_in = 0.25 * Fl_I.MN * Fl_I.MN;
  }
  Fl_I.MNdes = 0.4;
} //END D043
```

```
// -------------------------------
//      Turbine TrbL
// -------------------------------

Element Turbine TrbL {
#include "lptE3.map";
  S_map.parmMapDes   = 4.271;
  S_map.parmNcDes = 100.0;
  S_map.effDes       = 0.8777;
} //END TrbL


// -------------------------------
//      Bleed B045
// -------------------------------

Element Bleed B045 {

}


// -------------------------------
//      Nozzle NozPri
// -------------------------------

Element Nozzle NozPri {
  PsExhName = "Amb.Ps";
} //END NozPri

// -------------------------------
//      FlowEnds
// -------------------------------

Element FlowEnd FePri {
}
Element FlowEnd FeSec {
}

Element FlowEnd FeFanOB {
}

Element FlowEnd FelH{
}

Element FlowEnd FelL{
}
```

```
// ------------------------------
//      Shaft ShH
// ------------------------------

Element Shaft ShH {
  //  Mechanical Ports.  These are created as needed on the shaft.
  ShaftInputPort MeCmpH, MeTrbH;
  Nmech = 8997.43;
  inertia = .93243;       //30. lbm-ft2;
}   //END ShH


// ------------------------------
//      Shaft ShL
// ------------------------------

Element Shaft ShL {
  ShaftInputPort MeCmpFSec, MeCmpL, MeTrbL;
  Nmech = 3497.40;
  inertia = 2.73513;     //88. lbm-ft2;
}   //END ShL


// ------------------------------
//      PerfNASA Perf
// ------------------------------

Element EngPerf Perf {
} //END Perf


// ------------------------------
//      Cycle Cycle
// ------------------------------
Element Cycle Cycle {
  EPR_numName = "CmpH.Fl_O";
  EPR_denName = "InEng.Fl_O";
  FPR_numName = "CmpFSec.Fl_O";
  FPR_denName = "InEng.Fl_O";
} //END Cycle


// ------------------------------
//      Controls
// ------------------------------
#include "controls.cmp"
```

```
// --------------------------------
//      linkPorts
// --------------------------------
linkPorts( "InletStart.Fl_O", "InEng.Fl_I",         "F0"    );
linkPorts( "InEng.Fl_O",      "SpltFan.Fl_I",       "F01A"  );
// Primary section
linkPorts( "SpltFan.Fl_O1",   "CmpL.Fl_I",          "F025"  );
linkPorts( "CmpL.Fl_O",       "B025.Fl_I",          "F0251" );
linkPorts( "B025.Fl_O",       "D025.Fl_I",          "F0252" );
linkPorts( "D025.Fl_O",       "CmpH.Fl_I",          "F0253" );
linkPorts( "CmpH.Fl_O",       "BrnPri.Fl_I",        "F03"   );
linkPorts( "FusEng.Fu_O",     "BrnPri.Fu_I",        "FU036" );
// Primary Hot Section Connect Statements:
linkPorts( "BrnPri.Fl_O",     "B041.Fl_I",          "F041"  );
linkPorts( "B041.Fl_O",       "TrbH.Fl_I",          "F041a" );
linkPorts( "TrbH.Fl_O",       "B042.Fl_I",          "F042"  );
linkPorts( "B042.Fl_O",       "D043.Fl_I",          "F043"  );
linkPorts( "D043.Fl_O",       "TrbL.Fl_I",          "F044"  );
linkPorts( "TrbL.Fl_O",       "B045.Fl_I",          "F045"  );
linkPorts( "B045.Fl_O" ,      "NozPri.Fl_I",        "F07"   );
linkPorts( "NozPri.Fl_O",     "FePri.Fl_I",         "F09"   );
// Fan duct section:
linkPorts( "SpltFan.Fl_O2",   "CmpFSec.Fl_I",       "F12"   );
linkPorts( "CmpFSec.Fl_O",    "B025in.Fl_I",        "F11"   );
linkPorts( "B025in.Fl_O",     "Dfan.Fl_I",          "F16"   );
linkPorts( "Dfan.Fl_O",       "BFanOB.Fl_I",        "F165"  );
linkPorts( "BFanOB.Fl_O",     "NozSec.Fl_I",        "F17"   );
linkPorts( "NozSec.Fl_O",     "FeSec.Fl_I",         "F19"   );
// --------------------------------
//      Bleed Connections
// --------------------------------
// Component to Component Bleed
linkBleedCT( "CmpH", "TrbH",   .10, 1., 1., 1., 0, "ca1HPT" );
linkBleedCB( "CmpH", "B042",   .04, 1., 1.,        "ca2HPT" );
linkBleedCB( "CmpH", "B045",   .01, .5, .5,        "ca3HPT" );
linkBleedBB( "B025", "B025in",   .00, 1., 1.,      "surge"  );

//Overboard bleed
linkPorts( "BFanOB.BFanOB",   "FeFanOB.Fl_I",      "FL166");
linkPorts( "CmpH.Bld1out",    "FelH.Fl_I",      "FL31");
linkPorts( "CmpL.Bld1out",    "FelL.Fl_I",      "FL251");
// --------------------------------
//      Shaft Connect Statements
// --------------------------------
linkPorts( "CmpL.Sh_O",      "ShL.MeCmpL",    "MeCmpL" );
linkPorts( "CmpFSec.Sh_O",   "ShL.MeCmpFSec","MeCmpFSec" );
linkPorts( "TrbL.Sh_O"   ,   "ShL.MeTrbL",    "MeTrbL" );
linkPorts( "CmpH.Sh_O",      "ShH.MeCmpH",    "MeCmpH" );
linkPorts( "TrbH.Sh_O",      "ShH.MeTrbH",    "MeTrbH" );
```

2. Engine Run File

```
//Hi Bypass Fanjet model
//Created: 7/2000
//Modeified July 2012/1st lieutenant Anis Faidi/AFIT/ENY

#ifndef THERMO
#define THERMO GasTbl
#endif

//Set the thermo package
setThermoPackage("$THERMO");

//default includes
#include "nasa.view"            //default page viewer
#include "bleed_macros.fnc"   //bleed macros

//local includes
#include "Transient.view"     //transient viewer
#include "myViewer.view"
//model file
#include "fanjet.mdl"

//Set the day type

//Amb.switchDay="STD"; // default
//Amb.switchDay="COLD";
//Amb.switchDay="HOT";

//Throtlle setting
CONTROL.PLACS=50.0;

//case input files
#include "des8std.case"
//#include "des8cold.case"
//#include "des8hot.case"
```

3. Engine Control File

```
//class Control extends Element { }

//Element Control CONTROL {
Element CONTROL {
  // Variables and limits
  real PLACS, T1ACS, T25CS, P1ACS, P25CS, PS3CS, T41CS, P7CS, T7CS, WF36CS, TH1A  ;

  real T41H = 3206;
  real WFEL = 430;
  real PCNHR = 105;
  real PCNHH = 105;

  real PCNHRH, XN25CS, PCNHRS, EPCNHR, XNDHP, EPCNHH, EPNHRH, ET41, ERR1, WFED;
```

```
real XNHRD = 13000;

// Frame rate
real dtime = .05;

// Execute time
real execTime = 0;

real TSTD = 518.67;

void variableChanged(string name, string value) {
  // do nothing...
}
Option switchDes {
  allowedValues = { "DESIGN", "OFFDESIGN" }
  value = "DESIGN";
}

Option solutionMode {
  allowedValues = { "TRANSIENT", "STEADY_STATE", "ONE_PASS" }
  value = "STEADY_STATE";
}
// Get data from engine to control
void mapIn() {
  XN25CS = ShL.Nmech;
  T1ACS = F0.Tt;
  T25CS = F01A.Tt;
  P1ACS = F0.Pt;
  P25CS = F01A.Pt;
  PS3CS = F03.Ps;
  T41CS = F041.Tt;
  P7CS = F07.Pt;
  T7CS = F07.Tt;
  WF36CS = FusEng.Wfuel;
}
// Get data from control to engine
void mapOut() {
  if ( solutionMode == "TRANSIENT" ) { BrnPri.Wfuel = WFED * BrnPri.Wfuel;}
}

void calculate() {
  //steady state mode
  if ( solutionMode == "STEADY_STATE" ) {
    mapIn();
    steadyState();
  }
}
```

```
// Steady state
// Schedule fuel flow based on limits (from GE)
void steadyState() {

  TH1A = T1ACS / TSTD;

  if ( switchDes == "DESIGN" ) {
    XNDHP = XN25CS/ sqrt( TH1A );
  }
  // Calculate corrected speed
  TH1A = T1ACS / TSTD;
  PCNHRS = 100 * XN25CS / sqrt( TH1A )/ XNDHP;

  // Read demand fan speed from PLA
  PCNHR = PC_SKED( PLACS );

  // Calculate error between demand fan speed mand sensed fan speed
  EPCNHR = ( PCNHR - PCNHRS )/ 100.0;

  // Check max corrected fan speed limit
  EPCNHH = ( PCNHH - PCNHRS )/ 100;
  if ( EPCNHR > EPCNHH ) {
    EPCNHR = EPCNHH;
  }

  // Check max corrected fan speed as a function of physical speed
  PCNHRH = PCNHH * XNHRD / sqrt( TH1A )/ XNDHP;
  EPNHRH = ( PCNHRH - PCNHRS )/ 100;
  if ( EPCNHR > EPNHRH ) {
    EPCNHR = EPNHRH;
  }
  // Calculate error due to T41 max
  ET41 = ( T41H - T41CS )/ T41H;

  ERR1 = EPCNHR;
  if ( EPCNHR > ET41 ) {
    ERR1 = ET41;
  }
}

// Discrete calcs (done once per time step)
int runDiscreteCalcs( real time, real nextCalcTime ) {

  if ( abs ( nextCalcTime - execTime ) > .000001 ) {
    return FALSE;
  }
```

```
    // Check steady-state limits
    steadyState();

    real step = min( abs( ERR1 ), .005 );
    WFED =  ( 1 + ERR1 / abs ( ERR1 ) * step );

    // Map data from control to engine
    mapOut();

    return TRUE;
  }

  // Schedule of comp speed vs power code
  Table PC_SKED( real PL ) {
    PL = { 25, 40, 50 }
    PC_SKED = { 80, 90, 100 }
  }

  // Calculations performed after the cycle converges
  void updateHistory( ) {

    if ( abs ( time - execTime ) > .000001 ) {
      return;
    }

    // Determine the next time this executes
    execTime = execTime + dtime;

    // Get the data from the engine to the control
    mapIn();
  }

  // Intialize
  void initializeHistory() {

    execTime = time + dtime;
    // Get the data from the engine to the control
    mapIn();
  }

  // Tell the system at what time this thing needs to run
  real nextExecTime( real currentNextTime ) {
    return execTime;
  }

}
```

4. HPC Exit Bleed Air Off-take Case File

```
//cout << "Input File List \n\n" << inputFileList << endl;
//---------------------------------------------------
// Run a design  case
//---------------------------------------------------
cout <<"==============================running starting=========================="<<endl;
cout<<endl;

setOption( "switchDes", "DESIGN" );
autoSolverSetup();

cout << "\n\nDesign independents:\n" << solver.independentNames<<endl;
cout << "\n\nDesign Dependents:\n" << solver.dependentNames<<endl;
solver.debugLevel = "MATRIX_DETAILS";
solver.diagnosticFile = "solverDes.out";
CASE = CASE + 1;
run();
EngResultsRow.update();
ncpView.display();

setOption( "switchDes", "OFFDESIGN" );
autoSolverSetup();

cout << "\n\nDesign independents:\n" << solver.independentNames<<endl;
cout << "\n\nDesign Dependents:\n" << solver.dependentNames<<endl;
solver.debugLevel = "MATRIX_DETAILS";
solver.diagnosticFile = "solverOffDes.out";

solver.maxIterations = 100;
solver.maxJacobians = 100;

CASE = CASE + 1;
CmpH.Bld1out.fracBldW =0.01;
cout << "\n\nfracBldW =1%, SFC ="<<Perf.SFC<<endl;
run();
EngResultsRow.update();
ncpView.display();

cout<<"InEng.Fl_I.V  = "<<InEng.Fl_I.V<<endl;
cout<<"InEng.Fl_I.MN = "<<InEng.Fl_I.MN<<endl;

CASE = CASE + 1;
CmpH.Bld1out.fracBldW =0.02;
cout << "fracBldW =2%, SFC ="<<Perf.SFC<<endl;
run();
EngResultsRow.update();
ncpView.display();

CASE = CASE + 1;
CmpH.Bld1out.fracBldW =0.03;
cout << "fracBldW =3%, SFC ="<<Perf.SFC<<endl;
```

```
run();
EngResultsRow.update();
ncpView.display();

CASE = CASE + 1;
CmpH.Bld1out.fracBldW =0.04;
cout << "fracBldW =4%, SFC ="<<Perf.SFC<<endl;
run();
EngResultsRow.update();
ncpView.display();


CASE = CASE + 1;
CmpH.Bld1out.fracBldW =0.05;
cout << "fracBldW =5%, SFC ="<<Perf.SFC<<endl;
run();
EngResultsRow.update();
ncpView.display();

CASE = CASE + 1;
CmpH.Bld1out.fracBldW =0.06;
cout << "fracBldW =6%, SFC ="<<Perf.SFC<<endl;
run();
EngResultsRow.update();
ncpView.display();

CASE = CASE + 1;
CmpH.Bld1out.fracBldW =0.07;
cout << "fracBldW =7%, SFC ="<<Perf.SFC<<endl;
run();
EngResultsRow.update();
ncpView.display();

CASE = CASE + 1;
CmpH.Bld1out.fracBldW =0.08;
cout << "fracBldW =8%, SFC ="<<Perf.SFC<<endl;
run();
EngResultsRow.update();
ncpView.display();

CASE = CASE + 1;
CmpH.Bld1out.fracBldW =0.09;
cout << "fracBldW =9%, SFC ="<<Perf.SFC<<endl;
run();
EngResultsRow.update();
ncpView.display();

CASE = CASE + 1;
CmpH.Bld1out.fracBldW =0.10;
cout << "fracBldW =10%, SFC ="<<Perf.SFC<<endl;
run();
EngResultsRow.update();
ncpView.display();
EngResultsRow.display();
```

```
//set the transient mode runing
setOption("solutionMode","TRANSIENT");
transient.stopTime = 10.0;
transient.baseTimeStep = .05;
CONTROL.PLACS = 50;
postsolverSequence = { "transientTrace"};
run();
transientTrace.display()
cout <<"============================Design case running finishing================="<<endl;
cout <<endl;
```

5. Viewer File

```
// File: EngResultsRow.view
// Create an output stream named os_EngResultsRow
OutFileStream os_EngResultsRow {
    // Name of the output file that is created by this out stream
    filename = "case8Out"; // sent results to the command prompt
    //filename = "EngResults.txt";
}
```

```
// Create the Case Row Viewer named EngResultsRow
DataViewer CaseRowViewer EngResultsRow {

    // Specify the OutFileStream object to use for this viewer
    outStreamHandle = "os_EngResultsRow";

    // Set the default number format for real and scientific notation
    defRealFormat = "????????.??????";
    defSNFormat =   "??.??????E????";
    // List the variables that you want to print to the output file
    variableList = {

            //Engine Performance Obtaining
            "Perf.Fn  : ??????=Fn",
            "Perf.SFC : ?????.???=TSFC",
            "F041a.Tt  : ???????=Tt4",
            "FL251.W  : ??????.???=Fl251",
            "FL251.getExergy(FL251.Pt,FL251.Tt):?????.??=LExergy",
            "InEng.Fl_I.W:???.???=Wo",
            "InEng.Fl_I.ht:???.???=ho",
            "Perf.Fram  : ??????=Fram",
            "Perf.Fg  : ??????=Fg",
            "Perf.Wfuel : ???????=Wfuel",
            "FL31.W  : ??????.???=FL31",
            "FL31.getExergy(FL31.Pt,FL31.Tt):?????.??=HExergy",

            // Engine Shaft Torques Monitoring
            "ShH.trqIn : ??????.??",
            "ShH.trqOut : ??????.?? ",
            "ShL.trqIn : ??????.?? ",
            "ShL.trqOut : ??????.?? "
            "CmpL.effPoly:?.???",
            "CmpH.effPoly:?.???",
            "CmpH.effPoly:?.???",
            "TrbH.effPoly:?.???",
            "TrbL.effPoly:?.???",

            "F01A.W  : ???????=W0",
            "F12.W  : ???????=Wfan",
            "F025.W  : ???????=Wcore",
            "F0253.W  : ???????=Whpc",
            "F025.W  : ???????=Wlpc",
```

```
"F01A.W  : ???????=W0",
"F12.W  : ???????=Wfan",
"F025.W  : ???????=Wcore",
"F0253.W  : ???????=Whpc",
"F025.W  : ???????=Wlpc",

// Engine Operating Lines Obtaining parameters
"CmpFSec.Wc:???.???=FWc",
"CmpFSec.PR:???.???=FPR",
"CmpL.Wc:???.???=LWc",
"CmpL.PR:???.???=LPR",
"CmpH.Wc:???.???=HWc",
"CmpH.PR:???.???=HPR",
"CmpFSec.eff:???.???=FWc",
"CmpL.eff:???.???=LWc",
"CmpH.eff:???.???=HPR",
"F041a.Tt  : ???????=Tt4",
"Perf.Wfuel : ???????=Wfuel",

// Engine Surge Margins Parametrs Obtaining
"CmpFSec.S_map.S_eff.PRmapSMN:???.???=FPR_SMN",
"CmpFSec.S_map.S_eff.PRmapSMW:???.???=FPR_SMW",
"CmpFSec.S_map.S_eff.WcMapSMN:????.???=FWc_SMN",
"CmpFSec.S_map.S_eff.WcMapSMW:????.???=FWc_SMW",
"CmpL.S_map.S_eff.PRmapSMN:???.???=LPR_SMN",
"CmpL.S_map.S_eff.PRmapSMW:???.???=LPR_SMW",
"CmpL.S_map.S_eff.WcMapSMN:???.???=LWc_SMN",
"CmpL.S_map.S_eff.WcMapSMW:???.???=LWc_SMW",
"CmpH.S_map.S_eff.PRmapSMN:???.???=HPR_SMN",
"CmpH.S_map.S_eff.PRmapSMW:???.???=HPR_SMW",
"CmpH.S_map.S_eff.WcMapSMN:???.???=HWc_SMN",
"CmpH.S_map.S_eff.WcMapSMW:???.???=HWc_SMW",
```

```
            //Engine Operating Condition Monitoring
            "Amb.switchDay  : ?????=Day",
            "THERMPACKAGE:??????=THERMO",
            "CONTROL.PLACS :???.??=PLACS"
            "FL166.W  : ??????.???=Fl166",
            "FL31.W  : ??????.???=Fl31",
            "ShH.HPX  : ??????.???=HPXh",
            "ShL.HPX  : ??????.???=HPXl"
        }
    titleBody = "";
    titleVars = {};
    // Print the Case in the file header
    caseHeaderBody = "Case ???"; // Case header title to display
    caseHeaderVars = {"CASE"}; // Actual case number
    pageWidth = 10000;
    pageHeight = 10000.;
}
```

6. User Function File

```
// File name: EnginePerf.fnc

void EngineEnv(real MN, real startAlt, real endAlt, real numPts){
        // this function searches for baseline engine envelope
        numPts   =  max(numPts,1);
        real altStep  = (endAlt-startAlt)/(numPts-1);
        real Alt = startAlt;
        Amb.MN_in= MN;
        Amb.alt_in=Alt;
        CASE +=1;
        run();
        ncpView.display();
        baselinePerf.update();
        int i=1;//declare integer used for counting

        do {

            CASE +=1;
            i+=1;// increment the counter
            Alt=Alt+altStep;//calculate the next altitude number
            Amb.alt_in=Alt;//set the next altitude point
            run();// run the model
            ncpView.display();
            baselinePerf.update();
            } while(solver.converged==TRUE && i<numPts);
            cout<<"Done"<<endl;
            cout<<"numPts="<<numPts<<endl;
            cout<<"i="<<i<<endl;
}

void Fn_TSFC_Hooks(real Alt, real startMN, real endMN, real numPts){
        //This function run max Thrsut,TSFC and mass flow  for different flight conditions
        numPts   =  max(numPts,1);
        real MNstep  = (endMN-startMN)/(numPts-1);
        real MN = startMN;
        Amb.MN_in= MN;
        Amb.alt_in=Alt;
        CASE +=1;
        CONTROL.PLACS=50.0;
        CASE +=1;
        CONTROL.PLACS=50.0;
        run();
        ncpView.display();
        baselinePerf.update();
        int i=1;//declare integer used for counting
```

```
        do {

            CASE +=1;
            i+=1;// increment the counter
            MN=MN+MNstep;//calculate the next altitude number
            Amb.MN_in=MN;//set the next altitude point
            run();// run the model
            ncpView.display();
            baselinePerf.update();
            } while(solver.converged==TRUE && i<numPts);
            cout<<"Done"<<endl;
}

void ThrottleHooks(real Alt,real MN){
        // This function runs engine throttle hooks
        Amb.MN_in= MN;
        Amb.alt_in=Alt;
        CONTROL.PLACS=20.0;
        CASE +=1;
        run();
        ncpView.display();
        baselinePerf.update();

        do {
            CASE +=1;
            CONTROL.PLACS+=5;
            run();// run the model
            ncpView.display();
            baselinePerf.update();
            } while(solver.converged==TRUE && CONTROL.PLACS<51.0);
            cout<<"Done"<<endl;
}
```

Appendix-B

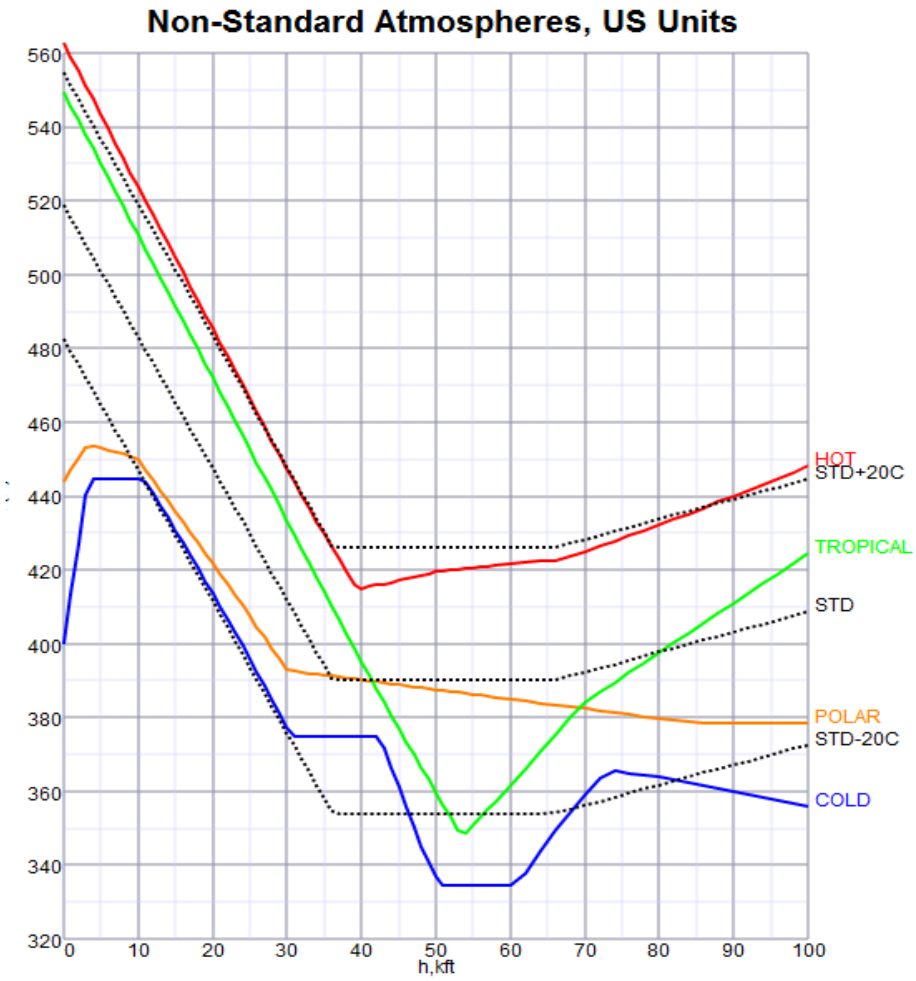

Figure B.1. MIL-STD-210A day type definition: US unit system

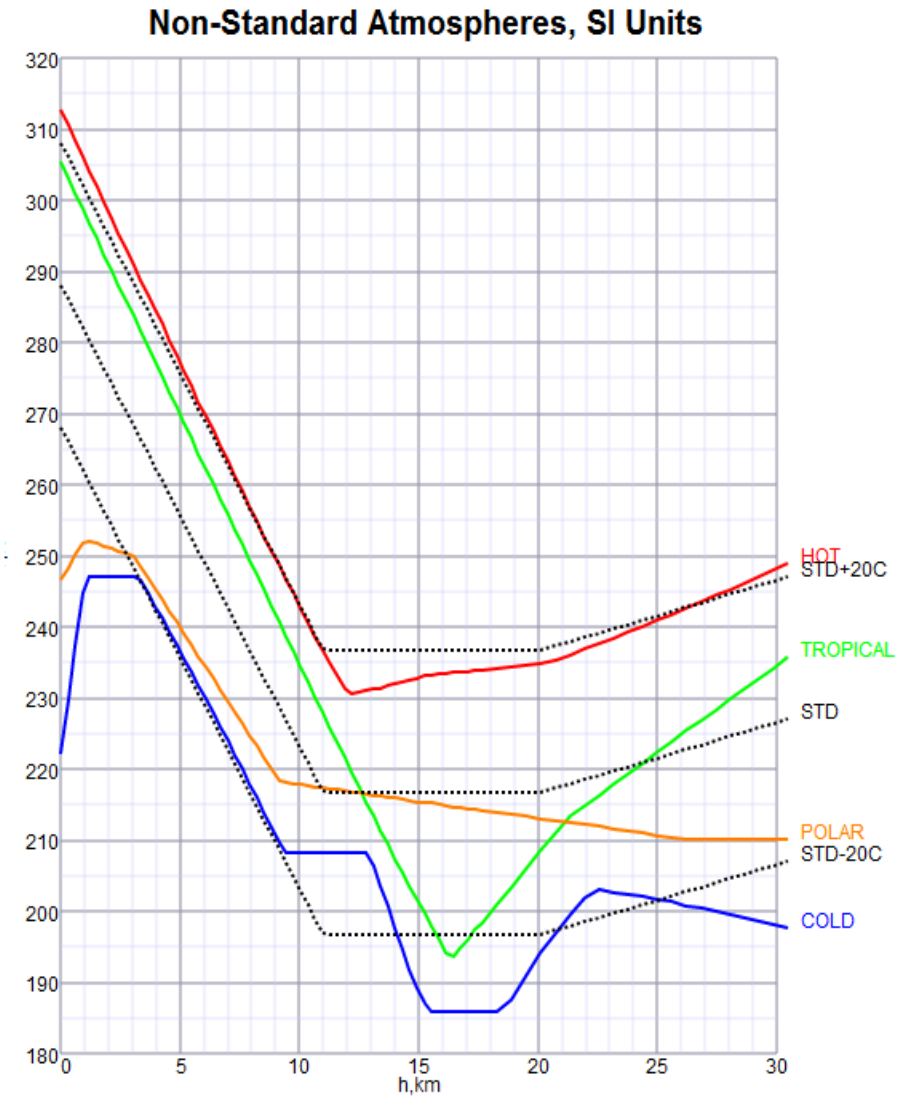

Figure B.2. MIL-STD-210A day type definition: SI unit system

Appendix-C

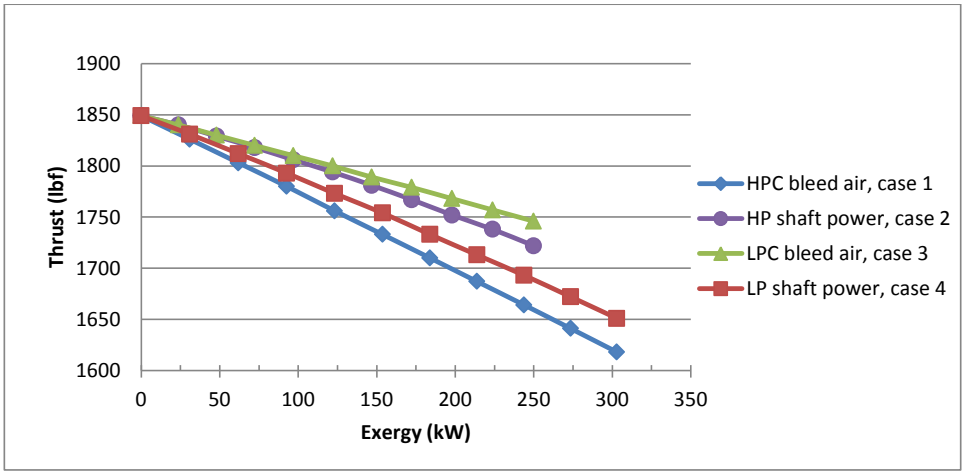

Figure C.1. Thrust versus exergy: mf = 0.35 lbm/s, Mach = 0.8, Alt = 35 kft on standard day

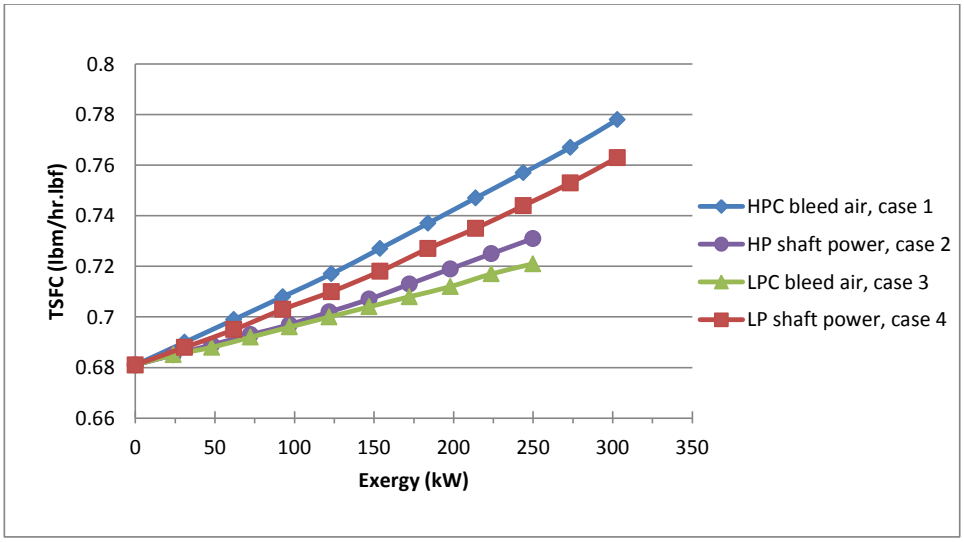

Figure C.2. TSFC versus exergy: mf = 0.35 lbm/s, Mach = 0.8, Alt = 35 kft on standard day

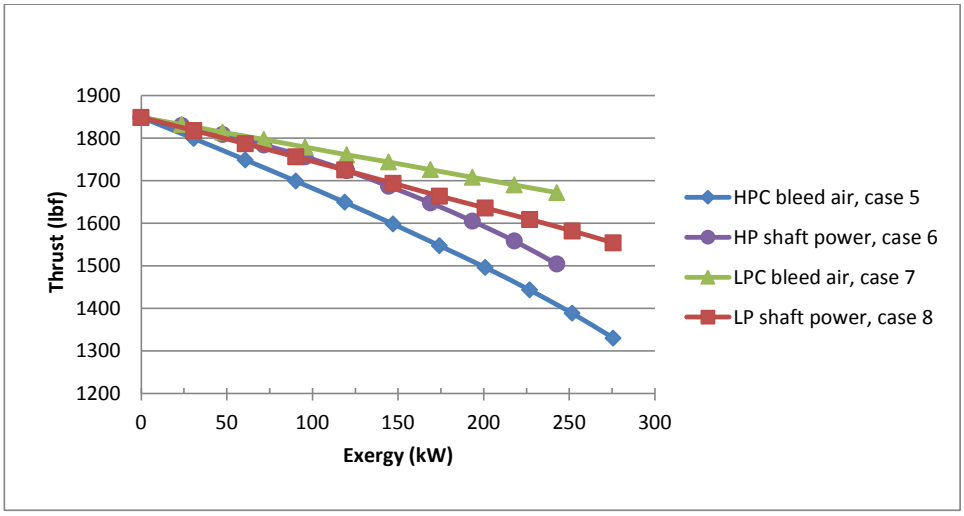

Figure C.3. Thrust versus exergy: Tt4 = 2270 R, Mach = 0.8, Alt = 35 kft on standard day

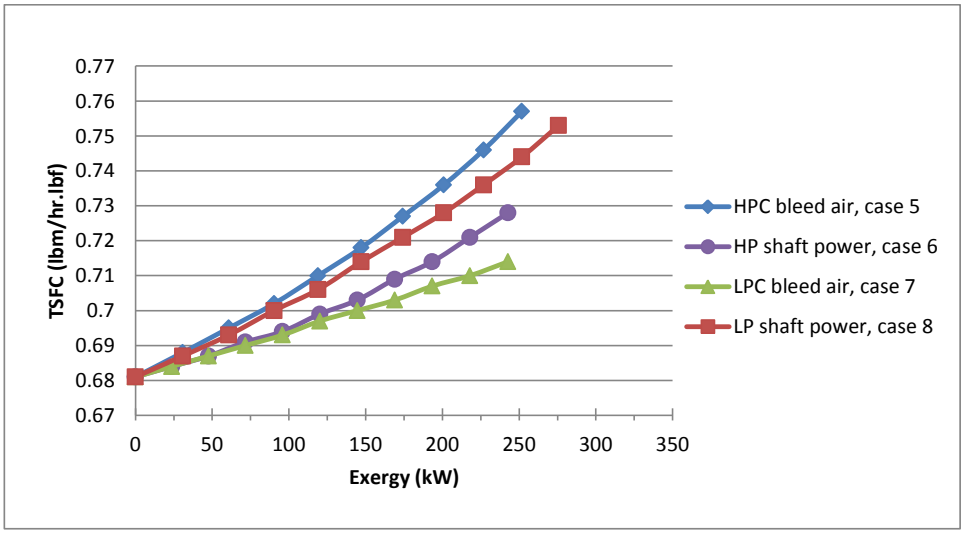

Figure C.4. TSFC versus exergy: Tt4 = 2270 R, Mach = 0.8, Alt = 35 kft on standard day

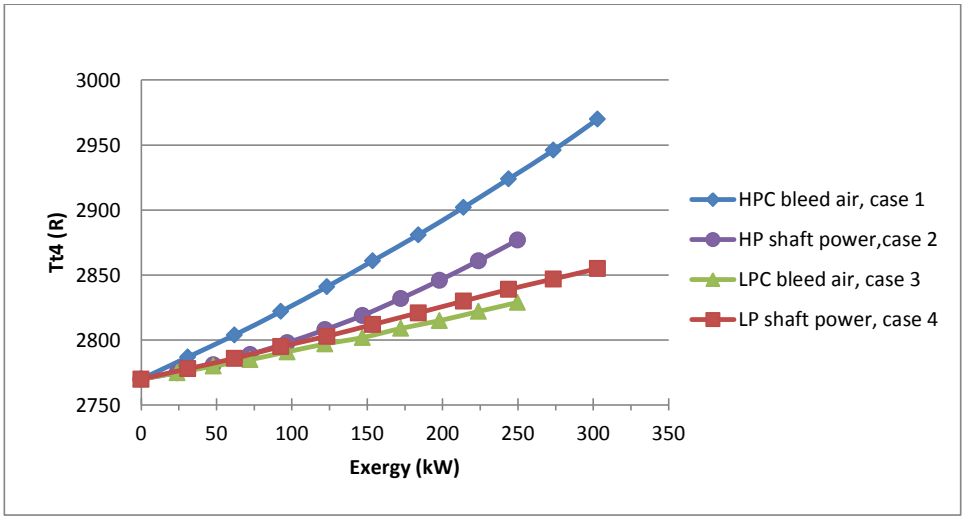

Figure C.5. Tt4 versus exergy: mf = 0.35 lbm/s, Mach = 0.8, Alt = 35 kft on standard day

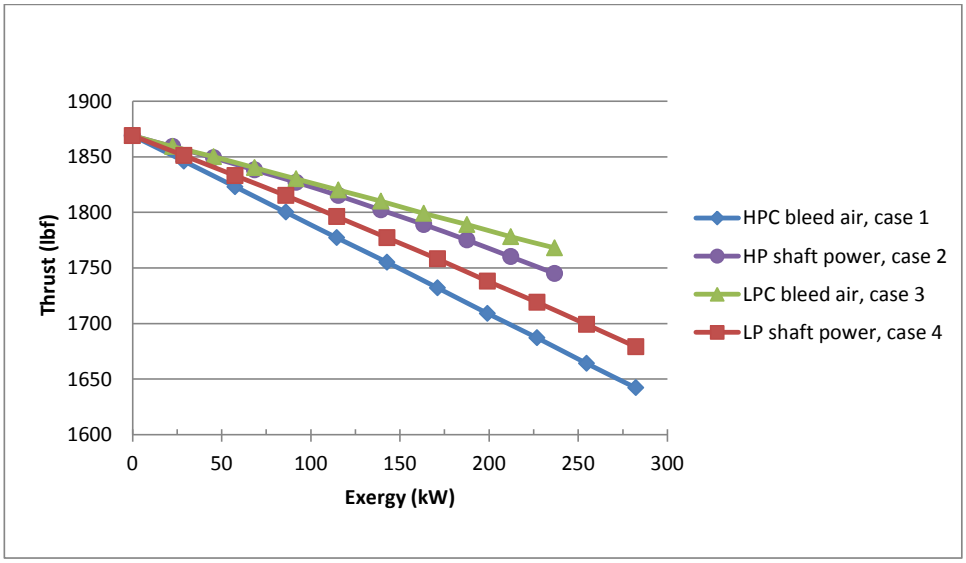

Figure C.6. Thrust versus exergy: mf = 0.35 lbm/s, Mach = 0.8, Alt = 35 kft on cold day

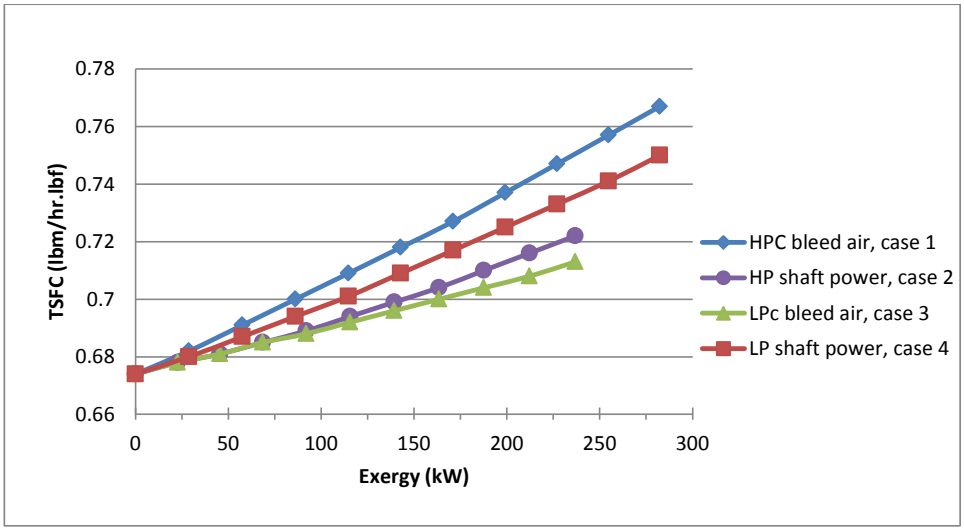

Figure C.7. TSFC versus exergy: mf = 0.35 lbm/s, Mach = 0.8, Alt = 35 kft on cold day

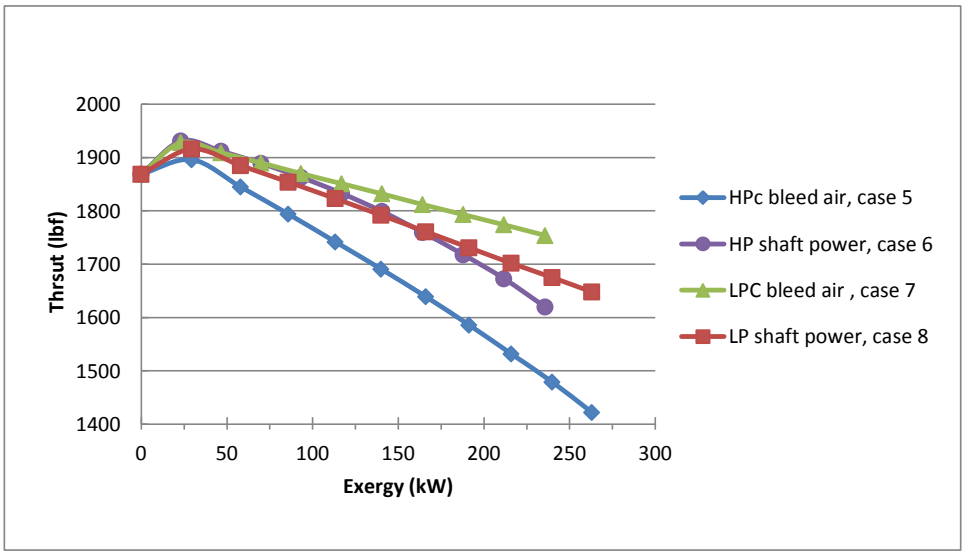

Figure C.8. Thrust versus exergy: Tt4 = 2270 R, Mach = 0.8, Alt = 35 kft on cold day

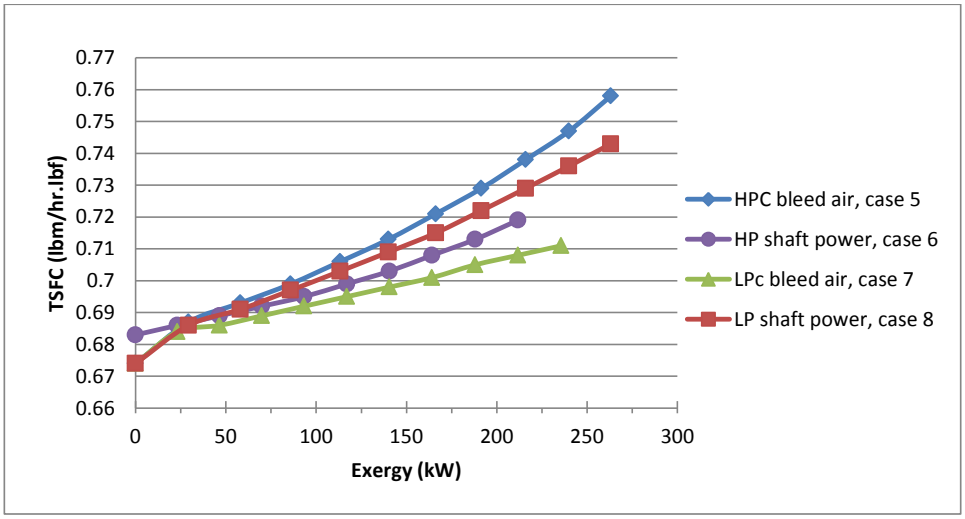

Figure C.9. TSFC versus exergy: Tt4 = 2270 R, Mach = 0.8, Alt = 35 kft on cold day

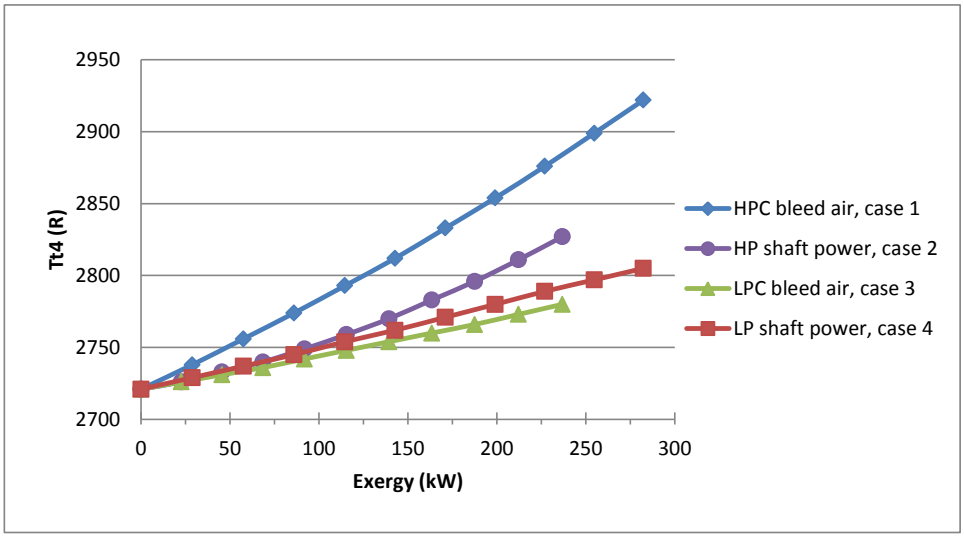

Figure C.10. Tt4 versus exergy: mf = 0.35 lbm/s, Mach = 0.8, Alt = 35 kft on cold day

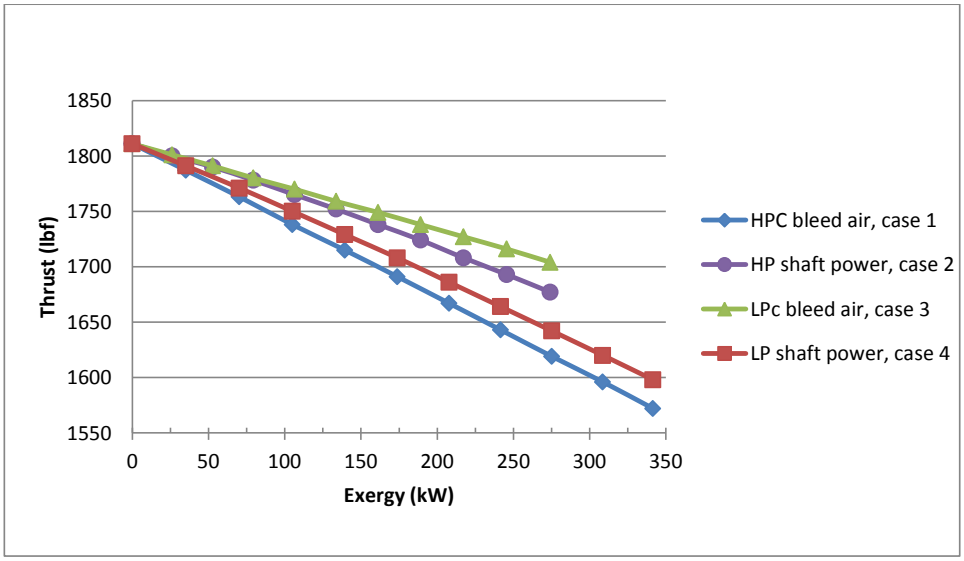

Figure C.11. Thrust versus exergy: mf = 0.35 lbm/s, Mach = 0.8, Alt = 35 kft on hot day

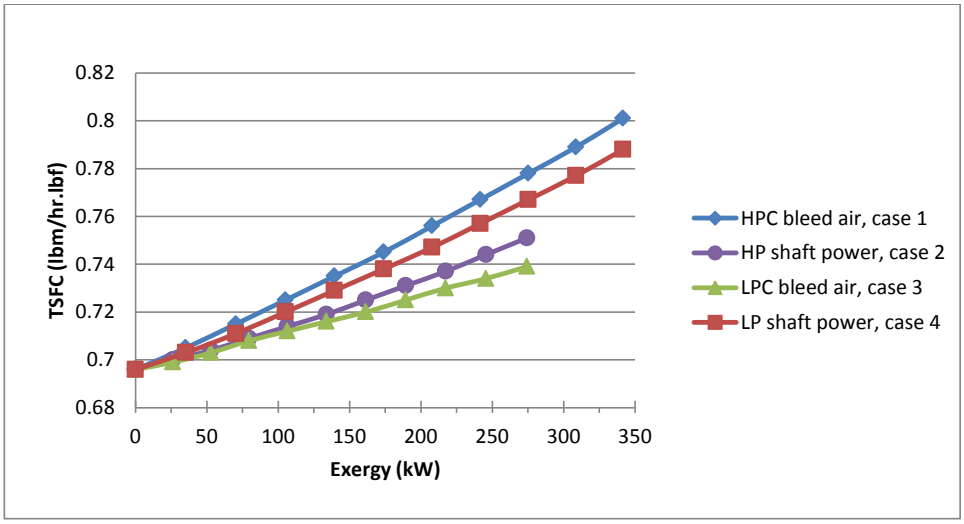

Figure C.12. TSFC versus exergy: mf = 0.35 lbm/s, Mach = 0.8, Alt = 35 kft on hot day

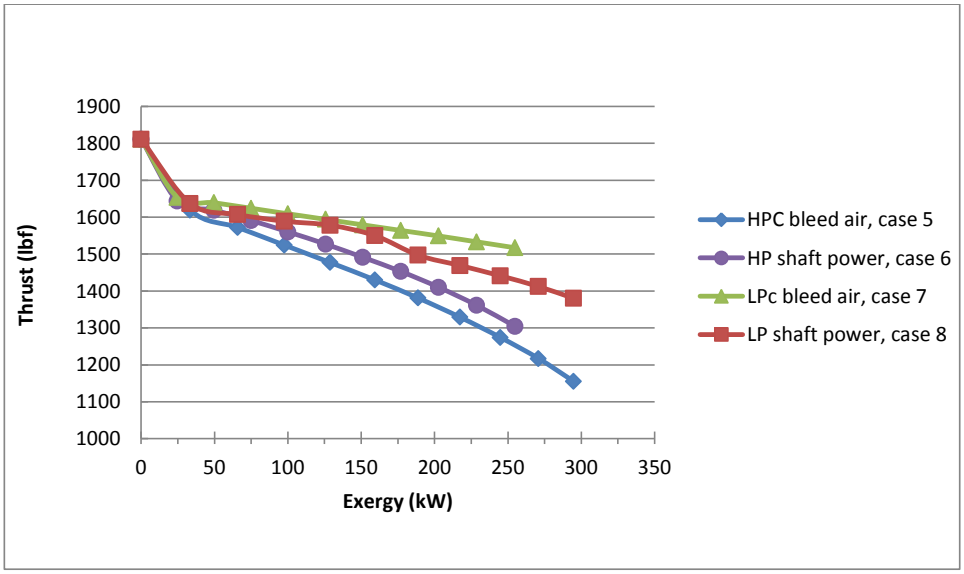

Figure C.13. Thrust versus exergy: Tt4 = 2770 R, Mach = 0.8, Alt = 35 kft on hot day

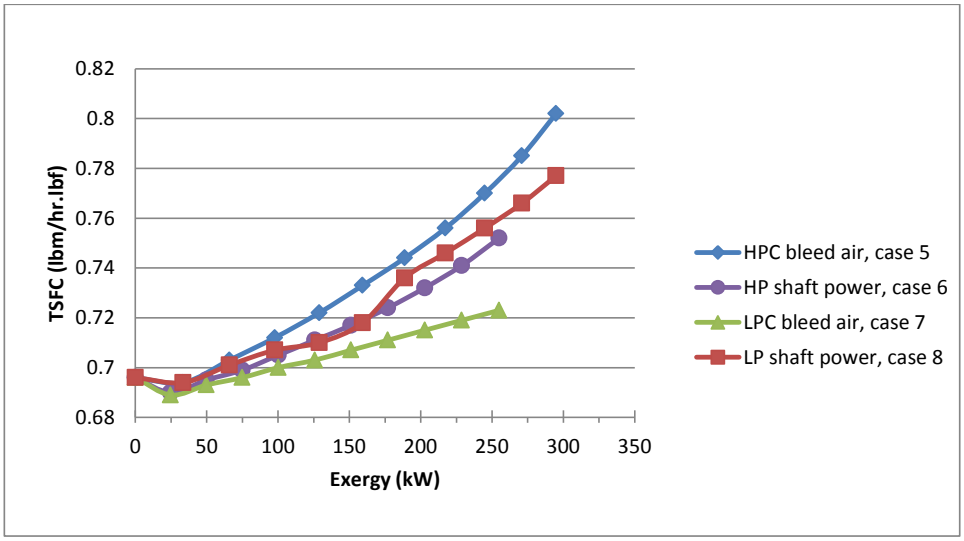

Figure C.14. TSFC versus exergy: Tt4 = 2770 R, Mach = 0.8, Alt = 35 kft on hot day

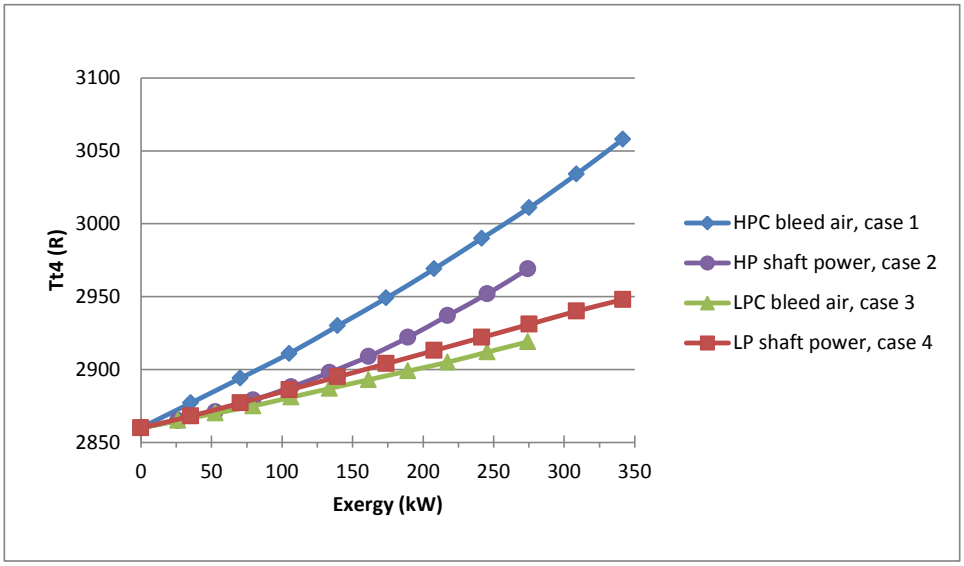

Figure C.15. Tt4 versus exergy: wf = 0.35 lbm/s, Mach = 0.8, Alt = 35 kft on hot day

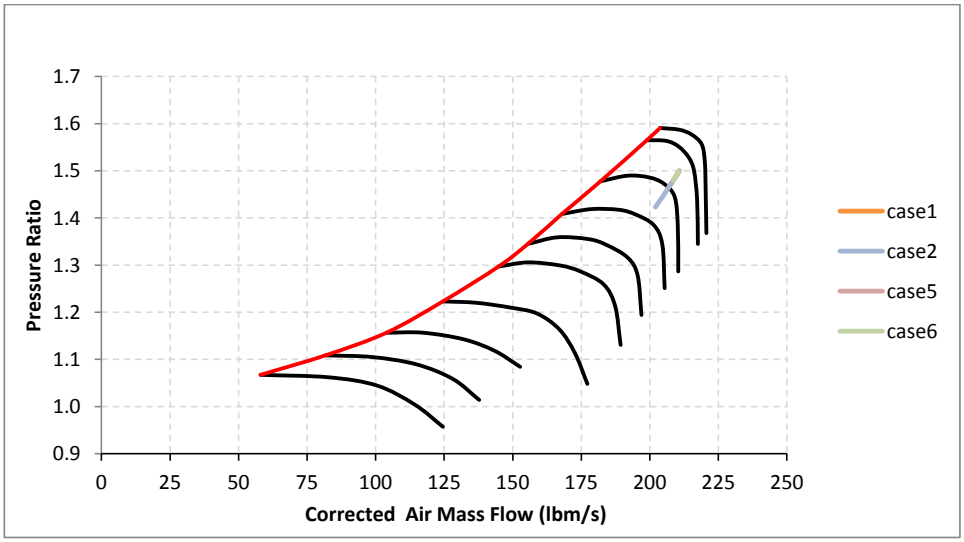

Figure C.16. Fan operating lines : wf = 0.35 lbm/s, Mach = 0.8, Alt = 35 kft on cold day

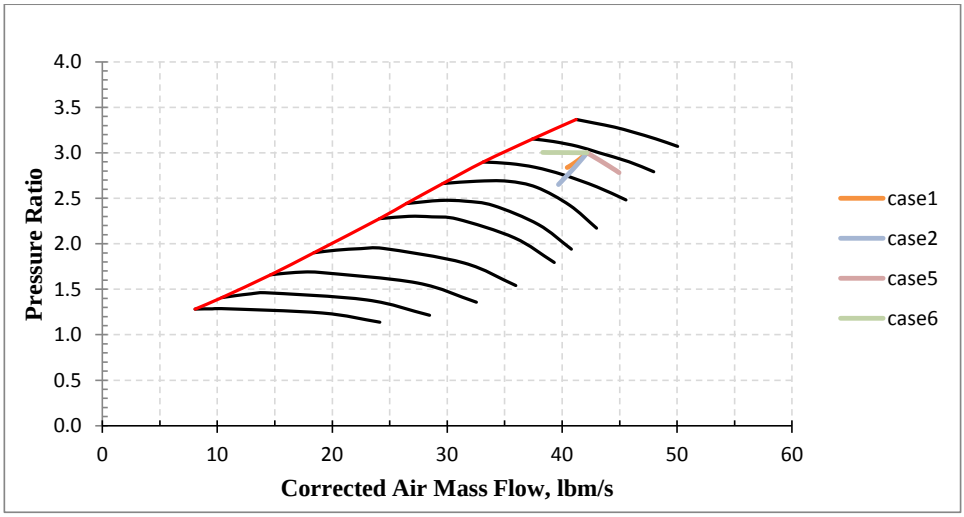

Figure C.17. LPC operating lines : wf = 0.35 lbm/s, Mach = 0.8, Alt = 35 kft on cold day

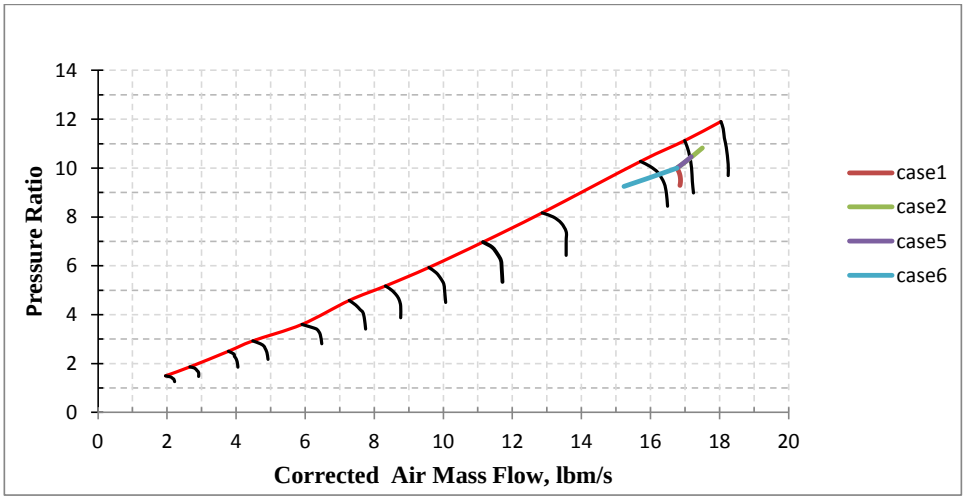

Figure C.18. HPC operating lines : wf = 0.35 lbm/s, Mach = 0.8, Alt = 35 kft on cold day

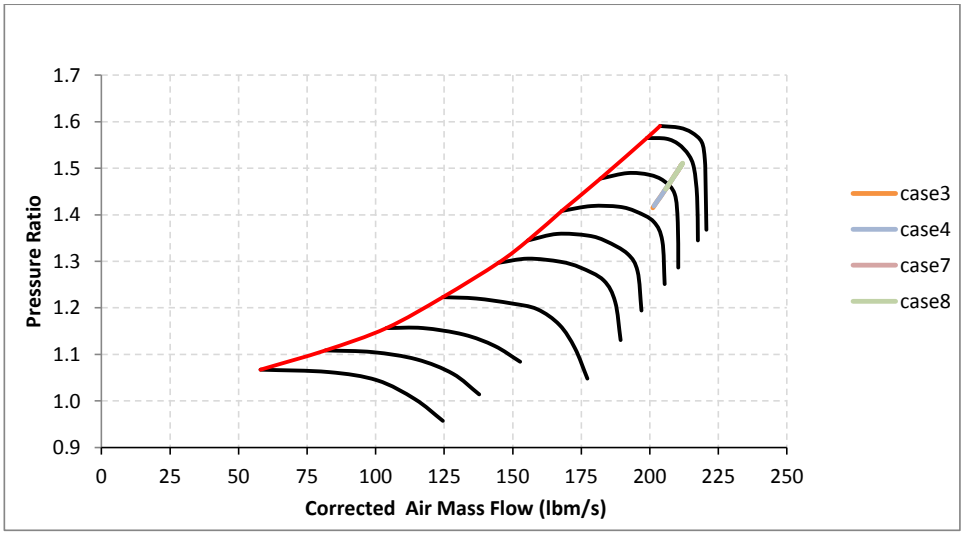

Figure C.19. Fan operating : Tt4 = 2270 R, Mach = 0.8, Alt = 35 kft on cold day

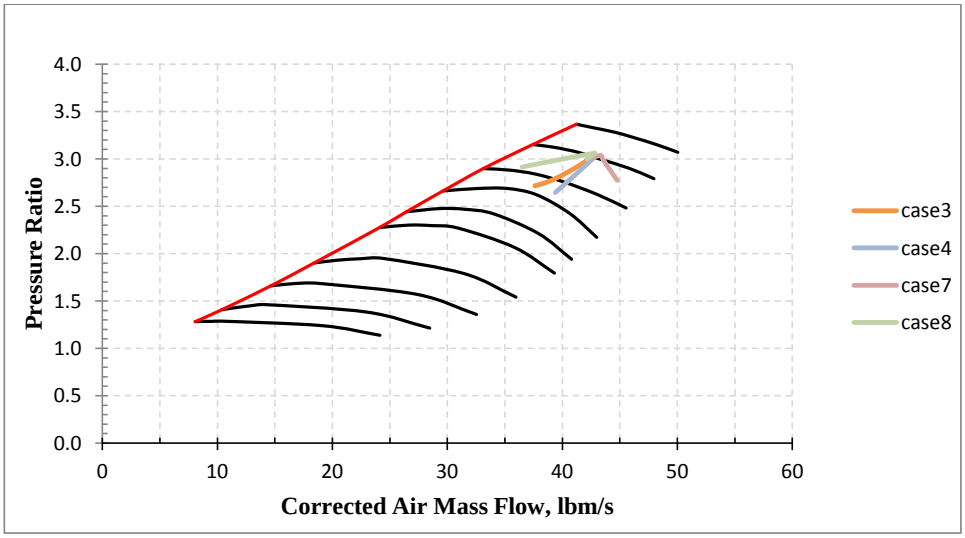

Figure C.20. LPC operating lines Tt4 = 2270 R, Mach = 0.8, Alt = 35 kft on cold day

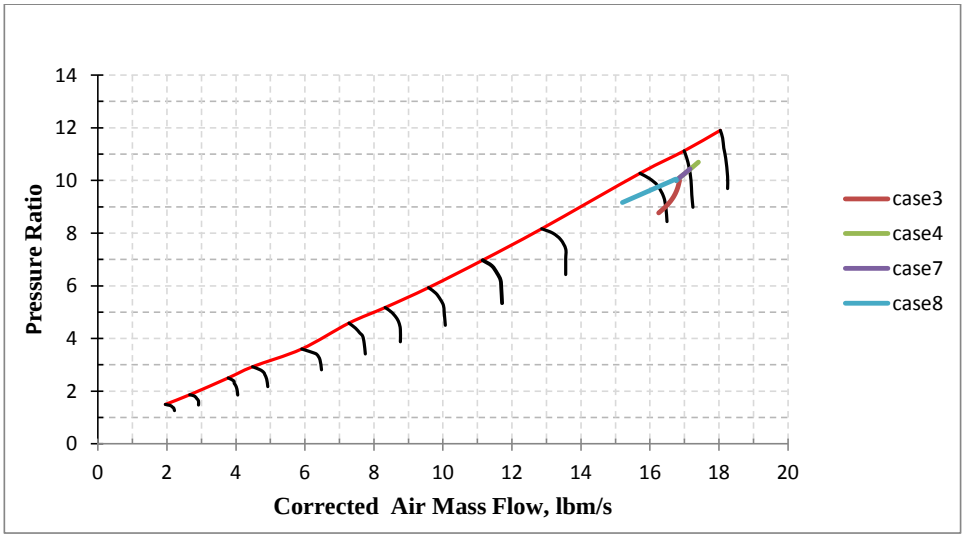

Figure C.21. HPC operating lines:Tt4 = 2270 R, Mach = 0.8, Alt = 35 kft on cold day

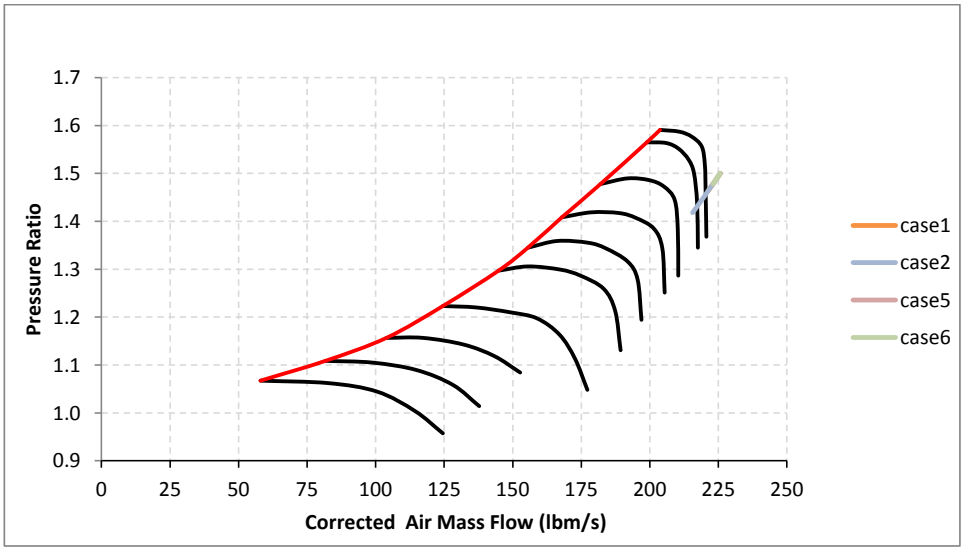

Figure C.22. Fan operating : wf = 0.35 lbm/s, Mach = 0.8, Alt = 35 kft on hot day

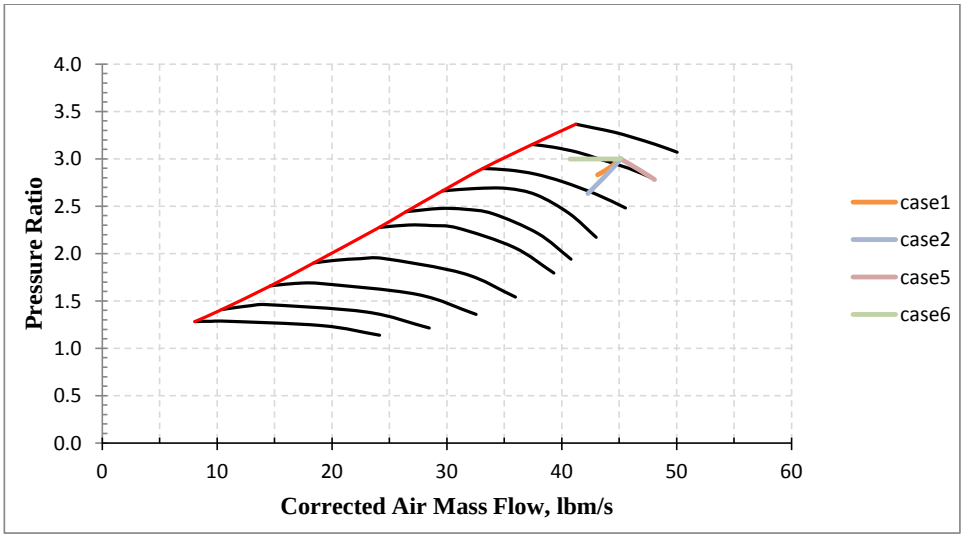

Figure C.23. LPC operating lines : wf = 0.35 lbm/s, Mach = 0.8, Alt = 35 kft on hot day

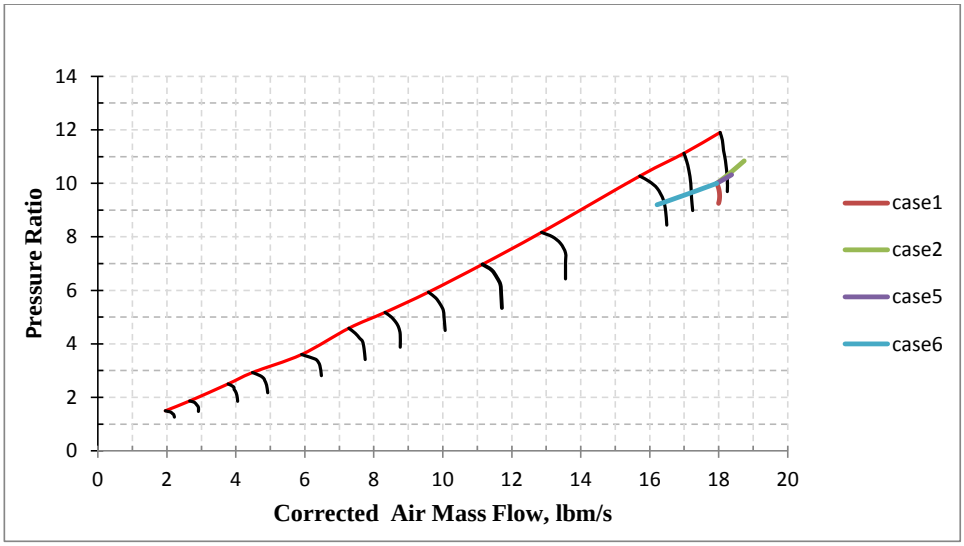

Figure C.24. HPC operating lines : wf = 0.35 lbm/s, Mach = 0.8, Alt = 35 kft on hot day

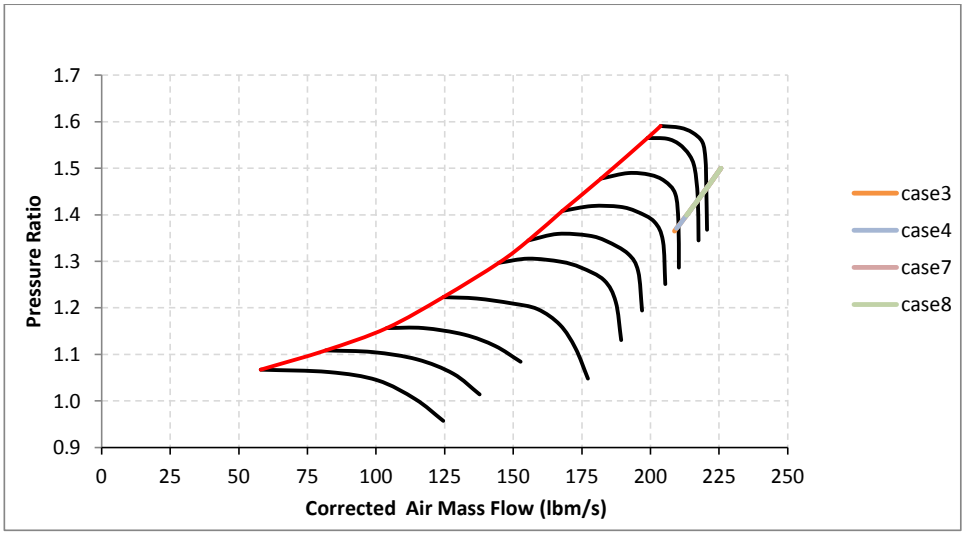

Figure C.25. Fan operating lines :Tt4 = 2270 R, Mach = 0.8, Alt = 35 kft on hot day

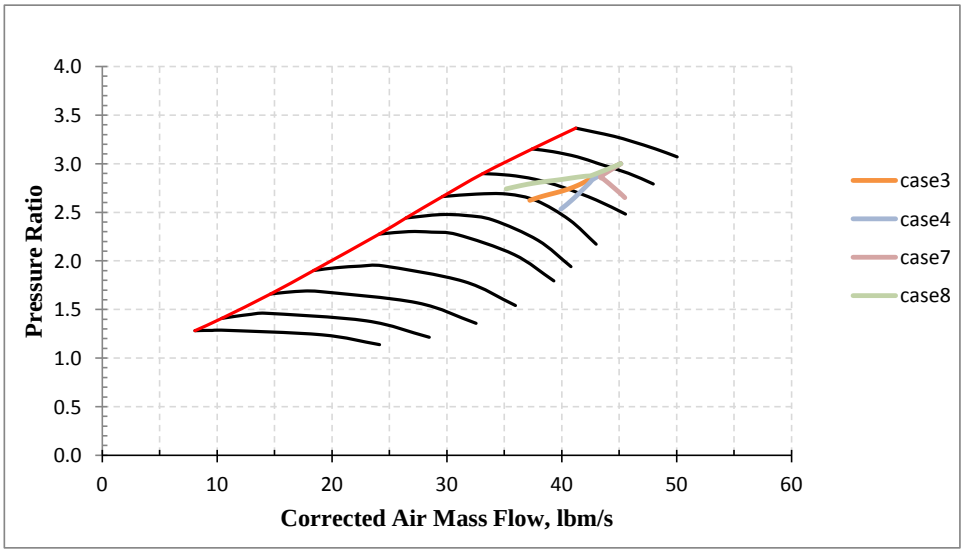

Figure C.26. LPC operating lines :Tt4 = 2270 R, Mach = 0.8, Alt = 35 kft on hot day

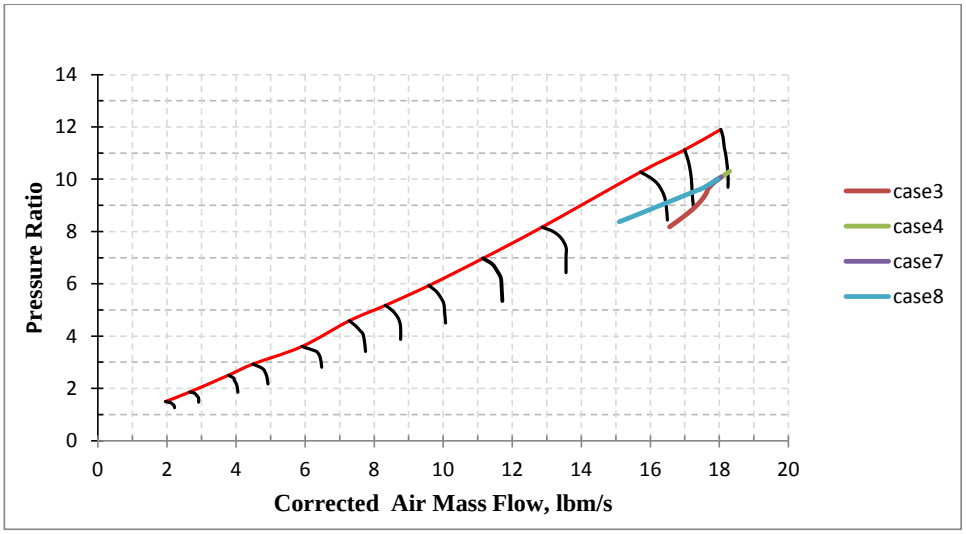

Figure 0.27. HPC operating lines :Tt4 = 2270 R, Mach = 0.8, Alt = 35 kft on hot day

Bibliography

1. A. Yuhas and R. Ray. " Effects of Bleed Air Extraction on Thrust Levels of the F404-GE-400 Turbofan Engine". AIAA-92-3092, 28th Joint Propulsion Conference and Exhibit, 6-8 July 1992, Nashville, TN.

2. Ronald Slingerland and Sijmen Zandstra. " Bleed Air Versus Electric Power Off-takes from a Turbofan over the Flight Cycle ". AIAA-2007-7848-925 . 7th AIAA Aviation Technology, Integration and Operations Conference, 18-20 September 2007, Belfast, Northern Ireland.

3. John H.Doty, José A.Camberos and Davis J. Moorhouse. " Benefits of Exergy-Based Analysis for Aerospace Applications: Part 1". AIAA-2008-4355-912. 40th Thermodynamics Conference, 23-26 June 200, Seattle, Washington.

4. John H.Doty, José A.Camberos and Davis J. Moorhouse. " Benefits of Exergy-Based Analysis for Aerospace Applications: Part 2". AIAA-2009-1598-214. 47th AIAA Aerospace Sciences Meeting Including The New Horizons Forum and Aerospace Exposition, 5-8 January 2009, Orlando, Florida.

5. John H.Doty, José A.Camberos and Davis J. Moorhouse. " Benefits of Exergy-Based Analysis for Aerospace Applications: Pert 1". AIAA-2008-4355-912. 40th Thermodynamics Conference, 23-26 June 200, Seattle, Washington.

6. Paul Osterbeck, Edward L. Butzin and Paul Johnson. " Air Vehicle Sizing and Performance Modeling in NPSS". AIAA-2009-5417-780. 45th AIAA/ASME/ASEE Joint Propulsion Conference & Exhibit, 2-5 August 2009, Denver, Colorado.

7. John K. Lytle. " Multi-fidelity Simulations of Air Breathing Propulsion Systems". AIAA-2006-4967-641. 42nd AIAA/ASME/ASEE Joint Propulsion Conference & Exhibit, 9-12 July 2006, Sacramento, California.

8. Russel W. Claus, Scott Townsend, Tom Lavelle, Cynthia Naiman, and Mark Turner. " A Case Study of High Fidelity Engine System Simulation". AIAA-2006-4971-555. 42nd AIAA/ASME/SAE/ASEE Joint Propulsion Conference & Exhibit, 9-12 July 2006, Sacramento, California.

9. Brian K. Kestner, Taewo Nam, Andrew J. Flett, J.Scott Wilson and Dimitri N. Mavris. " Integrated Engine and Aircraft Mission Performance Analysis Using NPSS". AIAA-2012-0841. 50th AIAA Aerospace Sciences Meeting Including The New Horizons Forum and Aerospace Exposition, 09-12 January 2012, Nashville, Tennessee.

10. Russel W. Claus, Tom Lavelle and Scott Townsend. " Variable Fidelity Analysis of Complete Engine Systems". AIAA-2007-5042-185. 43nd AIAA/ASME/SAE/ASEE Joint Propulsion Conference & Exhibit, 8-11 July 2006, Cincinnati, OH.

11. Rajiv Sampath, Rohinton Irani and Mahadevan Balasubramaniam. " High Fidelity System Simulation of Aerospace Vehicles Using NPSS". AIAA-2004-371-520. 42nd AIAA Aerospace Sciences Meeting and Exhibit, 5-8 January 2004, Reno, Nevada.

12. Scott M. Jones. " An Introduction to Thermodynamic Performance Analysis of Aircraft Gas Turbine Engine Cycles Using the Numerical Propulsion System Simulation Code". NASA/TM-2007-214690.

13. Mattingly, Jack D., Heiser, William H., and Pratt, David T., 2002. *Aircraft Engine Design, Second Edition*. AIAA Education Series

14. Wolverine Ventures, NPSS Modeling Tutorial, version 2.3.0.1.

15. The Ohio Aerospace Institute, *NPSS User Guide, version 2.3.0.*

16. Caitlin R. Thorn, Captain, USAF. *Off Design Analysis of a High Bypass Turbofan Using Pulsed Detonation Combustor* (Master's Thesis). Air Force Institute of Technology , 2010.

REPORT DOCUMENTATION PAGE

Form Approved
OMB No. 074-0188

1. REPORT DATE *(DD-MM-YYYY)*	**2. REPORT TYPE**	**3. DATES COVERED** *(From – To)*
26-09-2012	Master's Thesis	Sept2010-Sept2012

4. TITLE AND SUBTITLE

Effect Of Accessory Power Take-off Variation On A Turbofan Engine Performance

5a. CONTRACT NUMBER

5b. GRANT NUMBER

5c. PROGRAM ELEMENT NUMBER

6. AUTHOR(S)

Faidi, Anis., 1st Lieutenant, TUNAF

5d. PROJECT NUMBER

5e. TASK NUMBER

5f. WORK UNIT NUMBER

7. PERFORMING ORGANIZATION NAMES(S) AND ADDRESS(S)
Air Force Institute of Technology
Graduate School of Engineering and Management (AFIT/EN)
2950 Hobson Way
WPAFB OH 45433-8865

8. PERFORMING ORGANIZATION REPORT NUMBER

AFIT/GAE/ENY/12-S26

9. SPONSORING/MONITORING AGENCY NAME(S) AND ADDRESS(ES)
Intentionally left blank

10. SPONSOR/MONITOR'S ACRONYM(S)

11. SPONSOR/MONITOR'S REPORT NUMBER(S)

12. DISTRIBUTION/AVAILABILITY STATEMENT

APPROVED FOR PUBLIC RELEASE; DISTRIBUTION UNLIMITED.

13. SUPPLEMENTARY NOTES
This material is declared a work of the U.S. Government and is not subject to copyright protection in the United States.

14. ABSTRACT

Engine fuel efficiency of aerospace vehicles can be reached by different techniques. One way to do that is to reduce aircraft subsystems power supply effects on the engine performance. Previous research work has showed that extracting bleed air from the high pressure compressor exit is more efficient than extracting the equivalent amount of energy from the low pressure spool shaft. A high bypass turbofan engine was modeled using the Numerical Propulsion System Simulation (NPSS). The baseline engine performance was evaluated at different flight conditions of Mach number and altitude. To better understand the effect of air bleed take-off and shaft power extraction, four simulation cases are investigated at constant fuel flow and constant high pressure turbine inlet temperature setting. The first two cases extract bleed air from compressors while the last two cases extract equivalent power from engine shafts. Appropriate model modifications and port connections are made to consider the power extraction method. The effect of a bleed air fraction off-take from 1% to 10% and equivalent shaft power extraction on engine performance of thrust and thrust specific fuel consumption was investigated. Engine compressors operating lines and HPT inlet temperature were also checked. Results proved that shaft power extraction is more efficient for engine performance than bleeding an equivalent air fraction from compressors. Those results were shown to be consistent with a simulation run on the AEDsys simulation tool.

15. SUBJECT TERMS
Turbofan Engines, Combustion, NPSS Simulation, Aircraft Engines, Air Breathing Engines, Thermodynamic Cycles

16. SECURITY CLASSIFICATION OF:			**17. LIMITATION OF ABSTRACT**	**18. NUMBER O PAGES**	**19a. NAME OF RESPONSIBLE PERSON**
c. THIS PAGE	**b. ABSTRACT**	**c. THIS PAGE**			Dr. Paul I. King ADVISOR
U	**U**	**U**	**U**	130	**19b. TELEPHONE NUMBER** *(Include area code)* (937) 255-3636, ext 4628 (paul.king@afit.edu)

Standard Form 298 (Rev. 8-98)
Prescribed by ANSI Std. Z39-18